Rahlouni, Fatima R., Quantitative Proteomic Investigation of Estrogenic Endocrine-Disrupting Effects in the Rat Uterus. Doctor of Philosophy (Biochemistry and Cancer Biology), April, 2016, 144 pp., 8 tables, 28 illustrations, references: 167 titles.

The mammalian uterus is one of the most sensitive organs for estrogenicity. However, the widely used rat uterotrophic assay to assess known and potential estrogenic compounds only considers the uterine wet weight gain as an endpoint measurement. To complement this method with an advanced technology that reveals molecular targets, we analyzed changes in protein expression using label-free quantitative proteomic analysis by liquid chromatography–mass spectrometry from uterine protein extracts of ovariectomized rats after daily 17β-estradiol exposure for five days. We performed shotgun proteomic analysis of the uterus to identify candidate proteins for use as markers of estrogenicity. In addition, we mapped the differentially expressed proteins from untargeted analysis to signaling networks and biological processes through Ingenuity Pathway Analysis. We selected twelve of the top up- and down-regulated proteins for further evaluation by selected reaction monitoring-based targeted quantitation. Of the final six candidate markers, we verified all six as markers of estrogenicity by the application of the panel to testing rats exposed to a low and high dose of the known estrogenic compound bisphenol A. Altogether, the results of this study demonstrate the power of combining untargeted and targeted quantitative proteomic methods for a comprehensive analysis in rat uterus to evaluate changes in protein expression levels due to estrogen exposure, and to uncover candidate markers of estrogenicity in the development of a targeted proteomics panel.

QUANTITATIVE PROTEOMIC INVESTIGATION OF ESTROGENIC ENDOCRINE-DISRUPTING EFFECTS IN THE RAT UTERUS

DISSERTATION

Presented to the Graduate Council of the

Graduate School of Biomedical Sciences

University of North Texas

Health Science Center at Fort Worth

in Partial Fulfillment of the Requirements

For the Degree of

DOCTOR OF PHILOSOPHY

By

Fatima R. Rahlouni

Fort Worth, Texas

April 2016

ACKNOWLEDGEMENTS

First and foremost, I would like to thank my mentor Dr. Laszlo Prokai who has been my role model. His continuous encouragement and faith in my abilities have given me the perseverance and immense confidence in my work, as well as the strong desire to continually strive for the best. I could not have asked for a better mentor than him. He has been inspirational, supportive, tolerant and caring. In short, he has been a fatherly figure to me whom I have always approached for suggestions and guidance, be it in research or personal matters. He is a man of tremendous wisdom and patience, and I would like to thank him for bearing with me throughout this journey.

I would also like to express my innermost gratitude to my co-mentor Dr. Katalin Prokai-Tatrai who has provided me with continuous support, guidance, and encouragement throughout my doctoral training. I thank her for pushing me to develop into a more confident scientist with a critical eye, as well as a better person. I am forever grateful. I would also like to sincerely thank my other committee members: Dr. Andras Lacko, Dr. Julian Borejdo, and my University member Dr. Joseph Warren for their tremendous support, and taking time out of their busy schedules to help me along the way. To Dr. Vladimir Shulaev, thank you for your collaborations, knowledge, and guidance.

I would like to recognize and thank all of my current and former laboratory members for their friendliness, feedback and support. I am especially grateful to Dr. Szabolcs Szarka and Dr. Vien Nguyen for their help with the project and numerous discussions. I would also like to

acknowledge the administrative staff from the Department of Molecular Biology and Immunology, as well as the Department of Pharmacology and Neuroscience who have been very helpful and supportive throughout the course of my graduate studies.

I would like to recognize my family, friends, and fellow classmates for their support during my time as a graduate student. Thank you to my parents for their unconditional love and support. I would also like to thank my brother and sister for always believing in me. There are no words how infinitely grateful I am to my husband, Azeddine. He has been a pillar of constant support and encouragement. To my baby Layla, I love you so much. Without them, I do not think I would have come so far. I thank you for believing in me and making me believe in myself. Also, I would like to thank God for giving me the strength and opportunity, and blessing me at every step in my life.

Finally, I would like to thank the funding agencies that supported this work: Robert A. Welch Foundation (endowment BK-0031), NIH grant AG031535, and UNT Health Science Center Doctoral Student Bridge Grant RI6163.

TABLE OF CONTENTS

Page

V. SUMMARY AND DISCUSSION

ABBREVIATIONS

AQUA, Absolute quantification of proteins

AUC, Area under the curve

BPA, Bisphenol-A

CID, Collison-induced dissociation

DTT, Dithiothreitol

E1, Estrone

E2, 17β-Estradiol

E3, Estriol

E4, Estetrol

EDC, Endocrine disrupting chemical or endocrine disrupting compound

ESI, Electrospray ionization

H-ESI, Heated electrospray ionization

HPLC, High performance liquid chromatography

IAA, Iodoacetamide

iCAT™, Isotope-coded affinity tag

IPA®, Ingenuity Pathway Analysis®

iTRAQ, Isobaric tag for relative and absolute quantitation

LC, Liquid chromatography

LC-MRM-MS, Liquid chromatography coupled multiple reaction monitoring mass spectrometry

LC-MS, Liquid chromatography coupled mass spectrometry

LC-MS/MS, Liquid chromatography coupled tandem mass spectrometry

m/z, Mass-to-charge ratio

MRM, Multiple reaction monitoring

MS/MS or MS^2, Tandem mass spectrometry

NAT, Native peptide i.e. endogenous peptide

NSI, Nano-electrospray ionization

OVX, Ovariectomized i.e., ovaries surgically removed

QC, Quality control

RP-HPLC, Reversed-phase high performance liquid chromatography

RP-LC, Reversed-phase liquid chromatography

RP-LC/MS, Reversed-phase liquid chromatography mass spectrometry

SEM, Standard error of the mean

SILAC, Stable isotope labeling with amino acids in cell culture

SIS, Stable-isotope labeled internal standard

SRM, Selected reaction monitoring

US EPA, United States Environmental Protection Agency

LIST OF TABLES

CHAPTER III. TARGETED PROTEOMIC ASSAY DEVELOPMENT AND OPTIMIZATION FOR THE VERIFICATION OF ESTROGEN-REGULATED PROTEINS

LIST OF ILLUSTRATIONS

CHAPTER I

INTRODUCTION

Estrogens and the Uterus

Estrogens have many functions in the mammalian body, most important of which is in controlling the function of adult reproductive organs and processes (1, 2). Estrogen promotes the formation of the female secondary sex characteristics; its reproductive roles include the regulation of estrous and menstrual cycles, in addition to affecting fertility as well as playing a role in maternal and sexual behaviors (3-5). Estrogens are signaling molecules that coordinate multiple functions across the organs, cells and genes of the body (6). Some of the non-reproductive roles include maintaining bone strength and density (7), affecting blood lipid levels (8), water and salt balance (9), accelerating metabolism and fat deposition (10), maintaining healthy brain function (11), and playing an adverse role in various cancers (12, 13). Estrogens even play a minor role in signaling within male-specific functions like the reproductive role in sperm maturation (14). Estrogens are essential for embryonic and fetal development and survival (15). For each of its functions, estrogen levels are strictly regulated, and any shift in the delicate balance results in increased susceptibility to disease. Estrogen deficiency can lead to disease pathology such as in osteoporosis, atherosclerosis, and central nervous system degeneration. On the opposite end of the spectrum, elevated levels of estrogens can also lead to the development of tumors and cancer. In addition to these classical genomic functions via classical nuclear estrogen

receptor signaling, estrogens also have non-genomic functions (1, 6, 16-18). Taken altogether, this shows that there is a vast complexity with regards to estrogen signaling and response in maintaining health, preventing, causing and exacerbating disease.

Estrogens are a family of structurally related steroid hormones. They include estrone (E1), estradiol (E2), estriol (E3), and estetrol (E4) (Figure 1.1). E1, E2, and E3 are the three major endogenous estrogens in women, while E4 is produced only during pregnancy (18, 19). The uterus is the most receptive organ to and major target of estrogen. Estrogens are derived from cholesterol through a series of chemical reactions, with aromatase being the key enzyme in estrogen biosynthesis. 17β-Estradiol (E2) is a potent, biologically prevalent and active compound in the family of estrogens, and represents the principal circulating estrogen in humans. While the vast majority of E2 is produced from the ovaries, because of the presence of aromatase in a wide variety of tissues, E2 can also be produced to a lesser extent locally in the adrenal cortex, testes in men, from fat cells, and by the brain. E2 levels vary greatly based on the timing in the reproductive cycle, peaking right before ovulation; E2 levels are much lower in men and postmenopausal women (1-3, 6, 15-18). Because of these multiple roles and diverse functions with circulating E2 in the body, any slight disruption in function can harm the delicate balance struck by the body.

Endocrine Disrupting Chemicals

Endocrine disrupting chemicals (EDCs) are a class of chemicals that interfere with the biological actions of hormones, and there has been significant public concern about their adverse effect in the environment and on human health (20). They are broadly categorized according to the hormones that they interfere: either estrogens, androgens or thyroid hormones activities. The

US Environmental Protection Agency (EPA) has set up the Endocrine Disruptor Screening Program to screen the tens of thousands of chemicals for suspected endocrine disruption based on a directive from section 408(p) of the Federal Food, Drug and Cosmetic Act, and from the Food Quality Protection Act of 1996 and the Safe Drinking Water Act of 1996 to develop a chemical screening program using appropriate validated test systems to determine whether substances may have hormonal effects (21-23). The class of EDCs that we will focus on this dissertation is the estrogens. Estrogenicity, or mimicking the effect of an endogenous human estrogen such as E2, is one of the major concerns of the EPA and environmentalists.

The vast majority of these compounds that are tested for estrogenic effects in the uterus utilize the "gold standard" *in vivo* uterotrophic rat assay, as well as *in vitro* on rodent, yeast, and human cell lines as part of the complementary battery of assays implemented in the EPA's two-tier testing program (21-29). The uterotrophic assay is an *in vivo* assay that uses either sexually immature female rats or adult ovariectomized female rats, where there is no significant source of endogenous estrogen. In either version of the assay, multiple doses of a test compound are administered over consecutive days (a minimum of three days either orally or subcutaneously). This assay tests for whether or not a substance has estrogenic effects. The compounds that do have estrogenic effects cause uterotrophic response due to the imbibition of water and growth of the uterine cells. Statistically significant uterine weight increases compared to controls gives a positive result, and the compounds can be prioritized for further testing (Figure 1.2). Both the *in vivo* and *in vitro* methods have their limitations. The cell lines are not properly able to recapitulate the *in vivo* environment of the uterus within and interacting with the body. The rat uterotrophic assay merely uses uterine wet and dry weights as an endpoint of estrogenicity, not taking into account all of the complexities and other factors that play a role in exerting estrogen's

effect on the organ and body (24-32). This aside, many of the other groups that do work in this area examine the genomic or transcriptomic changes that take place (33-36). Focus has also been on understanding the developmental changes of the tissue and the effects on fertility (37, 38), while others explore the systemic effects due to environmental contaminants (39, 40).

One major EDC that has been widely publicized in recent years is bisphenol A (BPA) (Figure 1.3). Interestingly, BPA, as a monomer, was first developed as a synthetic estrogen in the 1890s (41), but it has never been employed in medicine. On the other hand, BPA-based polymers such as polycarbonate plastics (plastic #7) and epoxy resins are widely used. These polycarbonate plastics and epoxy resins have many applications; they are used to make water bottles, baby bottles, the coating of metal food cans, on thermal paper products such as cash register and ATM receipts, as well as some dental sealants (42, 43). BPA can leach form the plastic products it is coated on and enter the human body and environment to do harm (41, 42). Public concern about BPA exposure is so great because of its widespread use, and has led to a movement to specifically label products made without it as “BPA-free”. BPA is a weak estrogenic EDC and has become a major target for studies in recent years (30, 38, 41, 43-57).

With all the technology available, the uterotrophic assay itself is an overly simplified way to look at this problem. What is necessary is taking a hard look at the functional players of gene expression, the proteins, and their role and changes due to exposure to EDCs; i.e. taking an “omics” approach to this problem. Our lab has previously begun to investigate the gap in this area with an initial proteomics study on E2’s impact on the mouse uterus (58). However, others working in this area focus on protein expression signatures of EDCs from the environment focusing on either aquatic models or varying organs and tissues other than the uterus (45, 59-65),

while those studies focusing on uterine proteomics focus either on reproduction and fertility or cancer (66-70).

To our knowledge, one other study has been done using a proteomic analysis of estrogen effects in the rat uterus (71). While it is an untargeted investigation of the estrogen-induced changes in the rat uterus proteome, similar to our previous study in the mouse (58), this was a study focused on describing the methods and protocols in accomplishing such an experiment. They also did not use E2 to perturb estrogen exposure, but rather used ethinyl estradiol, a semisynthetic E2 derivative and most commonly used compound in oral contraceptive pills (72). They also made use of two-dimensional liquid chromatography, which in theory increases separation and resolving power to then increase the number of proteins identified (73). While this study compared the proteins differentially expressed upon estrogen exposure, they did not show which of the proteins they identified were regulated by the hormone in each group. This was a methods-based publication rather than a results-driven paper aimed at delving into the biological significance of proteins affected by estrogen exposure.

Experimental Strategy: Quantitative Proteomics

Proteomics, the large-scale study of a proteome (proteins in a cell or tissue) of an organism, has become an increasingly developed field. It goes hand-in-hand with mass spectrometry and its advances, making it the most comprehensive and versatile tool in proteomics (74-78). A mass spectrometer is an instrument that measures molecules that are ionized and then separated based on their mass-to-charge ratio (*m/z*). The information acquired from the mass spectrometer allows for protein identification, characterization and relative quantitation. Within the field of mass spectrometry-based proteomics are two branches:

discovery-driven, or untargeted shotgun, proteomics and targeted proteomics (Figure 1.4) (77-80). Both the discovery-driven and the targeted approaches will be applied in this dissertation.

(1) Discovery-driven Proteomics

Discovery-driven, or shotgun, proteomics is the branch of proteomics where no prior knowledge of the sample is needed for analysis. The goal in this approach is to identify as many proteins as possible. Via a "bottom-up" approach (81), the sample proteins are enzymatically digested into peptides, usually with trypsin. The peptides are separated, generally by reversed-phase liquid chromatography (RP-LC), to reduce the sample complexity and then analyzed by mass spectrometry. During mass spectrometric (MS) analysis, the *m/z* of peptide ions are determined and then these peptide ions are fragmented, most commonly by collision-induced dissociation (CID), to produce "tandem mass spectra" (MS/MS or MS^2) containing sequence ions for the assignment of peptide sequences and any post-translational modifications (82, 83). Proteins are identified from these mass spectra by utilizing software that make use of complex algorithms to match from sequence databases of proteins the experimental MS/MS spectra to the theoretical ones (84). The identifications are only as accurate as the databases used on the front end, and the algorithms are also probability-based. To make sense of these large datasets of identifications, systems biology is used. Systems biology is a biology-based interdisciplinary field of study that focuses on the interactions within biological systems by modeling these interactions into pathways and networks (85). This gives not only a bigger picture of what is happening within the cell, organ or organism, but also gives biological meaning and context to the lists of proteins identified within discovery-driven proteomics experiments (86, 87).

(2) Targeted Proteomics

Targeted proteomics, the 2012 Nature Methods method of the year (88), is the branch of proteomics where specific analytes, or targets, are detected and quantified (77-79, 89-92). Using selected reaction monitoring (SRM) after CID, or multiple SRMs which are considered multiple reaction monitoring (MRM), the capabilities of a triple quadrupole tandem mass spectrometer (a specific type of mass analyzer suited for MRM) are exploited most commonly for quantitative analyses. The first and third quadrupoles act as mass filters to specifically select predetermined *m/z* values corresponding to the peptide precursor ion and specific CID fragment ion of the peptide, where the second quadrupole acts as the collision cell (Figure 1.5). Several of these precursor/fragment ion pairs ("transitions") are monitored over time throughout the chromatographic separation. Utilizing mass selection by only monitoring for specific transitions with narrow windows results in higher selectivity over full scanning used in shotgun approaches, which increases sensitivity. These instruments also cover a wide dynamic range (up to five orders of magnitude), which enables the analysis of samples with low-abundance proteins. The improved selectivity, sensitivity, and dynamic range, allows for the quantitation of pre-selected proteins in highly complex biological samples making it possible in a robust, reliable and reproducible manner (92-94).

To establish a targeted proteomic assay, a list of protein targets first needs to be selected (79, 91, 93, 94). This is commonly achieved from the analysis of discovery-driven data of a given experiment. Once targets are selected, suitable peptides for each protein are necessary. These peptides should be unique to that protein (proteotypic); i.e., 100% homologous to that protein or isoform alone. Once proteotypic peptides are identified, the fragment ions that give the best signal intensity and distinguish the target peptide from the sample must be determined. The

transitions, precursor/fragment ion pairs, and their optimum collision energies are set up for an assay. These assays must also be optimized and validated with synthetic peptides. These transitions and optimal assay conditions take time on the front end to develop, but once set can be used indefinitely in any assay to quantify the given protein target (92-94). Taken together, untargeted and targeted analyses go hand in hand in complementing each other. Those proteins identified as biomarkers of disease using untargeted analyses are usually validated using targeted analysis (95). This is the approach that will be applied in this dissertation.

(3) Quantitative Label-free Methods

For both untargeted and targeted proteomics approaches, methodologies to be able to quantify the proteins are crucial. To this end, multiple techniques are in used that can be either label-free or label-based to be able to accurately and reliably quantify protein expression from complex samples (Figure 1.6). Label-based methods include modifying proteins and peptides with stable isotopes either via metabolic, enzymatic, or chemical means at varying points throughout the sample preparation process. These strategies include stable-isotope labels with amino acids in cell culture (SILAC), protein labeling with isotope-coded affinity tags (ICAT), peptide labeling with isobaric tags for relative quantitation (iTRAQ), and peptides modified at the N-terminus and lysine residues by reductive dimethylation via chemical reaction with different combinations of deuterated and ^{13}C-labeled formaldehyde and sodium cyanoborohydride (77, 78). While these labeling techniques are considered more accurate in quantifying protein abundance, their cost (due to expensive isotope labels) and limitations in number of samples analyzed per experiment make them a less practical choice for untargeted studies and, therefore, we did not use labeling for the discovery-driven studies summarized in

this dissertation. Other label-based approaches are used in targeted studies including the stable isotope dilution-based absolute quantification of proteins (AQUA) (77, 78, 96). This approach makes use of known amounts of stable isotope labeled peptides spiked into samples and used as internal standards for relative and absolute quantification. Isotope dilution-based mass spectrometry is the gold standard in analysis of small molecules and has crossed over into the targeted proteomics field.

Label-free quantitative methods fall under two categories based on which dimension of the mass spectra was used: either from the MS^1-level or the MS^2-level spectra (Figure 1.7). With quantification at the MS^1 level, the area under the curve (AUC) or signal intensity measurement from the precursor ion is used. At this level, the ion intensities of each peptide are measured as the peptides are eluted. Software processing the data need to take into account alignment of the retention times of the peptides to enable relative quantification across experiments (77, 78, 97). The second method of label-free quantitation is designated as “spectral counting”. Spectral counting is based on the concept that peptides that are more abundant will produce more MS^2 (MS/MS) spectra, and is therefore relative to protein abundance. This is a simple approach that has been diversified from merely summing spectra to take into account strategies for increasing accuracy (77, 78, 97). In this dissertation, we make use of the MS-based precursor intensity quantification (MS^1) method.

RESEARCH GOALS AND OBJECTIVES

Development of Targeted Proteomics Assay to Test for Estrogenicity

This dissertation involves adopting a two-fold quantitative proteomics approach for the evaluation and identification of estrogenic endpoints of endocrine disrupting chemicals (EDCs). Overall, we sought to develop a targeted proteomics assay to complement the rat uterotrophic assay with an advanced technology that reveals molecular targets. Initial focus will be on elucidating the broader effects of estrogen exposure on the rat uterus. By using traditional "bottom-up" discovery-driven proteomic methods utilizing liquid chromatography coupled tandem mass spectrometry (LC-MS/MS), we will survey the regulatory effects of E2, the biologically active estrogen, on the rat uterine proteome. We aim to identify E2-regulated proteins and biological processes on a global scale in the rat uterus. With an understanding of the biological processes and proteins that are affected by E2, we can pinpoint markers of estrogenicity for further validation. Therefore, it will be necessary to validate findings with the development of targeted proteomic assays for identifying markers of estrogenicity. Ultimately, any assay that is developed must be validated and be able to be applied to other EDCs for use. We propose to evaluate known estrogenic EDCs and EDCs with suspected estrogenic activity by applying our targeted estrogenic proteomic assay to rats exposed to bisphenol A. The results of this study have demonstrated the power of combining untargeted and targeted quantitative proteomic strategy to identify and verify candidate molecular markers for the evaluation of potential estrogenic endocrine disrupting chemicals to complement the conventional rat uterotrophic assay.

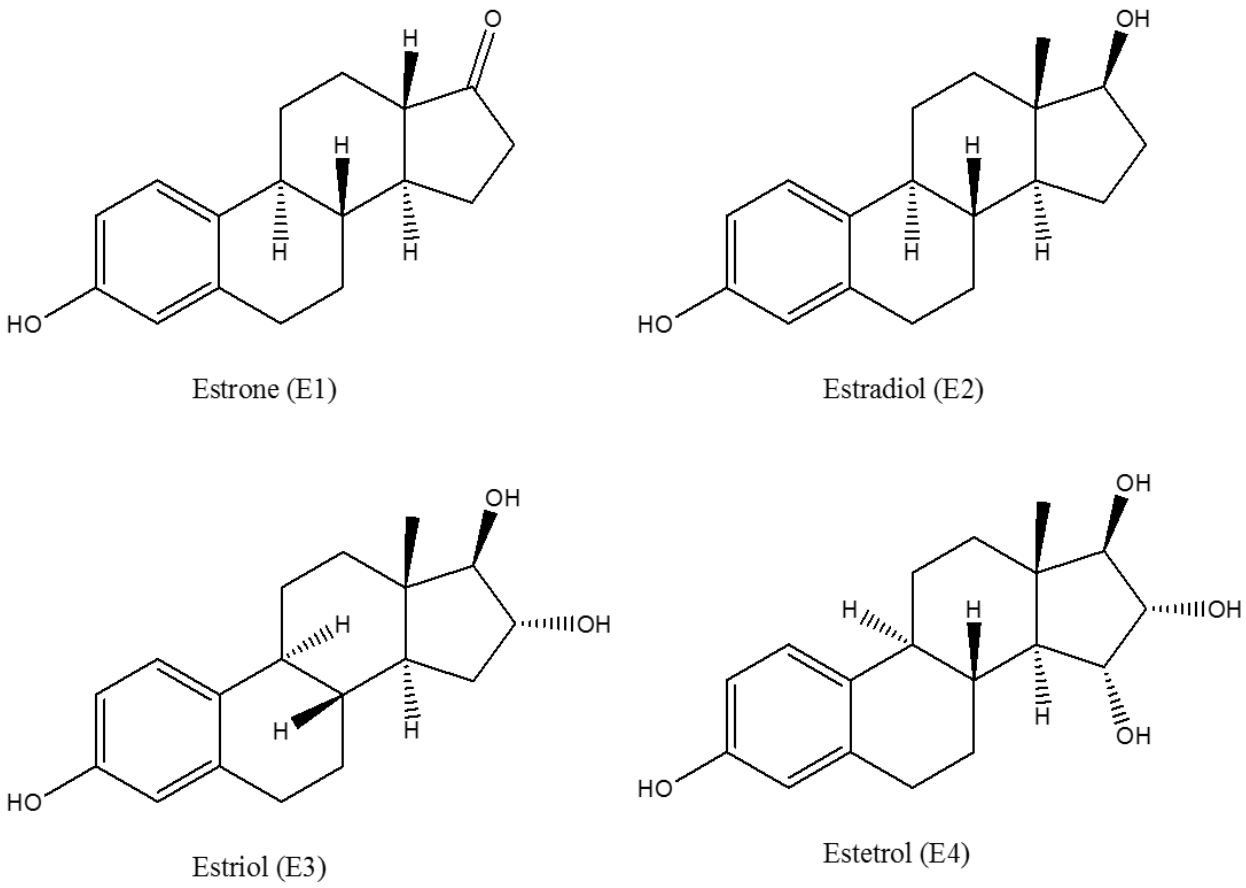

Figure 1.1. Chemical structures of endogenous estrogens: estrone (E1), estradiol (E2), estriol (E3), and estetrol (E4). There are three major endogenous estrogens E1, E2, and E3 present in women, while E4 is produced only during pregnancy.

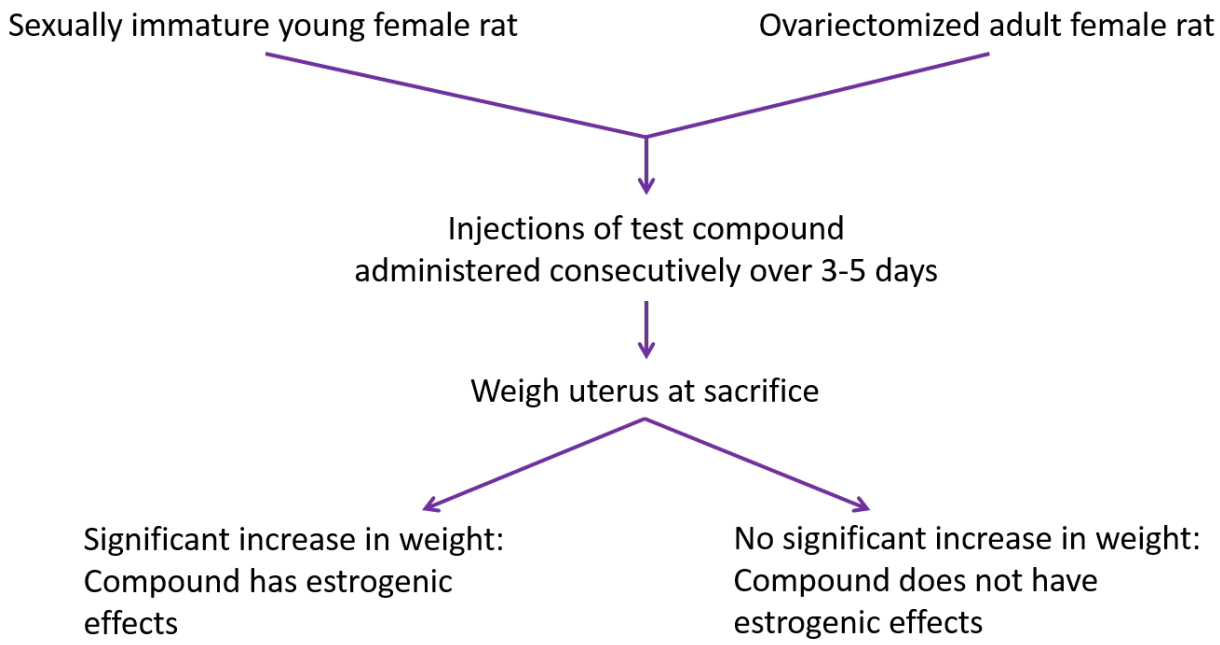

Figure 1.2. A schematic representation of the EPA's uterotrophic assay in rats.

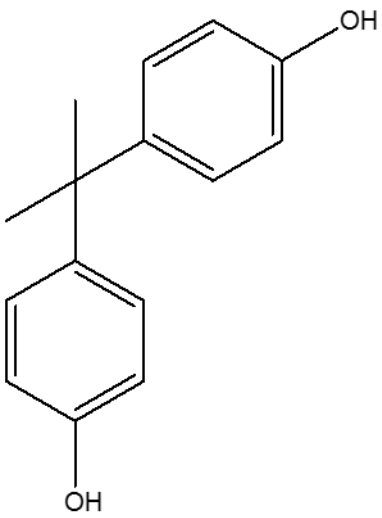

Bisphenol A (BPA)

Figure 1.3. Chemical structure of bisphenol A (BPA).

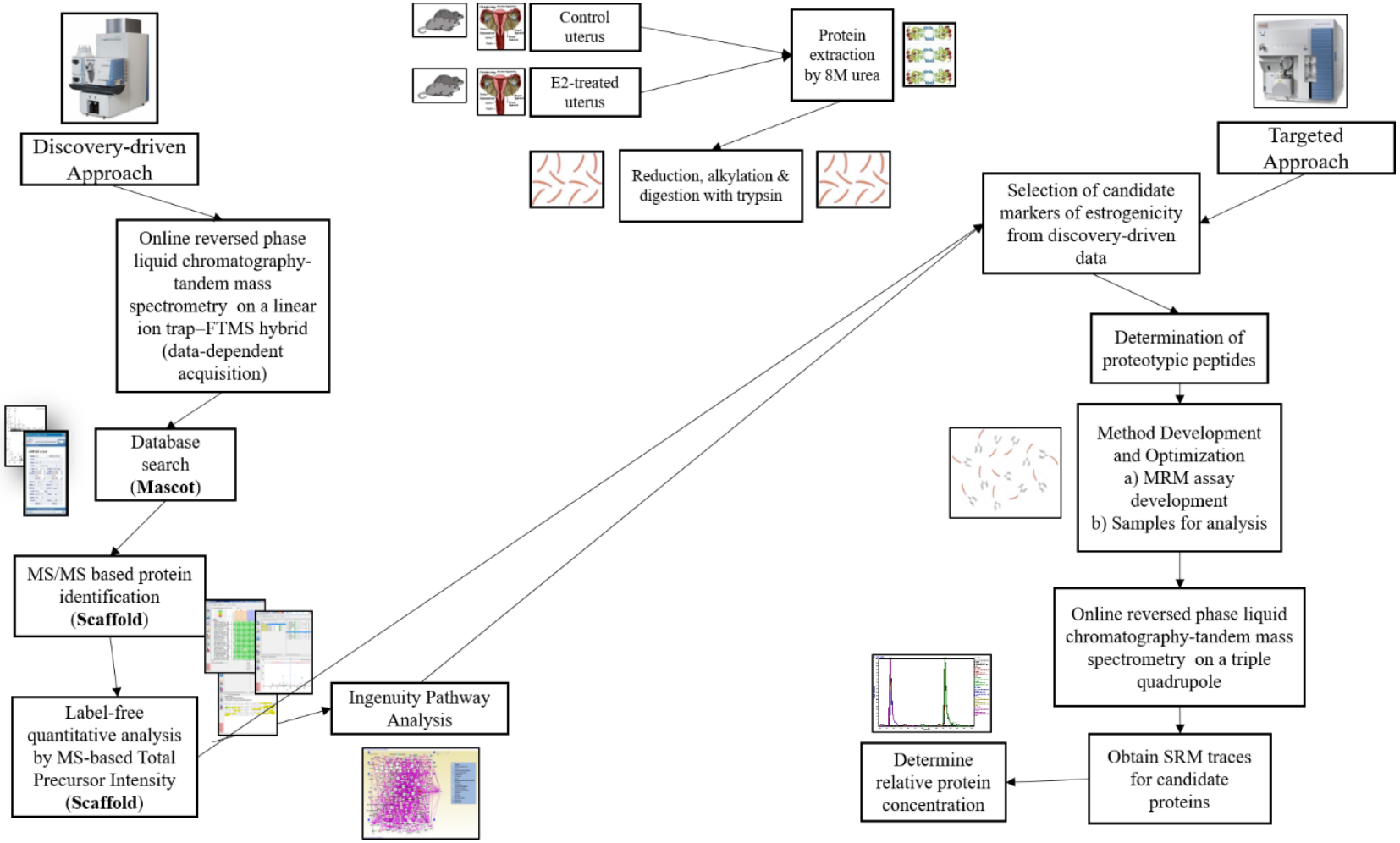

Figure 1.4. Quantitative proteomic methodologies. There are two branches of quantitative proteomics, untargeted and targeted analyses. The untargeted, discover-driven, approach aims to identify as many proteins as possible to gain the most comprehensive information. Information from untargeted studies directs targeted analyses, where protein hits also are validated.

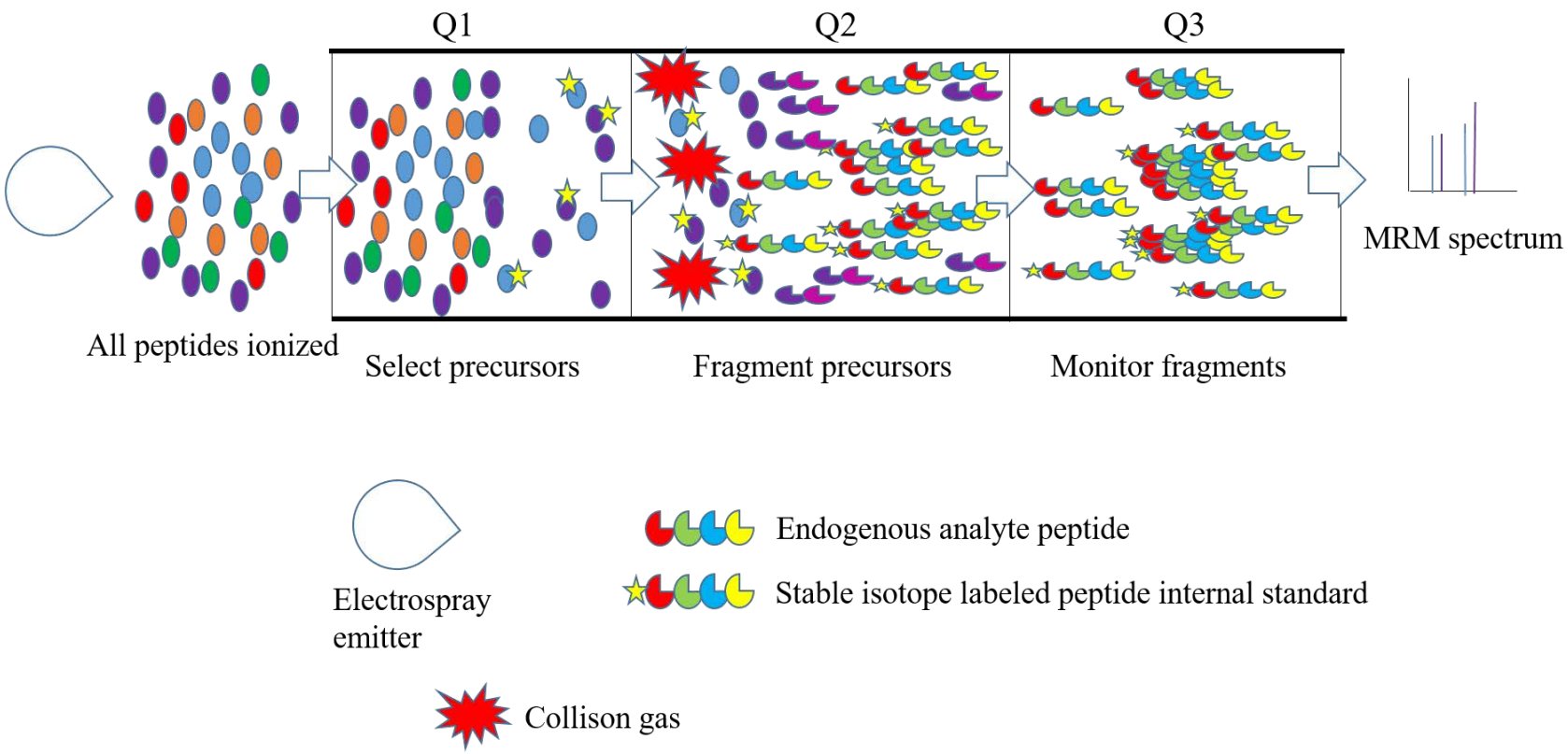

Figure 1.5. Schematic of a targeted multiple reaction monitoring (MRM) assay. In the LC-MS run, all ions are filtering in quadrupole 1 (Q1) from a predetermined set of precursors. Those that are selected move to quadrupole 2 (Q2), the collision cell, where ions are colliding with gas molecules and fragmented by CID. A predetermined set of fragments are filtered in quadrupole 3 (Q3) and detected, and MS/MS spectra are recorded. This scheme is inspired by and adapted from (90).

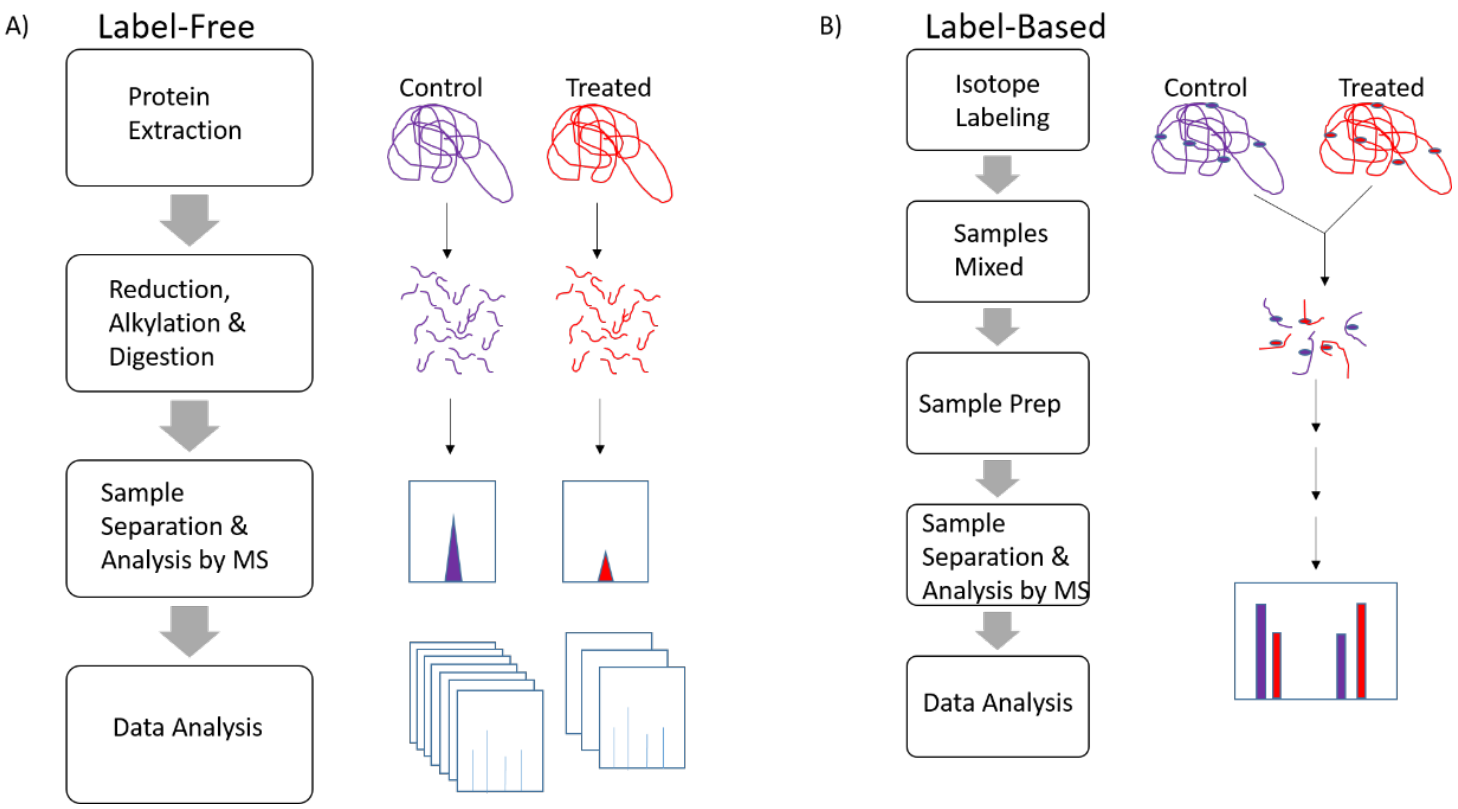

Figure 1.6. Label-free vs. label-based proteomics approaches. (A) In the label-free approach, each sample is processed individually and subjected to LC-MS/MS analysis followed by data analysis. (B) In the label-based approach, samples of different conditions are labeled with a specific isotope labeled molecule. After labeling, samples are combined and are processed together, followed by LC-MS/MS analysis and data analysis. This scheme is inspired by and adapted from (98).

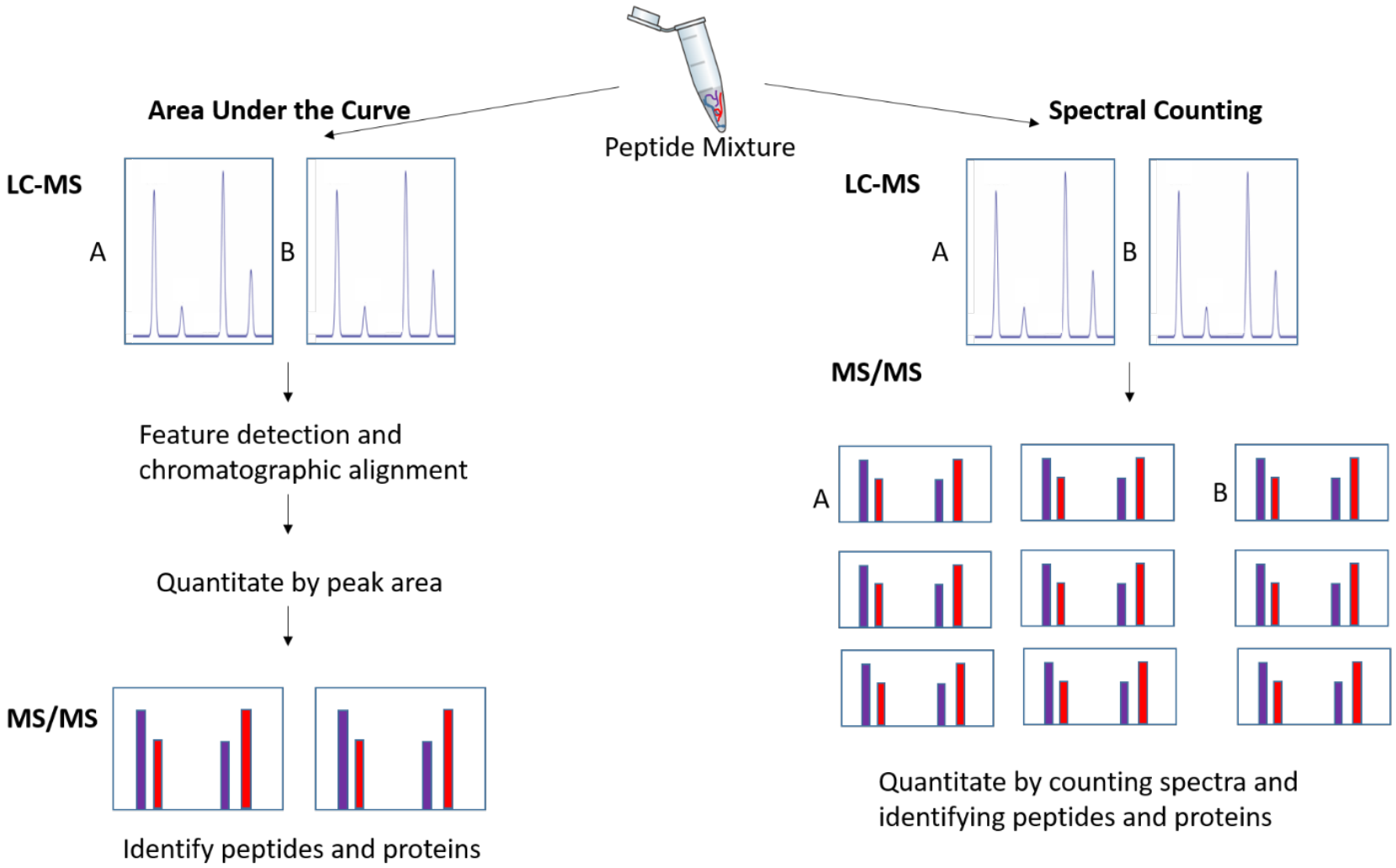

Figure 1.7. Schematic of the two major label-free quantitative approaches. In the LC-MS run, an ion is detected at a specific retention time and its intensity is recorded. The signal intensity has been observed to correlate with peptide abundance. Therefore,

quantifying the peptide, and associated protein, using the area under the curve (AUC) or precursor intensity measurement can be performed. The second approach to quantitation is known as spectral counting. This approach makes use of the sum of MS/MS spectra identified for a particular protein as a measure of protein abundance. These two commonly used label-free quantitative approaches are powerful tools in the analysis of differential protein expression in proteomics studies. This scheme is inspired by and adapted from (97).

REFERENCES

1. Vrtacnik, P.; Ostanek, B.; Mencej-Bedrac, S.; Marc, J., The many faces of estrogen signaling. *Biochem. Med.* **2014,** 24, (3), 329-342.

2. Korach, K. S., Selected biochemical actions of ovarian hormones. *Environ. Health Perspect.* **1981,** 38, 39-45.

3. Wall, E. H.; Hewitt, S. C.; Case, L. K.; Lin, C. Y.; Korach, K. S.; Teuscher, C., The role of genetics in estrogen responses: a critical piece of an intricate puzzle. *FASEB J.* **2014**.

4. Silberstein, S. D.; Merriam, G. R., Physiology of the menstrual cycle. *Cephalalgia* **2000,** 20, (3), 148-54.

5. Hirschberg, A. L., Sex hormones, appetite and eating behaviour in women. *Maturitas* **2012,** 71, (3), 248-56.

6. Diel, P., Tissue-specific estrogenic response and molecular mechanisms. *Toxicol. Lett.* **2002,** 127, (1-3), 217-24.

7. Vaananen, H. K.; Harkonen, P. L., Estrogen and bone metabolism. *Maturitas* **1996,** 23 Suppl, S65-9.

8. Tikkanen, M. J., Estrogens, progestins and lipid metabolism. *Maturitas* **1996,** 23 Suppl, S51-5.

9. Stachenfeld, N. S., Sex hormone effects on body fluid regulation. *Exerc. Sport Sci. Rev.* **2008,** 36, (3), 152-9.

10. Oosthuyse, T.; Bosch, A. N., Oestrogen's regulation of fat metabolism during exercise and gender specific effects. *Curr. Opin. Pharmacol.* **2012,** 12, (3), 363-71.

11. Toran-Allerand, C. D., Estrogen and the brain: beyond ER-alpha, ER-beta, and 17beta-estradiol. *Ann. N. Y. Acad. Sci.* **2005,** 1052, 136-44.

12. Losordo, D. W.; Isner, J. M., Estrogen and angiogenesis: A review. *Arterioscler. Thromb. Vasc. Biol.* **2001,** 21, (1), 6-12.

13. Liehr, J. G., Genotoxic effects of estrogens. *Mutat. Res.* **1990,** 238, (3), 269-76.

14. Carreau, S.; Bouraima-Lelong, H.; Delalande, C., Estrogen, a female hormone involved in spermatogenesis. *Adv. Med. Sci.* **2012,** 57, (1), 31-6.

15. Bondesson, M.; Hao, R.; Lin, C. Y.; Williams, C.; Gustafsson, J. A., Estrogen receptor signaling during vertebrate development. *Biochim. Biophys. Acta* **2014**.

16. Prokai, L.; Prokai-Tatrai, K.; Perjesi, P.; Simpkins, J. W., Mechanistic insights into the direct antioxidant effects of estrogens. *Drug Dev. Res.* **2005,** 66, (2), 118-125.

17. Prokai, L.; Simpkins, J. W., Structure-nongenomic neuroprotection relationship of estrogens and estrogen-derived compounds. *Pharmacol. Ther.* **2007,** 114, (1), 1-12.

18. Thomas, M. P.; Potter, B. V., The structural biology of oestrogen metabolism. *J. Steroid Biochem. Mol. Biol.* **2013,** 137, 27-49.

19. Holinka, C. F.; Diczfalusy, E.; Coelingh Bennink, H. J., Estetrol: a unique steroid in human pregnancy. *J. Steroid Biochem. Mol. Biol.* **2008,** 110, (1-2), 138-43.

20. Colborn, T.; vom Saal, F. S.; Soto, A. M., Developmental effects of endocrine-disrupting chemicals in wildlife and humans. *Environ. Health Perspect.* **1993,** 101, (5), 378-84.

21. United States Environmental Protection Agency, Research Plan for Endocrine Disruptors. In Feb 1998 EPA/600/R-98/087 ed.; Office of Research and Development, Ed. 1998.

22. United States Environmental Protection Agency Endocrine Disruptor Screening Program (EDSP). http://www.epa.gov/endo/ (Nov),

23. United States Environmental Protection Agency, Next Generation Risk Assessment: Incorporation of Recent Advances in Molecular, Computational, and Systems Biology. In Sept

2014 EPA/600/R-14/004 ed.; National Center for Environmental Assessment Office of Research and Development, Ed. 2014.

24. Baker, V. A., Endocrine disrupters--testing strategies to assess human hazard. *Toxicol. In Vitro* **2001,** 15, (4-5), 413-9.

25. Clode, S. A., Assessment of in vivo assays for endocrine disruption. *Best Pract. Res. Clin. Endocrinol. Metab.* **2006,** 20, (1), 35-43.

26. Gelbke, H. P.; Kayser, M.; Poole, A., OECD test strategies and methods for endocrine disruptors. *Toxicology* **2004,** 205, (1-2), 17-25.

27. Marty, M. S.; O'Connor, J. C., Key learnings from the Endocrine Disruptor Screening Program (EDSP) Tier 1 rodent uterotrophic and Hershberger assays. *Birth Defects Res. B Dev. Reprod. Toxicol.* **2014,** 101, (1), 63-79.

28. Owens, J. W.; Ashby, J., Critical review and evaluation of the uterotrophic bioassay for the identification of possible estrogen agonists and antagonists: in support of the validation of the OECD uterotrophic protocols for the laboratory rodent. Organisation for Economic Co-operation and Development. *Crit. Rev. Toxicol.* **2002,** 32, (6), 445-520.

29. O'Connor, J. C.; Cook, J. C.; Marty, M. S.; Davis, L. G.; Kaplan, A. M.; Carney, E. W., Evaluation of Tier I screening approaches for detecting endocrine-active compounds (EACs). *Crit. Rev. Toxicol.* **2002,** 32, (6), 521-549.

30. Yoon, K.; Kwack, S. J.; Kim, H. S.; Lee, B. M., Estrogenic endocrine-disrupting chemicals: molecular mechanisms of actions on putative human diseases. *J. Toxicol. Environ. Health B Crit. Rev.* **2014,** 17, (3), 127-74.

31. Kiyama, R.; Wada-Kiyama, Y., Estrogenic endocrine disruptors: Molecular mechanisms of action. *Environ. Int.* **2015,** 83, 11-40.

32. Tyler, C. R.; Jobling, S.; Sumpter, J. P., Endocrine disruption in wildlife: a critical review of the evidence. *Crit. Rev. Toxicol.* **1998,** 28, (4), 319-61.

33. Watanabe, H.; Suzuki, A.; Kobayashi, M.; Takahashi, E.; Itamoto, M.; Lubahn, D. B.; Handa, H.; Iguchi, T., Analysis of temporal changes in the expression of estrogen-regulated genes in the uterus. *J. Mol. Endocrinol.* **2003,** 30, (3), 347-358.

34. Watanabe, H.; Suzuki, A.; Mizutani, T.; Khono, S.; Lubahn, D. B.; Handa, H.; Iguchi, T., Genome-wide analysis of changes in early gene expression induced by oestrogen. *Genes Cells* **2002,** 7, (5), 497-507.

35. Bauersachs, S.; Mitko, K.; Ulbrich, S. E.; Blum, H.; Wolf, E., Transcriptome studies of bovine endometrium reveal molecular profiles characteristic for specific stages of estrous cycle and early pregnancy. *Exp. Clin. Endocrinol. Diabetes* **2008,** 116, (7), 371-384.

36. Zama, A. M.; Uzumcu, M., Epigenetic effects of endocrine-disrupting chemicals on female reproduction: an ovarian perspective. *Front. Neuroendocrinol.* **2010,** 31, (4), 420-439.

37. Spencer, T. E.; Dunlap, K. A.; Filant, J., Comparative developmental biology of the uterus: insights into mechanisms and developmental disruption. *Mol. Cell. Endocrinol.* **2012,** 354, (1-2), 34-53.

38. LaRocca, J.; Boyajian, A.; Brown, C.; Smith, S. D.; Hixon, M., Effects of in utero exposure to Bisphenol A or diethylstilbestrol on the adult male reproductive system. *Birth Defects Res. B Dev. Reprod. Toxicol.* **2011,** 92, (6), 526-533.

39. Sahambi, S. K.; Pelland, A.; Cooke, G. M.; Schrader, T.; Tardif, R.; Charbonneau, M.; Krishnan, K.; Haddad, S.; Cyr, D. G.; Devine, P. J., Oral p-tert-octylphenol exposures induce minimal toxic or estrogenic effects in adult female Sprague-Dawley rats. *J. Toxicol. Environ. Health A* **2010,** 73, (9), 607-622.

40. Seidlova-Wuttke, D.; Christoffel, J.; Rimoldi, G.; Jarry, H.; Wuttke, W., Comparison of effects of estradiol with those of octylmethoxycinnamate and 4-methylbenzylidene camphor on fat tissue, lipids and pituitary hormones. *Toxicol. Appl. Pharmacol.* **2006,** 214, (1), 1-7.

41. Rochester, J. R., Bisphenol A and human health: a review of the literature. *Reprod. Toxicol.* **2013,** 42, 132-55.

42. National Institute of Environmental Health Sciences Bisphenol A (BPA). https://www.niehs.nih.gov/health/topics/agents/sya-bpa/ (April 3),

43. Kitamura, S.; Suzuki, T.; Sanoh, S.; Kohta, R.; Jinno, N.; Sugihara, K.; Yoshihara, S.; Fujimoto, N.; Watanabe, H.; Ohta, S., Comparative study of the endocrine-disrupting activity of bisphenol A and 19 related compounds. *Toxicol. Sci.* **2005,** 84, (2), 249-59.

44. Ashby, J., Increasing the sensitivity of the rodent uterotrophic assay to estrogens, with particular reference to bisphenol A. *Environ. Health Perspect.* **2001,** 109, (11), 1091-4.

45. Bhandari, R. K.; Deem, S. L.; Holliday, D. K.; Jandegian, C. M.; Kassotis, C. D.; Nagel, S. C.; Tillitt, D. E.; Vom Saal, F. S.; Rosenfeld, C. S., Effects of the environmental estrogenic contaminants bisphenol A and 17alpha-ethinyl estradiol on sexual development and adult behaviors in aquatic wildlife species. *Gen. Comp. Endocrinol.* **2014**.

46. Kim, H. S.; Han, S. Y.; Yoo, S. D.; Lee, B. M.; Park, K. L., Potential estrogenic effects of bisphenol-A estimated by in vitro and in vivo combination assays. *J. Toxicol. Sci.* **2001,** 26, (3), 111-8.

47. Kim, H. S.; Kang, T. S.; Kang, I. H.; Kim, T. S.; Moon, H. J.; Kim, I. Y.; Ki, H.; Park, K. L.; Lee, B. M.; Yoo, S. D.; Han, S. Y., Validation study of OECD rodent uterotrophic assay for the assessment of estrogenic activity in Sprague-Dawley immature female rats. *J. Toxicol. Environ. Health A* **2005,** 68, (23-24), 2249-62.

48. Laws, S. C.; Carey, S. A.; Ferrell, J. M.; Bodman, G. J.; Cooper, R. L., Estrogenic activity of octylphenol, nonylphenol, bisphenol A and methoxychlor in rats. *Toxicol. Sci.* **2000,** 54, (1), 154-67.

49. Liao, C.; Kannan, K., Concentrations and profiles of bisphenol A and other bisphenol analogues in foodstuffs from the United States and their implications for human exposure. *J. Agric. Food. Chem.* **2013,** 61, (19), 4655-62.

50. Markey, C. M.; Michaelson, C. L.; Veson, E. C.; Sonnenschein, C.; Soto, A. M., The mouse uterotrophic assay: a reevaluation of its validity in assessing the estrogenicity of bisphenol A. *Environ. Health Perspect.* **2001,** 109, (1), 55-60.

51. Matthews, J. B.; Twomey, K.; Zacharewski, T. R., In vitro and in vivo interactions of bisphenol A and its metabolite, bisphenol A glucuronide, with estrogen receptors alpha and beta. *Chem. Res. Toxicol.* **2001,** 14, (2), 149-57.

52. Ohta, R.; Takagi, A.; Ohmukai, H.; Marumo, H.; Ono, A.; Matsushima, Y.; Inoue, T.; Ono, H.; Kanno, J., Ovariectomized mouse uterotrophic assay of 36 chemicals. *J. Toxicol. Sci.* **2012,** 37, (5), 879-89.

53. Tinwell, H.; Joiner, R.; Pate, I.; Soames, A.; Foster, J.; Ashby, J., Uterotrophic activity of bisphenol A in the immature mouse. *Regul. Toxicol. Pharmacol.* **2000,** 32, (1), 118-26.

54. Wu, M.; Xu, H.; Shen, Y.; Qiu, W.; Yang, M., Oxidative Stress in Zebrafish Embryos Induced by Short-Term Exposure to Bisphenol A, Nonylphenol, and their Mixture. *Environ. Toxicol. Chem.* **2011,** 30, (10), 2335-2341.

55. Yamasaki, K.; Sawaki, M.; Takatsuki, M., Immature rat uterotrophic assay of bisphenol A. *Environ. Health Perspect.* **2000,** 108, (12), 1147-50.

56. Yamasaki, K.; Takeyoshi, M.; Sawaki, M.; Imatanaka, N.; Shinoda, K.; Takatsuki, M., Immature rat uterotrophic assay of 18 chemicals and Hershberger assay of 30 chemicals. *Toxicology* **2003,** 183, (1-3), 93-115.

57. Yang, C. Z.; Yaniger, S. I.; Jordan, V. C.; Klein, D. J.; Bittner, G. D., Most plastic products release estrogenic chemicals: a potential health problem that can be solved. *Environ. Health Perspect.* **2011,** 119, (7), 989-96.

58. Prokai, L.; Stevens, S. M., Jr.; Rauniyar, N.; Nguyen, V., Rapid label-free identification of estrogen-induced differential protein expression in vivo from mouse brain and uterine tissue. *J. Proteome Res.* **2009,** 8, (8), 3862-71.

59. De Wit, M.; Keil, D.; van der Ven, K.; Vandamme, S.; Witters, E.; De Coen, W., An integrated transcriptomic and proteomic approach characterizing estrogenic and metabolic effects of 17 alpha-ethinylestradiol in zebrafish (Danio rerio). *Gen. Comp. Endocrinol.* **2010,** 167, (2), 190-201.

60. Kling, P.; Forlin, L., Proteomic studies in zebrafish liver cells exposed to the brominated flame retardants HBCD and TBBPA. *Ecotoxicol. Environ. Saf.* **2009,** 72, (7).

61. Biales, A. D.; Bencic, D. C.; Villeneuve, D. L.; Ankley, G. T.; Lattier, D. L., Proteomic analysis of zebrafish brain tissue following exposure to the pesticide prochloraz. *Aquat. Toxicol.* **2011,** 105, (3-4), 618-28.

62. Huang, Q.-Y.; Huang, H.-Q., Differential expression profile of membrane proteins in zebrafish (Danio rerio) brain exposed to methyl parathion. *Proteomics* **2011,** 11, (18).

63. Shrader, E. A.; Henry, T. R.; Greeley, M. S.; Bradley, B. P., Proteomics in zebrafish exposed to endocrine disrupting chemicals. *Ecotoxicology* **2003,** 12, (6), 485-488.

64. Abdullah, L.; Crynen, G.; Reed, J.; Bishop, A.; Phillips, J.; Ferguson, S.; Mouzon, B.; Mullan, M.; Mathura, V.; Mullan, M.; Ait-Ghezala, G.; Crawford, F., Proteomic CNS profile of delayed cognitive impairment in mice exposed to Gulf War agents. *Neuromolecular. Med.*. **2011,** 13, (4), 275-288.

65. Benninghoff, A., Toxicoproteomics--the next step in the evolution of environmental biomarkers. *Toxicol. Sci.* **2007,** 95, (1), 1-4.

66. Senapati, S.; Barnhart, K. T., Biomarkers for ectopic pregnancy and pregnancy of unknown location. *Fertil. Steril.* **2013,** 99, (4), 1107-1116.

67. Munoz, M.; Corrales, F. J.; Caamano, J. N.; Diez, C.; Trigal, B.; Mora, M. I.; Martin, D.; Carrocera, S.; Gomez, E., Proteome of the early embryo-maternal dialogue in the cattle uterus. *J. Proteome Res.* **2012,** 11, (2), 751-766.

68. Wang, T.; Zhou, R.; Zhang, L.; Wang, Y.; Song, C.; Lin, W.; Niu, X.; Lin, Y.; Hu, H., Proteins in leaked amniotic fluid as biomarkers diagnostic for prelabor rupture of membranes. *Proteomics Clin. Appl.* **2011,** 5, (7-8), 415-421.

69. Gemoll, T.; Habermann, J. K.; Lahmann, J.; Szymczak, S.; Lundgren, C.; Bundgen, N. K.; Jungbluth, T.; Nordstrom, B.; Becker, S.; Lomnytska, M. I.; Bruch, H. P.; Ziegler, A.; Hellman, U.; Auer, G.; Roblick, U. J.; Jornvall, H., Protein profiling of genomic instability in endometrial cancer. *Cell. Mol. Life Sci.* **2012,** 69, (2), 325-333.

70. Upadhyay, R. D.; Balasinor, N. H.; Kumar, A. V.; Sachdeva, G.; Parte, P.; Dumasia, K., Proteomics in reproductive biology: beacon for unraveling the molecular complexities. *Biochim. Biophys. Acta* **2013,** 1834, (1), 8-15.

71. Callegari, E. A., Shotgun Proteomics Analysis of Estrogen Effects in the Uterus Using Two-Dimensional Liquid Chromatography and Tandem Mass Spectrometry. *Methods Mol. Biol.* **2016,** 1366, 131-48.

72. Evans, G.; Sutton, E. L., Oral contraception. *Med. Clin. North Am.* **2015,** 99, (3), 479-503.

73. Bedani, F.; Schoenmakers, P. J.; Janssen, H. G., Theories to support method development in comprehensive two-dimensional liquid chromatography--a review. *J. Sep. Sci.* **2012,** 35, (14), 1697-711.

74. Aebersold, R.; Goodlett, D. R., Mass spectrometry in proteomics. *Chem. Rev.* **2001,** 101, (2), 269-95.

75. Aebersold, R.; Mann, M., Mass spectrometry-based proteomics. *Nature* **2003,** 422, (6928), 198-207.

76. Domon, B.; Aebersold, R., Mass spectrometry and protein analysis. *Science* **2006,** 312, (5771), 212-7.

77. Bantscheff, M.; Schirle, M.; Sweetman, G.; Rick, J.; Kuster, B., Quantitative mass spectrometry in proteomics: a critical review. *Anal. Bioanal. Chem.* **2007,** 389, (4), 1017-31.

78. Bantscheff, M.; Lemeer, S.; Savitski, M. M.; Kuster, B., Quantitative mass spectrometry in proteomics: critical review update from 2007 to the present. *Anal. Bioanal. Chem.* **2012,** 404, (4), 939-65.

79. Doerr, A., Mass spectrometry–based targeted proteomics. *Nat. Methods* **2013,** 10, (1), 23.

80. Wasinger, V. C.; Zeng, M.; Yau, Y., Current status and advances in quantitative proteomic mass spectrometry. *Int. J. Proteomics* **2013,** 2013, 180605.

81. Zhang, Y.; Fonslow, B. R.; Shan, B.; Baek, M. C.; Yates, J. R., 3rd, Protein analysis by shotgun/bottom-up proteomics. *Chem. Rev.* **2013,** 113, (4), 2343-2394.

82. Steen, H.; Mann, M., The ABC's (and XYZ's) of peptide sequencing. *Nat. Rev. Mol. Cell Biol.* **2004,** 5, (9), 699-711.

83. Bogdanov, B.; Smith, R. D., Proteomics by FTICR mass spectrometry: top down and bottom up. *Mass Spectrom. Rev.* **2005,** 24, (2), 168-200.

84. Mueller, L. N.; Brusniak, M. Y.; Mani, D. R.; Aebersold, R., An assessment of software solutions for the analysis of mass spectrometry based quantitative proteomics data. *J. Proteome Res.* **2008,** 7, (1), 51-61.

85. Ideker, T.; Galitski, T.; Hood, L., A new approach to decoding life: systems biology. *Annu. Rev. Genomics Hum. Genet.* **2001,** 2, 343-72.

86. Jacobs, A. T.; Marnett, L. J., Systems analysis of protein modification and cellular responses induced by electrophile stress. *Acc. Chem. Res.* **2010,** 43, (5), 673-683.

87. Bensimon, A.; Heck, A. J.; Aebersold, R., Mass spectrometry-based proteomics and network biology. *Annu. Rev. Biochem.* **2012,** 81, 379-405.

88. Method of the Year 2012. *Nat. Methods* **2013,** 10, (1), 1.

89. Marx, V., Targeted proteomics. *Nat. Methods* **2012,** 10, (1), 19-22.

90. Gillette, M. A.; Carr, S. A., Quantitative analysis of peptides and proteins in biomedicine by targeted mass spectrometry. *Nat. Methods* **2013,** 10, (1), 28-34.

91. Harlan, R.; Zhang, H., Targeted proteomics: a bridge between discovery and validation. *Expert Rev. Proteomics* **2014,** 11, (6), 657-61.

92. Boja, E. S.; Rodriguez, H., Mass spectrometry-based targeted quantitative proteomics: achieving sensitive and reproducible detection of proteins. *Proteomics* **2012,** 12, (8), 1093-1110.

93. Picotti, P.; Aebersold, R., Selected reaction monitoring-based proteomics: workflows, potential, pitfalls and future directions. *Nat. Methods* **2012,** 9, (6), 555-66.

94. Lange, V.; Picotti, P.; Domon, B.; Aebersold, R., Selected reaction monitoring for quantitative proteomics: a tutorial. *Mol. Syst. Biol.* **2008,** 4, 222.

95. Hathout, Y., Proteomic methods for biomarker discovery and validation. Are we there yet? *Expert Rev. Proteomics* **2015,** 12, (4), 329-31.

96. Villanueva, J.; Carrascal, M.; Abian, J., Isotope dilution mass spectrometry for absolute quantification in proteomics: concepts and strategies. *J. Proteomics* **2014,** 96, 184-99.

97. Neilson, K. A.; Ali, N. A.; Muralidharan, S.; Mirzaei, M.; Mariani, M.; Assadourian, G.; Lee, A.; van Sluyter, S. C.; Haynes, P. A., Less label, more free: approaches in label-free quantitative mass spectrometry. *Proteomics* **2011,** 11, (4), 535-53.

98. Zhu, W.; Smith, J. W.; Huang, C. M., Mass spectrometry-based label-free quantitative proteomics. *J. Biomed. Biotechnol.* **2010,** 2010, 840518.

CHAPTER II

UNTARGETED PROTEOMIC ANALYSIS OF ESTROGEN EFFECTS IN THE RAT UTERUS

INTRODUCTION

The uterus is the major target of E2's action. By using a "bottom-up" label-free discovery-driven proteomic method, a strategy for the quantitative survey of a complex proteome used previously in our lab, we seek to identify E2-regulated proteins on a global-scale in the rat uterus with the aim of elucidating the biological processes and networks impacted by E2. We will also develop a list of targets of E2's action to be used for targeted validation in further studies. The immediate goal will be to identify a focused panel of potential biomarker candidates for the evaluation of potential estrogenic compounds and thereby complementing the classical uterotrophic assay.

EXPERIMENTAL STRATEGY

Chemicals

HPLC grade solvents were all obtained from Fisher Scientific (Atlanta, GA). Sequencing grade trypsin was from Applied Biosystems (Foster City, CA). All other chemicals were acquired through Sigma-Aldrich (St. Louis, MO), unless otherwise stated.

Animals

Ovariectomized adult Sprague Dawley rats weighing 200−250 g were obtained from Charles Rivers Laboratories (Wilmington, DE, USA). Animals were kept under the standard 12 h light/12 h dark cycle, and the room temperature was maintained at 21 °C. Animals had full access to standard diet and water. Rats were treated according to institutional animal care and use guidelines.

Ovariectomy of the animals was done by their supplier (Charles River Laboratories, Wilmington, MA). The animals were shipped approximately one week after ovariectomy and were allowed to adapt in the animal facility of the University of North Texas Health Science Center for approximately two weeks before starting daily injections with the vehicle (corn oil, 60 µL per injection) control, or E2 (50 µg/kg body weight in corn oil vehicle) for 5 consecutive days between 10:00 a.m. and 12:00 a.m. The animals were sacrificed by cervical dislocation, decapitated, and their brains were removed. An abdominal incision was then made and the uterus was removed by cutting at the junction of the uterus and vagina and at the site of the ovariectomy on each horn. Excess fat and connective tissues were removed, and the organ was blotted and weighed. All tissues were stored at -80 °C until sample preparation and analysis.

Sample Preparation

Approximately one-tenth of the whole uterus (10 mg control and 50 mg E2-treated) was incubated in 200 µL of 8M urea for 30 minutes. The samples were centrifuged for 5 minutes at 1400x g and the supernatant was collected. Protein content of uterine extracts was determined by a microBCA assay (Bio-RAD, CA). Approximately 100 µg of protein from each sample was used for further processing. Samples were reduced with 1 mM dithiothreitol (DTT) for 30 minutes at 65°C to reduce the disulfide bonds. Carbamidomethylation of the thiol groups was performed by the addition of 5 mM iodoacetamide (IAA) and incubation for 30 minutes at room temperature in the dark. Excess IAA was quenched by the addition of DTT for 5 minutes. The samples were diluted with 50 mM ammonium bicarbonate to lower the urea concentration to less than 2M. Samples were digested with sequencing grade trypsin (1:50, Applied Biosystems, Foster City, CA) overnight. Following tryptic digestion, the enzymatic reaction was terminated by acidifying the samples to pH <2.0 with acetic acid and the digests were desalted using C18 Sep-Pak solid-phase extraction cartridges (Waters, Milford, MA). The desalted uterine tryptic digests were further dried with a SpeedVac and subsequently reconstituted in 20 µL of 5% (v/v) acetonitrile in water containing 0.1% (v/v) acetic acid and aliquots of 5 µL were used for LC-MS/MS analyses.

Data-dependent LC-MS/MS

The samples were analyzed in triplicate using a hybrid linear ion trap−Fourier transform ion cyclotron resonance (7-T) mass spectrometer (LTQ-FT, Thermo Scientific) equipped with a nano-electrospray ionization (ESI) source and operated with Xcalibur (version 2.2) and LTQ Tune Plus (version 2.2) data acquisition software. Online reversed-phase high performance

liquid chromatography (RP-HPLC) was performed with an Eksigent nano-LC-2D (Eksigent, Dublin, CA) system. An amount of 5 µL of the sample was automatically loaded onto the IntegraFrit™ sample trap (2.5 cm x 75 µm) (New Objective, Woburn, MA), for sample concentration and desalting, at a flow rate of 1.5 µl/min in a loading solvent containing 0.1% (v/v) acetic acid and 5% (v/v) acetonitrile in 94.9% (v/v) water prior to injection onto a reverse-phase column (NAN75-15-03-C18-PM; 75 µm i.d. x 15 cm, LC Packings, Sunnyvale, CA) packed with C18 beads (3 µm, 100 Å pore size, PepMap). Mobile-phase buffer A consisted of 0.1% (v/v) acetic acid and 99.9% (v/v) water, and mobile-phase buffer B consisted of 0.1% (v/v) acetic acid and 99.9% (v/v) acetonitrile. Following desalting and injection onto the analytical column, peptides were separated using the following gradient conditions: (1) 5 min in 95% solvent A for equilibration; (2) linear gradient to 40% solvent B over 90 min and holding at 40% solvent B for isocratic elution for 5 min; (3) increasing the gradient to 90% solvent B and maintaining for 5 min; and finally (4) 95% solvent A in the next 20 min. The flow rate through the column was 250 nL/min. Peptides eluted through a Picotip emitter (internal diameter 10 ± 1 µm; New Objective, Woburn, MA) and were directly sampled by the nano-electrospray source of the mass spectrometer. Spray voltage and capillary temperature during the gradient run were maintained at 2.0 kV and 250 ºC. Conventional data-dependent mode of acquisition was utilized in which an accurate m/z survey scan was performed in the FTICR cell followed by parallel MS/MS linear ion trap analysis of the top five most intense precursor ions. FTICR full-scan mass spectra were acquired at 50000 mass resolving power (m/z 400) from m/z 350 to 1500 using the automatic gain control mode of ion trapping. Peptide fragmentation was performed by collision-induced dissociation (CID) in the linear ion trap using a 3.0-Th isolation width and 35% normalized collision energy with helium as the target gas. The precursor ion that had been

selected for CID was dynamically excluded from further MS/MS analysis for 60 s. The raw data from these experiments have been deposited to the ProteomeXchange (1) with identifier PXD003906, which will be made available after publication of the results in a peer-reviewed paper.

Database Search, Label-free Relative Quantification, and Signaling Pathway Analysis

MS/MS data generated by data-dependent acquisitions were extracted by BioWorks version 3.3 and searched against a composite UniProt rat protein sequence database (release 2014_07, 41267 entries) (2) using the Mascot (version 2.2, Matrix Science) search algorithm within Proteome Discoverer (version 1.4, Thermo Scientific). The Proteome Discoverer application reverses all protein sequences to achieve a decoy database to search and calculates false discovery rates using the Percolator node. Mascot was searched with a fragment ion mass tolerance of 0.80 Da and a parent ion tolerance of 25.0 ppm assuming the digestion enzyme trypsin with the possibility of one missed cleavage. Carbamidomethylation of cysteine was specified as a fixed modification while oxidation of methionine and deamidation of asparagine and glutamine were specified as variable modifications in the database search.

The software program Scaffold (version 4.3.0, Proteome Software Inc, Portland, OR) was employed to validate MS/MS-based peptide and protein identifications. Peptide information was accepted if they could be established at greater than 95.0% probability as specified by the Peptide Prophet (3) algorithm. Protein identifications, where protein probabilities were assigned by the Protein Prophet (4), were accepted if they could be established at greater than 99.0% probability and contained at least two identified peptides.

Scaffold 4 readily extracts the MS-based peptide precursor ion abundance calculated from Proteome Discoverer's peak area quantitation for each identified peptide, and calculates the total precursor intensity for each protein. To test for significant changes in protein expression between treatments, the Student's *t*-test was performed on the normalized precursor intensity values and accepted at $p<0.05$ requiring at least a 1.5-fold change. Additionally, Ingenuity Pathway Analysis® (IPA®, QIAGEN Redwood City, CA) was utilized to derive annotations along with potential protein interaction networks from the associated proteins in the rat uterus.

RESULTS AND DISCUSSION

Discovery-driven proteomic analysis was performed using an adult ovariectomized female rat model, just as is described for use in testing EDCs using the EPA's uterotrophic assay (5, 6). As expected, the administration of E2 to these animals resulted in a visibly pronounced effect on the uterus. In addition to the apparent increase of wet weight in the uteri, we also measured the concentration of E2 in the uterus and serum, using a validated stable isotope dilution LC-MS/MS assay (7), to verify the extent of E2 exposure on the uterus (Table 2.1).

Here, we adapted a rapid tissue proteomics-based approach used previously (8) for a quantitative survey of the uterine proteome. Using the Mascot database search algorithm, 253 proteins passed rigorous validation criteria by both Peptide Prophet (3) and Protein Prophet (4) with at least two unique tryptic peptides identified for each protein. The complete list of identified proteins is provided in Supplemental Table 2.1.

For label-free quantification, we used an MS-based total precursor intensity based approach to detect quantitative differences as previously reported (9). Label-free quantitation

was performed using the MS-based precursor intensities rather than spectral counting or MS^2-TIC, which was previously shown to be best quantitative method comparing the different approaches (9). Spectral counting is a quantitative method which counts and compares the number of fragment spectra identifying peptides of any protein. MS^2-TIC considers the peak intensities from the MS/MS spectra combined with the counting of the spectra. MS-based precursor intensity measures and compares the MS signal intensity of the peptide precursor ions belonging to a protein. Using high resolution LC-MS, precursor intensity quantitation was shown to have a superior performance in terms of reproducibility, missing data, quantitative dynamic range, quantitative accuracy and biomarker discovery (9).

Using rigorous criteria for the evaluation of significant protein expression differences, 143 confidently identified proteins were markedly affected by E2 exposure, with 100 up-regulated and 43 down-regulated (Table 2.2 and 2.3). Several of the estrogen-regulated proteins, such as the vitamin D-dependent calcium-binding protein S100G and transglutaminase 2 (TGM2), have been previously reported from transcriptomic (10-12) studies. However, we show, for the first time, their regulation in the uterus *in vivo* using proteomics.

We used IPA® to find functional interactions between the up- and down-regulated proteins identified in our study. Of the 143 proteins significantly affected by E2, 139 were mapped across 9 networks. The networks could not be combined into one comprehensive and meaningful figure because of the limitations of the software program and the number of connections involved, and are shown individually (Figures 2.1-2.9). These networks show proteins that are associated with: 1) Cancer, organismal injury and abnormalities, immunological disease; 2) Cell death and survival, metabolic disease; 3) Cell morphology; 4) Free radical scavenging, organismal injury and abnormalities; 5) Cancer; 6) Carbohydrate metabolism, amino

acid metabolism, cell morphology; 7) Cell morphology, cellular assembly and organization, connective tissue disorders; 8) Organ morphology, inflammatory disease; and 9) Cellular movement, inflammatory response. A summary of the pathways and biological functions represented by the E2-regulated proteins is shown in Table 2.4. Identification of statistically significant pathways and networks involved will aid in the understanding of the impact E2 has on the uterus. Top pathways include metabolic pathways, as well as steroid signaling pathways and stress response pathways. IPA analysis not only revealed processes already recognized to be impacted by estrogen exposure, but also uncovered protein associations hitherto unknown at the proteome level and worthy of future pursuit as potential indicators of estrogenicity. One such protein was the transglutaminase 2 (TGM2), which is a crucial node shown in a network (Figure. 2.2).

Previously established E2-regulated proteins from transcriptomic (10-12) and proteomic (8) studies include but are not limited to the following proteins identified in this study: elongation factor 2, vitamin D-dependent calcium-binding protein S100G, transglutaminase 2, ATP synthase subunit alpha, glutathione S-transferase, selenium binding protein, lumican, GTP-binding nuclear protein Ran, retinol-binding protein 1, and macrophage-capping protein. Novel findings included dipeptidyl peptidase 2. These proteins will be further discussed as putative markers of estrogenicity worthy of targeted validation.

EF2 belongs to the GTP-binding translational elongation factor family. It is essential for protein synthesis, as it catalyzes the GTP-dependent ribosomal translocation step in translation. EF2 is a well-known up-regulated marker of estrogen exposure (8, 13, 14) shown previously in mouse uterus and cancer cells, and may play a critical role in E2 exerting its role as transcriptional regulator, as EF2 is an important checkpoint in transcriptional translation. EF2 is

activated upon E2 exposure, which could be explained by the need for an increase in proteins synthesized to keep up with demands of the growth of the organ. This is consistent with our discovery data showing the majority of proteins that are differentially regulated are activated.

S100G belongs to a family of calcium-binding proteins, and is also known as Calbindin-D9k. S100G mediates the transport of calcium. Shown to be activated by exposure to E2 via transcriptomic and western blot studies (15-19), S100G could play a role in the influx of Ca^{2+} ions to mediate signaling cascades involved in not only the growth of the organ, but possibly also with getting the uterus ready for carrying a pregnancy. S100G is a novel finding as it has not been shown previously *in vivo* using proteomics.

TGM2 is in a class of enzymes that catalyze the crosslinking of proteins by epsilon-gamma glutamyl lysine isopeptide bonds. TGM2 was shown to be activated in bovine uterus and mouse liver studies (12, 20). TGM2, while being involved in this Ca^{2+}-dependent transamidation of proteins, it is also involved in roles that are nonenzymatic and roles that are not Ca^{2+}-dependent. These additional roles include ATP and GTP hydrolysis, signal transduction through G-protein coupled receptors, as well as protein kinase, protein disulfide isomerase activities. In addition to all these enzymatic roles, TGM2 also has multiple interactions with protein scaffolds (21). Taken together, the many functions of TGM2, it potentially plays a critical role in remodeling the cytoskeletal structure and maintaining structural integrity, and variation in its abundance could contribute to the major morphological changes involved with the growth of the uterus upon E2 exposure. TGM2 is another novel finding as it has not been shown previously *in vivo* using proteomics, and is a significant finding given its importance in the protein interaction network.

ATP synthase subunit alpha forms the F_1 catalytic core, along with ATP synthase subunit beta, of the mitochondrial membrane ATP synthase. This is part of the complex (Complex V) that produces ATP from ADP in the presence of a proton gradient formed from the electron transport chain during the process of oxidative phosphorylation. Shown previously as activated upon E2 exposure (8, 22), the activation of ATP synthase is in line with the increased metabolic demand of the organ required for growth during normal conditions, but under endocrine disrupting conditions would be cause for stress in the cell.

Glutathione S-transferases are a family of enzymes that catalyze the conjugation of the reduced form of glutathione to xenobiotics for the purpose of detoxification. These have been shown to be repressed upon E2 exposure (8, 11). The loss of this protective enzyme leaves the cells vulnerable to the toxic effects of estrogen or its metabolites, and potentially exacerbates the stress the cell is under by amplifying the stress response.

Selenium binding protein 1, a protein that binds selenium, a trace elemental component of nonconventional amino acids selenocysteine and selenomethionine as well as selenoproteins, may be involved in the sensing of reactive xenobiotics in the cytoplasm, and may be involved in intra-Golgi protein transport (23-25). SBP1 expression has been shown to be down-regulated upon E2 exposure in the uterus via transcriptomics as well as in cancer cells (11, 26). Its role is not fully understood, however as a binding protein of selenium its role is important in maintaining the redox state of the cell in keeping free selenium concentrations low, as it is toxic to the cell in large amounts but necessary for the function of those antioxidant selenoproteins. E2 exposure, a stressor, could cause a shift in the redox state of the cell and could cause a loss in the protective function of SBP1. SBP1 is a novel finding as it has not been shown previously *in vivo* using proteomics.

Lumican belongs to the family of small leucine-rich proteoglycans. It is an extracellular matrix protein whose presence in the uterus varies depending on the hormonal levels during estrous cycle (27-29). As the E2 levels increase in the cycle, lumican levels are lower. This is in line with previous study that showed the repression of lumican upon E2 exposure (8), as well as the present study. As the uterus is remodeled and grows, this extracellular matrix "filler" is not needed and is removed and replaced with other protein scaffolding.

GTP-binding nuclear protein ran (RAN) is a GTP-binding protein involved in nucleocytoplasmic transport. It is required for the import of proteins into the nucleus and the export of RNA out to the cytoplasm. It is also involved in control of the cell cycle, as well as playing a role mitotic spindle formation during mitosis (2). It has been shown previously to be activated by estrogen action (10). Given the nature of the growing organ during estrogen stimulation, it makes sense that RAN activity would increase to allow for the cells to divide and help the organ grow. RAN is a novel finding as it has not been shown previously *in vivo* using proteomics.

Retinol binding protein 1 (RBP1) belongs to a family of enzymes that is involved in the intracellular transport of retinol, and it regulates the uptake and esterification of retinol and its bioavailability (2, 30). Given the importance of retinol (i.e., Vitamin A) and its involvement in cell growth and differentiation, this protein plays a significant role during the estrous cycle. Additionally, retinol binding proteins have been established as progesterone-induced proteins in the uterus (31, 32), which would correlate with its estrogen repression similar to its family member RBP4 (12, 22, 33). To our knowledge, RBP1 has not been shown as estrogen-regulated previously *in vivo* using proteomics.

Macrophage-capping protein (CAPG) is a calcium sensitive protein that reversibly blocks the barbed ends of actin filaments, as well as may play an important role in macrophage function (2). Through its interactions with actin, an increase in CAPG correlates with an increase in cell division and remodeling to meet the needs of the growing organ. Interestingly, one role of macrophages is in muscle repair, growth and regeneration, which is exactly what is going on throughout the estrous cycle—the building of the endometrium in preparation for a pregnancy and the subsequent tear-down during menstruation. CAPG, although shown to be regulated by estrogen *in vitro* using transcriptomics with cancer cells (34), it is a novel finding with regards to regulation by E2 exposure *in vivo* using proteomics.

Dipeptidyl peptidase 2 (DPP2) is an enzyme that plays an important role in the degradation of oligopeptides, preferentially tripeptides. It catalyzes the release of the N-terminal dipeptide Xaa-Yaa, where Yaa is Ala or Pro (2). DPP2, is a novel finding with regards to regulation by E2. The degradation of oligopeptides would not be the goal during the proliferation that the uterus is undergoing with organ growth, but rather the building up of proteins to support the growing organ, which would correlate with the repression of this protein to allow for uterine growth.

CONCLUSIONS

Using the rat uterus with a label-free proteomic approach, we were able to identify a number of proteins differentially regulated by E2 exposure. In addition to confirming the previously established estrogen regulation of a number of proteins, we showed for the first time *in vivo* using proteomics that proteins such as S100G and TGM2 were up-regulated by estrogen

exposure, findings which had been shown previously using transcriptomic approaches (10-12). Our studies also revealed novel estrogen-regulated proteins in the rat uterus, such as DDP2. Identification of statistically significant pathways and networks involved also will provide useful information to understand of estrogens' impact on the uterus. Specifically, metabolic, steroid signaling and stress response pathways were the top pathways revealed on proteome level in our study.

Table 2.1. Uterus wet weight, E2 content and serum E2 content given as average ± standard error. Measurements were performed according to a procedure reported previously by us in the literature (7, 35).

	Vehicle-treated Control	E2-treated
Uterine wet weight (mg)	81 ± 4.7	347 ± 14.6
Uterine E2 concentration (pg/g)	988 ± 146	4765 ± 312
Serum E2 concentration (pg/mL)	4.6 ± 0.3	525 ± 53

Table 2.2. Significantly up-regulated proteins identified by Mascot database search and MS-based Precursor Intensity feature generated in Scaffold 4 software comparing control rat uterus to E2-treated rat uterus. Minimum protein identification confidence: 99%, minimum peptide identification confidence: 95% requiring at least 2 peptides per protein. Student *t*-test was accepted at $p < 0.05$ with at least a 1.5-fold change. Total MS precursor intensities are given as average ± standard error.

Protein Name	Accession Number	Molecular Weight (kDa)	Student *t*-test ($p<0.05$)	Control Average Total MS Precursor Intensity	E2-treated Average Total MS Precursor Intensity
Protein S100-G	S100G_RAT	9 kDa	<0.001	U.E.	3.43E+07 ± 2.15E+06
Transglutaminase 2	Q9WVJ6_RAT	77 kDa	<0.001	U.E.	3.23E+07 ± 1.81E+06
Elongation factor 2	EF2_RAT	95 kDa	<0.001	U.E.	1.20E+07 ± 5.59E+05
6-phosphogluconate dehydrogenase, decarboxylating	6PGD_RAT	53 kDa	<0.001	U.E.	7.80E+06 ± 4.78E+05
Annexin A1	ANXA1_RAT	39 kDa	<0.001	U.E.	7.13E+06 ± 1.23E+06
Keratin, type I cytoskeletal 18	K1C18_RAT	48 kDa	<0.001	U.E.	6.57E+06 ± 6.09E+05
Rho GDP dissociation inhibitor (GDI) beta	Q5M860_RAT	23 kDa	<0.001	U.E.	6.28E+06 ± 1.35E+06
Protein LOC679816	G3V9A3_RAT Q5EBB0_RAT	28 kDa	<0.001	U.E.	6.08E+06 ± 7.64E+05
Lactoperoxidase (Predicted)	D4A400_RAT	78 kDa	0.003	U.E.	5.97E+06 ± 2.05E+06

Acyl-CoA-binding protein	ACBP_RAT M0RDC5_RAT	10 kDa	<0.001	U.E.	5.84E+06 ± 9.47E+05
Ezrin	EZRI_RAT	69 kDa	<0.001	U.E.	5.83E+06 ± 4.88E+05
Nucleoside diphosphate kinase B	NDKB_RAT	17 kDa	<0.001	U.E.	5.46E+06 ± 7.11E+05
Tubulin beta-2A chain	TBB2A_RAT TBB2B_RAT	50 kDa	0.031	U.E.	5.33E+06 ± 2.76E+06
Lamin A, isoform CRA_b	G3V8L3_RAT	74 kDa	<0.001	U.E.	4.21E+06 ± 9.03E+05
Macrophage-capping protein	CAPG_RAT	39 kDa	<0.001	U.E.	3.41E+06 ± 4.34E+05
CArG-binding factor A	Q9QX80_RAT Q9QX81_RAT	31 kDa	<0.001	U.E.	3.09E+06 ± 1.80E+05
Protein Naca	M0R9L0_RAT	220 kDa	<0.001	U.E.	2.82E+06 ± 6.85E+05
Polypyrimidine tract binding protein 1, isoform CRA_c	D3ZB30_RAT F1M18_RAT PTBP1_RAT	57 kDa	<0.001	U.E.	2.75E+06 ± 2.86E+05
Alpha-1B-glycoprotein	A1BG_RAT	56 kDa	0.028	U.E.	2.62E+06 ± 1.32E+06
Citrate synthase	G3V936_RAT	52 kDa	0.001	U.E.	2.48E+06 ± 6.80E+05

Peptidyl-prolyl cis-trans isomerase B	PPIB_RAT	24 kDa	<0.001	U.E.	2.26E+06 ± 4.92E+05
Eukaryotic translation elongation factor 1 beta 2	B5DEN5_RAT	25 kDa	0.009	U.E.	2.03E+06 ± 8.25E+05
GTP-binding nuclear protein Ran	RAN_RAT	24 kDa	<0.001	U.E.	1.96E+06 ± 2.23E+05
14-3-3 protein eta	1433F_RAT	28 kDa	0.001	U.E.	1.76E+06 ± 5.06E+05
40S ribosomal protein S7	RS7_RAT	22 kDa	0.001	U.E.	1.74E+06 ± 5.03E+05
Heat shock 70 kDa protein 4	F1LRV4_RAT HSP74_RAT	94 kDa	<0.001	U.E.	1.49E+06 ± 1.85E+05
ATP synthase subunit alpha, mitochondrial	ATPA_RAT F1LP05_RAT	60 kDa	0.001	U.E.	1.47E+06 ± 4.34E+05
Serine/threonine-protein phosphatase PP1-alpha catalytic subunit	PP1A_RAT PP1B_RAT PP1G_RAT	38 kDa	<0.001	U.E.	1.40E+06 ± 1.39E+05
Sulfated glycoprotein 1	F7EPE0_RAT SAP_RAT	62 kDa	<0.001	U.E.	1.35E+06 ± 3.67E+05
60S ribosomal protein L12	RL12_RAT	18 kDa	<0.001	U.E.	1.13E+06 ± 2.51E+05

Calumenin	G3V6S3_RAT	37 kDa	0.048	U.E.	9.71E+05 ± 5.56E+05
PYD and CARD domain containing	G3V8L1_RAT	22 kDa	0.009	U.E.	8.50E+05 ± 3.45E+05
Cytosolic non-specific dipeptidase	CNDP2_RAT	53 kDa	<0.001	U.E.	8.13E+05 ± 1.72E+05
Isoform 2 of Fibrinogen beta chain	FIBB_RAT	57 kDa	0.019	U.E.	7.50E+05 ± 3.51E+05
Protein Tln1	G3V852_RAT	270 kDa	0.014	U.E.	7.26E+05 ± 3.21E+05
Guanine nucleotide-binding protein subunit beta-2-like 1	GBLP_RAT	35 kDa	0.005	U.E.	6.87E+05 ± 2.53E+05
60S acidic ribosomal protein P0	RLA0_RAT	34 kDa	0.004	U.E.	6.53E+05 ± 2.35E+05
Protein Ppp2r1a	Q5XI34_RAT	65 kDa	0.008	U.E.	6.29E+05 ± 2.54E+05
Protein Itih4	D3ZFC6_RAT Q5EBC0_RAT	103 kDa	<0.001	U.E.	6.13E+05 ± 1.19E+05
Basic transcription factor 3	Q5U3Y8_RAT	18 kDa	0.029	U.E.	5.17E+05 ± 2.63E+05
Ribonuclease inhibitor	E2RUH2_RAT	50 kDa	0.031	U.E.	4.72E+05 ± 2.44E+05
Phosphoglucomutase-1	PGM1_RAT Q499Q4_RAT	61 kDa	0.017	U.E.	4.16E+05 ± 1.89E+05
Protein Susd2	D3ZEV8_RAT	90 kDa	0.028	U.E.	2.61E+05 ± 1.32E+05

L-lactate dehydrogenase A chain	LDHA_RAT	36 kDa	<0.001	2.09E+05 ± 1.12E+05	2.94E+07 ± 2.81E+06
Keratin complex 2, basic, gene 7, isoform CRA_a	G3V712_RAT	51 kDa	<0.001	1.07E+05 ± 1.07E+05	1.51E+07 ± 1.23E+06
Keratin, type I cytoskeletal 19	K1C19_RAT	45 kDa	<0.001	5.99E+05 ± 3.01E+05	4.98E+07 ± 1.76E+06
Serine (Or cysteine) proteinase inhibitor, clade H, member 1, isoform CRA_b	Q5RJR9_RAT	47 kDa	<0.001	2.86E+05 ± 1.89E+05	1.56E+07 ± 1.12E+06
Histone H2B	D3ZNH4_RAT D3ZWM5_RAT D4A817_RAT G3V8B3_RAT G3V9C7_RAT H2B1_RAT M0R4L7_RAT	15 kDa	<0.001	3.79E+05 ± 3.79E+05	1.79E+07 ± 3.30E+06
Elongation factor 1-alpha 1	EF1A1_RAT M0R757_RAT	50 kDa	<0.001	1.23E+06 ± 1.17E+06	5.48E+07 ± 5.20E+06
Alpha-2 antiplasmin	Q80ZA3_RAT	46 kDa	<0.001	3.29E+04 ± 3.29E+04	1.37E+06 ± 1.06E+05

Adenylyl cyclase-associated protein 1	CAP1_RAT	52 kDa	<0.001	8.40E+04 ± 8.40E+04	3.07E+06 ± 5.79E+05
Phosphoglycerate kinase 1	PGK1_RAT	45 kDa	<0.001	2.79E+05 ± 2.79E+05	8.13E+06 ± 1.57E+06
Isoform M2 of Pyruvate kinase PKM	KPYM_RAT	58 kDa	<0.001	1.93E+06 ± 9.83E+05	2.85E+07 ± 3.72E+06
Transitional endoplasmic reticulum ATPase	TERA_RAT	89 kDa	<0.001	3.71E+05 ± 1.67E+05	5.09E+06 ± 5.04E+05
Keratin, type II cytoskeletal 8	K2C8_RAT	54 kDa	<0.001	3.30E+06 ± 9.22E+05	3.98E+07 ± 4.44E+05
Desmin	Q6P725_RAT	53 kDa	<0.001	1.27E+07 ± 1.83E+06	1.41E+08 ± 9.81E+06
Protein Pkn3	D3ZC07_RAT D4ADL2_RAT SET_RAT	107 kDa	0.027	8.71E+04 ± 8.71E+04	8.11E+05 ± 3.38E+05
Endoplasmin	ENPL_RAT	93 kDa	<0.001	1.19E+06 ± 6.48E+05	1.09E+07 ± 8.82E+05
Lambda-crystallin homolog	CRYL1_RAT	35 kDa	0.017	1.67E+05 ± 1.11E+05	1.52E+06 ± 5.95E+05
Complement C3	M0RBF1_RAT	186 kDa	<0.001	3.63E+06 ± 1.16E+06	2.89E+07 ± 1.52E+06
Lymphocyte cytosolic protein 1	Q5XI38_RAT	70 kDa	<0.001	7.48E+05 ± 3.10E+05	5.87E+06 ± 4.28E+05
Eukaryotic translation initiation factor 4A1	Q6P3V8_RAT	46 kDa	0.002	1.43E+05 ± 9.48E+04	1.11E+06 ± 2.70E+05

Glucose-6-phosphate isomerase	G6PI_RAT	63 kDa	<0.001	1.54E+06 ± 7.02E+05	1.08E+07 ± 1.36E+06
Eukaryotic translation initiation factor 5A2 (Predicted)	G3V7J7_RAT IF5A1_RAT	17 kDa	<0.001	8.74E+05 ± 5.84E+05	5.77E+06 ± 8.74E+05
Protein disulfide-isomerase A6	PDIA6_RAT	48 kDa	0.001	9.44E+05 ± 4.38E+05	6.09E+06 ± 1.31E+06
Tubulin alpha-1B chain	TBA1B_RAT	50 kDa	<0.001	1.32E+06 ± 4.55E+05	8.21E+06 ± 5.09E+05
Ab2-417	Q7TMC7_RAT TRFE_RAT	107 kDa	<0.001	1.67E+06 ± 5.07E+05	9.53E+06 ± 5.59E+05
Calponin-1	CNN1_RAT	33 kDa	<0.001	6.77E+06 ± 1.63E+06	3.47E+07 ± 5.10E+06
Fructose-bisphosphate aldolase A	ALDOA_RAT	39 kDa	0.002	8.05E+05 ± 4.06E+05	3.84E+06 ± 7.65E+05
Heat shock protein HSP 90-alpha	HS90A_RAT	85 kDa	0.001	2.78E+06 ± 1.71E+06	1.32E+07 ± 1.27E+06
Protein disulfide-isomerase	PDIA1_RAT	57 kDa	<0.001	5.55E+06 ± 1.57E+06	2.52E+07 ± 2.21E+06
Protein disulfide-isomerase A3	PDIA3_RAT	57 kDa	<0.001	5.57E+06 ± 1.31E+06	2.48E+07 ± 2.45E+06
Group specific component	Q68FY4_RAT	54 kDa	<0.001	4.18E+06 ± 1.37E+06	1.61E+07 ± 1.89E+06
Prolargin	PRELP_RAT	43 kDa	<0.001	2.77E+06 ± 1.00E+06	1.00E+07 ± 7.85E+05
Histone H2A	D3ZVK7_RAT	14 kDa	<0.001	3.78E+06 ± 1.07E+06	1.36E+07 ± 9.71E+05

	D4ACV3_RAT				
	G3V9C0_RAT				
	H2A1C_RAT				
	H2A1E_RAT				
	H2A1F_RAT				
	H2A1_RAT				
	H2A2A_RAT				
	H2A3_RAT				
	H2A4_RAT				
	H2AJ_RAT				
	M0RCL5_RAT				
	M0RDM4_RAT				
	Q6I8Q6_RAT				
Glyceraldehyde-3-phosphate dehydrogenase	G3P_RAT	36 kDa	<0.001	1.63E+07 ± 2.53E+06	5.83E+07 ± 5.26E+06
Malate dehydrogenase, mitochondrial	MDHM_RAT	36 kDa	<0.001	1.16E+07 ± 3.28E+06	3.97E+07 ± 1.82E+06

60 kDa heat shock protein, mitochondrial	CH60_RAT	61 kDa	0.048	7.23E+05 ± 5.35E+05	2.47E+06 ± 5.53E+05
Rab GDP dissociation inhibitor beta	GDIB_RAT	51 kDa	<0.001	2.65E+06 ± 7.80E+05	8.82E+06 ± 3.46E+05
Superoxide dismutase [Cu-Zn]	SODC_RAT	16 kDa	0.001	2.38E+06 ± 3.69E+05	7.81E+06 ± 1.40E+06
Rho GDP-dissociation inhibitor 1	GDIR1_RAT	23 kDa	<0.001	6.32E+06 ± 2.15E+06	2.07E+07 ± 1.37E+06
Cathepsin B	CATB_RAT Q6IN22_RAT	37 kDa	0.010	2.66E+06 ± 1.28E+06	8.52E+06 ± 1.38E+06
Cofilin-1	COF1_RAT	19 kDa	<0.001	8.05E+06 ± 1.87E+06	2.54E+07 ± 1.52E+06
Peptidyl-prolyl cis-trans isomerase FKBP1A	FKB1A_RAT	12 kDa	0.005	1.42E+06 ± 5.09E+05	4.42E+06 ± 7.82E+05
Tubulin beta-5 chain	TBB5_RAT	50 kDa	0.001	4.49E+06 ± 1.09E+06	1.37E+07 ± 2.27E+06
78 kDa glucose-regulated protein	GRP78_RAT	72 kDa	<0.001	1.27E+07 ± 2.36E+06	3.87E+07 ± 3.39E+06
Heat shock 70 kDa protein 1A/1B	HSP71_RAT	70 kDa	<0.001	5.78E+06 ± 1.02E+06	1.74E+07 ± 2.36E+06
Alpha-1-macroglobulin	A1M_RAT	167 kDa	0.004	2.85E+06 ± 8.31E+05	8.27E+06 ± 1.50E+06
Peroxiredoxin-1	PRDX1_RAT	22 kDa	0.003	5.65E+06 ± 1.63E+06	1.47E+07 ± 1.70E+06
Annexin A5	ANXA5_RAT Q66HH8_RAT	36 kDa	<0.001	7.76E+06 ± 1.66E+06	1.99E+07 ± 1.73E+06

Profilin-1	PROF1_RAT	15 kDa	<0.001	2.30E+07 ± 4.08E+06	5.81E+07 ± 1.98E+06
Transgelin	TAGL_RAT	23 kDa	<0.001	1.24E+08 ± 1.40E+07	2.96E+08 ± 1.78E+07
Heat shock protein HSP 90-beta	HS90B_RAT	83 kDa	0.002	1.05E+07 ± 2.77E+06	2.48E+07 ± 1.94E+06
Serum albumin	ALBU_RAT	69 kDa	<0.001	1.66E+09 ± 2.74E+08	3.81E+09 ± 6.62E+07
Vinculin	R9PXU6_RAT VINC_RAT	117 kDa	0.010	7.80E+06 ± 2.55E+06	1.77E+07 ± 1.19E+06
Transketolase	G3V826_RAT TKT_RAT	71 kDa	<0.001	3.31E+06 ± 5.76E+05	7.12E+06 ± 4.37E+05
Heat shock cognate 71 kDa protein	HSP7C_RAT	71 kDa	<0.001	4.36E+07 ± 7.05E+06	9.23E+07 ± 2.52E+06
Calreticulin	CALR_RAT	48 kDa	0.036	8.92E+06 ± 2.97E+06	1.84E+07 ± 2.08E+06
Destrin	DEST_RAT	19 kDa	0.044	7.56E+06 ± 2.49E+06	1.52E+07 ± 1.81E+06
Actin, cytoplasmic 1	ACTB_RAT ACTG_RAT V9GZ85_RAT	42 kDa	<0.001	3.82E+08 ± 4.20E+07	6.86E+08 ± 3.11E+07

U.E. – Unique to E2-treated i.e., not detected in control

Table 2.3. Significantly down-regulated proteins identified by Mascot database search and MS-based Precursor Intensity feature generated in Scaffold 4 software comparing control rat uterus to E2-treated rat uterus. Minimum protein identification confidence: 99%, minimum peptide identification confidence: 95% requiring at least 2 peptides per protein. Student *t*-test was accepted at $p < 0.05$ with at least a 1.5-fold change. Total MS TIC are given as average ± standard error.

Protein Name	Accession Number	Molecular Weight (kDa)	Student *t*-test ($p<0.05$)	Control Average Total MS Precursor Intensity	E2-treated Average Total MS Precursor Intensity
Selenium binding Protein 1	F1LRJ9_RAT SBP1_RAT	52 kDa	<0.001	1.28E+07 ± 2.01E+06	U.C.
Barrier-to-autointegration factor	BAF_RAT	10 kDa	<0.001	1.22E+07 ± 1.12E+06	U.C.
C-reactive protein	CRP_RAT	25 kDa	0.032	5.08E+06 ± 1.71E+06	U.C.
Keratin, type II cytoskeletal 1	K2C1_RAT	65 kDa	0.002	4.38E+06 ± 8.91E+05	U.C.
Retinol-binding protein 1	RET1_RAT	16 kDa	<0.001	3.47E+06 ± 5.02E+05	U.C.
Serine/arginine-rich splicing factor 2	SRSF2_RAT	25 kDa	0.029	1.43E+06 ± 4.67E+05	U.C.
Carbonic anhydrase 2	CAH2_RAT	29 kDa	0.008	4.47E+06 ± 1.13E+06	5.84E+04 ± 5.84E+04
Carboxylesterase 1C	D3ZGK7_RAT EST1C_RAT	60 kDa	0.032	4.91E+06 ± 1.62E+06	7.85E+04 ± 7.85E+04
Dipeptidyl peptidase 2	DPP2_RAT	55 kDa	0.003	3.93E+06 ± 8.57E+05	6.89E+04 ± 6.89E+04

Dermatopontin (Predicted), isoform CRA_c	D4A9H2_RAT	20 kDa	0.001	3.53E+07 ± 6.02E+06	1.76E+06 ± 8.33E+05
Glutathione S-transferase P	GSTP1_RAT	23 kDa	0.007	8.52E+07 ± 2.04E+07	4.74E+06 ± 5.29E+05
Keratin, type II cytoskeletal 6A	K2C6A_RAT	59 kDa	0.008	6.60E+06 ± 1.58E+06	3.82E+05 ± 2.68E+05
Phosphatidylethanolamine-binding protein 1	PEBP1_RAT	21 kDa	0.001	6.86E+07 ± 1.20E+07	4.62E+06 ± 6.13E+05
Protein Srsf7	D4A720_RAT	27 kDa	0.018	4.48E+06 ± 1.20E+06	3.58E+05 ± 3.58E+05
Carbonic anhydrase 3	CAH3_RAT	29 kDa	0.043	1.61E+07 ± 5.27E+06	1.40E+06 ± 8.92E+05
Nuclear transport factor 2	NTF2_RAT	14 kDa	0.015	5.69E+06 ± 1.48E+06	4.93E+05 ± 1.78E+05
Lumican	LUM_RAT	38 kDa	0.001	3.66E+08 ± 6.04E+07	3.49E+07 ± 3.66E+06
SH3 domain-binding glutamic acid-rich-like protein	B5DFD8_RAT	13 kDa	0.001	2.98E+07 ± 4.95E+06	3.04E+06 ± 6.08E+05
Glutathione S-transferase Mu 2	GSTM2_RAT	26 kDa	0.001	1.29E+07 ± 2.31E+06	1.38E+06 ± 1.10E+05
Glyoxalase domain-containing protein 4	GLOD4_RAT	33 kDa	<0.001	4.12E+06 ± 5.09E+05	4.73E+05 ± 1.52E+05
Alpha-2-HS-glycoprotein	FETUA_RAT	38 kDa	0.002	1.39E+08 ± 2.48E+07	1.81E+07 ± 2.31E+06
Complement factor D	CFAD_RAT	28 kDa	0.041	3.50E+06 ± 1.04E+06	5.09E+05 ± 3.27E+05

	G3V7H3_RAT				
Serine protease inhibitor A3K	SPA3K_RAT	47 kDa	0.047	1.85E+07 ± 5.64E+06	3.13E+06 ± 2.75E+05
Hemoglobin subunit beta-2	HBB2_RAT	16 kDa	0.001	6.15E+08 ± 8.80E+07	1.12E+08 ± 3.70E+07
Hemoglobin subunit beta-1	HBB1_RAT	16 kDa	<0.001	1.01E+09 ± 7.13E+07	1.90E+08 ± 6.04E+07
Microfibrillar-associated protein 4	D4A7W8_RAT G3V6A9_RAT	29 kDa	0.033	2.16E+07 ± 5.84E+06	4.36E+06 ± 4.07E+05
Cathepsin D	CATD_RAT Q6P6T6_RAT	45 kDa	0.019	8.74E+06 ± 2.07E+06	1.80E+06 ± 4.71E+05
Apolipoprotein E	APOE_RAT	36 kDa	0.010	1.42E+07 ± 2.72E+06	3.35E+06 ± 1.40E+06
Alpha-1-antiproteinase	A1AT_RAT	46 kDa	0.042	5.06E+07 ± 1.34E+07	1.26E+07 ± 3.62E+06
Hemoglobin subunit alpha-1/2	HBA_RAT	15 kDa	0.002	8.81E+08 ± 1.19E+08	2.55E+08 ± 8.18E+07
Gamma-enolase	ENOG_RAT	47 kDa	0.021	1.20E+07 ± 2.15E+06	3.51E+06 ± 2.22E+06
Peroxiredoxin-5, mitochondrial (Fragment)	D3ZEN5_RAT PRDX5_RAT	17 kDa	0.003	5.89E+06 ± 8.90E+05	1.75E+06 ± 2.02E+05
Tropomyosin alpha-4 chain	TPM4_RAT	29 kDa	0.034	1.37E+08 ± 2.91E+07	4.36E+07 ± 1.99E+07
Peptidyl-prolyl cis-trans isomerase A	PPIA_RAT	18 kDa	0.001	3.76E+08 ± 4.90E+07	1.32E+08 ± 5.65E+06

Triosephosphate isomerase	TPIS_RAT	27 kDa	0.008	4.03E+07 ± 6.61E+06	1.45E+07 ± 7.96E+05
Protein Hbb-b1	Q62669_RAT	16 kDa	0.001	3.94E+07 ± 2.15E+06	1.55E+07 ± 5.69E+06
Osteoglycin (Predicted)	D3ZVB7_RAT	34 kDa	0.007	4.09E+07 ± 5.94E+06	1.69E+07 ± 1.32E+06
Purine nucleoside phosphorylase (Fragment)	D3ZXK9_RAT PNPH_RAT	32 kDa	0.006	3.60E+07 ± 4.79E+06	1.58E+07 ± 2.03E+06
Protein DJ-1	PARK7_RAT	20 kDa	0.018	1.12E+07 ± 1.76E+06	4.96E+06 ± 9.31E+05
Serine protease inhibitor A3L	SPA3L_RAT	46 kDa	0.016	2.78E+07 ± 4.29E+06	1.26E+07 ± 1.55E+06
Polymerase I and transcript release factor	G3V8L9_RAT	44 kDa	0.009	1.71E+07 ± 1.84E+06	9.75E+06 ± 9.40E+05
Peroxiredoxin-2	PRDX2_RAT	22 kDa	0.002	1.50E+07 ± 1.08E+06	8.55E+06 ± 1.33E+06
Isoform 2 of Tropomyosin beta chain	TPM2_RAT	33 kDa	0.006	2.29E+08 ± 2.30E+07	1.34E+08 ± 5.80E+06

U.C. – Unique to control i.e., not detected in E2-treated

Table 2.4. IPA® Analysis: Summary of top pathways and biological functions represented by rat uterus proteins significantly regulated by E2 exposure using an MS-based total precursor intensity based label-free quantitative approach.

Canonical Pathways	***p*-value**
Glycolysis I	2.57E-10
LXR/RXR Activation	1.05E-08
FXR/RXR Activation	1.67E-08
Diseases and Disorders	***p*-value**
Cancer	2.01E-03 – 3.50E-26
Hematological Disease	2.01E-03 – 7.47E-17
Immunological Disease	2.01E-03 – 7.47E-17
Molecular and Cellular Functions	***p*-value**
Cell Death and Survival	1.97E-03 – 9.25E-18
Cellular Growth and Proliferation	1.93E-03 – 7.05E-17
Cellular Movement	1.83E-03 – 1.46E-13
Physiological System Development and Function	***p*-value**
Immune Cell Trafficking	1.74E-03 – 2.17E-08
Tissue Development	1.93E-03 – 2.28E-05
Tissue Morphology	9.52E-04 – 2.82E-05
Tox Lists	***p*-value**
LXR/RXR Activation	1.23E-08
FXR/RXR Activation	1.67E-08
NRF2-mediated Oxidative Stress Response	4.82E-06

Supplementary Table 2.1. A list of proteins identified from E2-regulated rat uterus extracts identified using standard MS^2 data-dependent acquisition.

#	Identified Proteins (253)	Accession Number	Molecular Weight
1	Protein S100-G	S100G_RAT	9 kDa
2	Transglutaminase 2	Q9WVJ6_RAT	77 kDa
3	Elongation factor 2	EF2_RAT	95 kDa
4	6-phosphogluconate dehydrogenase, decarboxylating	6PGD_RAT	53 kDa
5	Annexin A1	ANXA1_RAT	39 kDa
6	Keratin, type I cytoskeletal 18	K1C18_RAT	48 kDa
7	Rho GDP dissociation inhibitor (GDI) beta	Q5M860_RAT	23 kDa
8	Protein LOC679816	G3V9A3_RAT (+1)	28 kDa
9	Lactoperoxidase (Predicted)	D4A400_RAT	78 kDa
10	Acyl-CoA-binding protein	ACBP_RAT (+1)	10 kDa
11	Ezrin	EZRI_RAT	69 kDa
12	Nucleoside diphosphate kinase B	NDKB_RAT	17 kDa
13	Tubulin beta-2A chain	TBB2A_RAT (+1)	50 kDa
14	Lamin A, isoform CRA_b	G3V8L3_RAT	74 kDa
15	Macrophage-capping protein	CAPG_RAT	39 kDa
16	CArG-binding factor A	Q9QX80_RAT (+1)	31 kDa
17	Protein Naca	M0R9L0_RAT	220 kDa

18	Polypyrimidine tract binding protein 1, isoform CRA_c	D3ZB30_RAT (+3)	57 kDa
19	Alpha-1B-glycoprotein	sp|Q9EPH1|A1BG_RAT	56 kDa
20	Citrate synthase	G3V936_RAT	52 kDa
21	Peptidyl-prolyl cis-trans isomerase B	PPIB_RAT	24 kDa
22	Eukaryotic translation elongation factor 1 beta 2	B5DEN5_RAT	25 kDa
23	GTP-binding nuclear protein Ran	RAN_RAT	24 kDa
24	14-3-3 protein eta	1433F_RAT	28 kDa
25	40S ribosomal protein S7	RS7_RAT	22 kDa
26	Heat shock 70 kDa protein 4	F1LRV4_RAT (+1)	94 kDa
27	ATP synthase subunit alpha, mitochondrial	ATPA_RAT (+1)	60 kDa
28	Serine/threonine-protein phosphatase PP1-alpha catalytic subunit	PP1A_RAT (+3)	38 kDa
29	Sulfated glycoprotein 1	F7EPE0_RAT (+1)	62 kDa
30	60S ribosomal protein L12	RL12_RAT	18 kDa
31	Calumenin	G3V6S3_RAT	37 kDa
32	PYD and CARD domain containing	G3V8L1_RAT	22 kDa
33	Cytosolic non-specific dipeptidase	CNDP2_RAT	53 kDa
34	Isoform 2 of Fibrinogen beta chain	sp|P14480-2|FIBB_RAT (+1)	57 kDa

35	Protein Tln1	G3V852_RAT	270 kDa
36	Guanine nucleotide-binding protein subunit beta-2-like 1	GBLP_RAT	35 kDa
37	60S acidic ribosomal protein P0	RLA0_RAT	34 kDa
38	Protein Ppp2r1a	Q5XI34_RAT	65 kDa
39	Protein Itih4	D3ZFC6_RAT (+1)	103 kDa
40	Basic transcription factor 3	Q5U3Y8_RAT	18 kDa
41	Ribonuclease inhibitor	E2RUH2_RAT	50 kDa
42	Phosphoglucomutase-1	PGM1_RAT (+1)	61 kDa
43	Protein Susd2	D3ZEV8_RAT	90 kDa
44	L-lactate dehydrogenase A chain	LDHA_RAT	36 kDa
45	Keratin complex 2, basic, gene 7, isoform CRA_a	G3V712_RAT	51 kDa
46	Keratin, type I cytoskeletal 19	K1C19_RAT	45 kDa
47	Serine (Or cysteine) proteinase inhibitor, clade H, member 1, isoform CRA_b	Q5RJR9_RAT	47 kDa
48	Histone H2B	D3ZNH4_RAT (+6)	15 kDa
49	Elongation factor 1-alpha 1	EF1A1_RAT (+1)	50 kDa
50	Alpha-2 antiplasmin	Q80ZA3_RAT	46 kDa
51	Adenylyl cyclase-associated protein 1	CAP1_RAT	52 kDa
52	Phosphoglycerate kinase 1	PGK1_RAT	45 kDa

53	Isoform M2 of Pyruvate kinase PKM	sp|P11980-2|KPYM_RAT	58 kDa
54	Transitional endoplasmic reticulum ATPase	TERA_RAT	89 kDa
55	Keratin, type II cytoskeletal 8	K2C8_RAT	54 kDa
56	Desmin	Q6P725_RAT	53 kDa
57	Protein Pkn3	D3ZC07_RAT (+3)	107 kDa
58	Endoplasmin	sp|Q66HD0|ENPL_RAT	93 kDa
59	Lambda-crystallin homolog	CRYL1_RAT	35 kDa
60	Complement C3	M0RBF1_RAT	186 kDa
61	Lymphocyte cytosolic protein 1	Q5XI38_RAT	70 kDa
62	Eukaryotic translation initiation factor 4A1	Q6P3V8_RAT	46 kDa
63	Glucose-6-phosphate isomerase	G6PI_RAT	63 kDa
64	Eukaryotic translation initiation factor 5A2 (Predicted)	G3V7J7_RAT (+1)	17 kDa
65	Protein disulfide-isomerase A6	PDIA6_RAT	48 kDa
66	Tubulin alpha-1B chain	TBA1B_RAT	50 kDa
67	Ab2-417	Q7TMC7_RAT (+1)	107 kDa
68	Calponin-1	CNN1_RAT	33 kDa
69	Fructose-bisphosphate aldolase A	ALDOA_RAT	39 kDa
70	Heat shock protein HSP 90-alpha	HS90A_RAT	85 kDa
71	Protein disulfide-isomerase	PDIA1_RAT	57 kDa

72	Protein disulfide-isomerase A3	PDIA3_RAT	57 kDa
73	Group specific component	Q68FY4_RAT	54 kDa
74	Prolargin	PRELP_RAT	43 kDa
75	Histone H2A	D3ZVK7_RAT (+13)	14 kDa
76	Glyceraldehyde-3-phosphate dehydrogenase	G3P_RAT	36 kDa
77	Malate dehydrogenase, mitochondrial	MDHM_RAT	36 kDa
78	60 kDa heat shock protein, mitochondrial	CH60_RAT	61 kDa
79	Rab GDP dissociation inhibitor beta	GDIB_RAT	51 kDa
80	Superoxide dismutase [Cu-Zn]	SODC_RAT	16 kDa
81	Rho GDP-dissociation inhibitor 1	GDIR1_RAT	23 kDa
82	Cathepsin B	CATB_RAT (+1)	37 kDa
83	Cofilin-1	COF1_RAT	19 kDa
84	Peptidyl-prolyl cis-trans isomerase FKBP1A	FKB1A_RAT	12 kDa
85	Tubulin beta-5 chain	sp|P69897|TBB5_RAT	50 kDa
86	78 kDa glucose-regulated protein	GRP78_RAT	72 kDa
87	Heat shock 70 kDa protein 1A/1B	HSP71_RAT	70 kDa
88	Alpha-1-macroglobulin	A1M_RAT	167 kDa
89	Peroxiredoxin-1	PRDX1_RAT	22 kDa

90	Annexin A5	ANXA5_RAT (+1)	36 kDa
91	Profilin-1	PROF1_RAT	15 kDa
92	Transgelin	TAGL_RAT	23 kDa
93	Heat shock protein HSP 90-beta	HS90B_RAT	83 kDa
94	Serum albumin	ALBU_RAT	69 kDa
95	Vinculin	R9PXU6_RAT (+1)	117 kDa
96	Transketolase	G3V826_RAT (+1)	71 kDa
97	Heat shock cognate 71 kDa protein	HSP7C_RAT	71 kDa
98	Calreticulin	CALR_RAT	48 kDa
99	Destrin	DEST_RAT	19 kDa
100	Actin, cytoplasmic 1	ACTB_RAT (+2)	42 kDa
101	Selenium binding protein 1	F1LRJ9_RAT (+1)	52 kDa
102	Barrier-to-autointegration factor	BAF_RAT	10 kDa
103	C-reactive protein	CRP_RAT	25 kDa
104	Keratin, type II cytoskeletal 1	K2C1_RAT	65 kDa
105	Retinol-binding protein 1	RET1_RAT	16 kDa
106	Serine/arginine-rich splicing factor 2	SRSF2_RAT	25 kDa
107	Carbonic anhydrase 2	CAH2_RAT	29 kDa
108	Carboxylesterase 1C	D3ZGK7_RAT (+1)	60 kDa
109	Dipeptidyl peptidase 2	DPP2_RAT	55 kDa
110	Dermatopontin (Predicted), isoform CRA_c	D4A9H2_RAT	20 kDa

111	Glutathione S-transferase P	GSTP1_RAT	23 kDa
112	Keratin, type II cytoskeletal 6A	K2C6A_RAT	59 kDa
113	Phosphatidylethanolamine-binding protein 1	PEBP1_RAT	21 kDa
114	Protein Srsf7	D4A720_RAT	27 kDa
115	Carbonic anhydrase 3	CAH3_RAT	29 kDa
116	Nuclear transport factor 2	NTF2_RAT	14 kDa
117	Lumican	LUM_RAT	38 kDa
118	SH3 domain-binding glutamic acid-rich-like protein	B5DFD8_RAT	13 kDa
119	Glutathione S-transferase Mu 2	GSTM2_RAT	26 kDa
120	Glyoxalase domain-containing protein 4	GLOD4_RAT	33 kDa
121	Alpha-2-HS-glycoprotein	FETUA_RAT	38 kDa
122	Complement factor D	CFAD_RAT (+1)	28 kDa
123	Serine protease inhibitor A3K	SPA3K_RAT	47 kDa
124	Hemoglobin subunit beta-2	HBB2_RAT	16 kDa
125	Hemoglobin subunit beta-1	HBB1_RAT	16 kDa
126	Uncharacterized protein (Fragment)	D4A7W8_RAT (+1)	29 kDa
127	Cathepsin D	CATD_RAT (+1)	45 kDa
128	Apolipoprotein E	APOE_RAT	36 kDa
129	Alpha-1-antiproteinase	A1AT_RAT	46 kDa
130	Hemoglobin subunit alpha-1/2	HBA_RAT	15 kDa

131	Gamma-enolase	ENOG_RAT	47 kDa
132	Peroxiredoxin-5, mitochondrial (Fragment)	D3ZEN5_RAT (+2)	17 kDa
133	Tropomyosin alpha-4 chain	TPM4_RAT	29 kDa
134	Peptidyl-prolyl cis-trans isomerase A	PPIA_RAT	18 kDa
135	Triosephosphate isomerase	TPIS_RAT	27 kDa
136	Protein Hbb-b1	Q62669_RAT	16 kDa
137	Osteoglycin (Predicted)	D3ZVB7_RAT	34 kDa
138	Purine nucleoside phosphorylase (Fragment)	D3ZXK9_RAT (+1)	32 kDa
139	Protein DJ-1	PARK7_RAT	20 kDa
140	Serine protease inhibitor A3L	SPA3L_RAT	46 kDa
141	Polymerase I and transcript release factor	G3V8L9_RAT	44 kDa
142	Peroxiredoxin-2	PRDX2_RAT	22 kDa
143	Isoform 2 of Tropomyosin beta chain	sp|P58775-2|TPM2_RAT	33 kDa
144	Alpha-actinin-1	ACTN1_RAT	103 kDa
145	Aldehyde dehydrogenase, mitochondrial	ALDH2_RAT (+1)	56 kDa
146	10 kDa heat shock protein, mitochondrial	CH10_RAT	11 kDa

147	Coactosin-like protein	COTL1_RAT	16 kDa
148	Transgelin-2	TAGL2_RAT	22 kDa
149	Myl9 protein	B0BMS8_RAT	20 kDa
150	Parathymosin	PTMS_RAT	12 kDa
151	Fetuin-B	FETUB_RAT (+1)	42 kDa
152	Nucleophosmin	sp|P13084|NPM_RAT	33 kDa
153	Myosin-11	E9PTU4_RAT	227 kDa
154	N(G),N(G)-dimethylarginine dimethylaminohydrolase 2	DDAH2_RAT	30 kDa
155	ADP-ribosylation factor 1	ARF1_RAT (+1)	21 kDa
156	Actin-related protein 3	ARP3_RAT	47 kDa
157	Ac2-248	Q7TPI9_RAT	66 kDa
158	Protein Hmg1l1 GN=Hmg1l1	D3ZCR3_RAT (+3)	25 kDa
159	Tropomyosin 1, alpha, isoform CRA_c	F7FK40_RAT	33 kDa
160	Adenosylhomocysteinase	SAHH_RAT	48 kDa
161	T-kininogen 2	KNT2_RAT	48 kDa
162	Adenylate kinase isoenzyme 1	KAD1_RAT	22 kDa
163	Fatty acid-binding protein, adipocyte	FABP4_RAT (+1)	15 kDa
164	Protein LOC679748	D3ZE63_RAT (+1)	13 kDa
165	Protein Mylk	D3ZFU9_RAT	215 kDa
166	Calmodulin	CALM_RAT	17 kDa

167	40S ribosomal protein S12	D3ZHB3_RAT (+2)	14 kDa
168	Myosin light polypeptide 6	MYL6_RAT	17 kDa
169	Ras-related protein Rab-7a	RAB7A_RAT	24 kDa
170	Non-muscle caldesmon	CALD1_RAT (+1)	61 kDa
171	Heterogeneous nuclear ribonucleoprotein Q	HNRPQ_RAT (+1)	60 kDa
172	Afamin	AFAM_RAT (+1)	69 kDa
173	Uncharacterized protein (Fragment)	F1LPQ6_RAT (+1)	39 kDa
174	Serine/threonine-protein phosphatase 2A catalytic subunit beta isoform	PP2AB_RAT	36 kDa
175	F-actin-capping protein subunit alpha-2	CAZA2_RAT	33 kDa
176	Glutathione peroxidase 3	GPX3_RAT	25 kDa
177	Actin, aortic smooth muscle	ACTA_RAT	42 kDa
178	Fibulin-1	D3ZQ25_RAT	78 kDa
179	Isoform 2 of Cell surface glycoprotein MUC18	sp|Q9EPF2-2|MUC18_RAT (+1)	67 kDa
180	Heterogeneous nuclear ribonucleoprotein K	HNRPK_RAT (+1)	51 kDa
181	Protein Abracl	D3ZSL2_RAT	9 kDa
182	Ras-related protein Rab-1A	E9PU16_RAT (+1)	34 kDa
183	Creatine kinase B-type	KCRB_RAT	43 kDa

184	Retinoid-inducible serine carboxypeptidase	RISC_RAT	51 kDa
185	40S ribosomal protein SA	RSSA_RAT	33 kDa
186	14-3-3 protein gamma	1433G_RAT	28 kDa
187	Apolipoprotein A-IV	APOA4_RAT	44 kDa
188	Peroxiredoxin-6	PRDX6_RAT	25 kDa
189	Protein-L-isoaspartate(D-aspartate) O-methyltransferase	PIMT_RAT	25 kDa
190	Protein LOC100362751	D4A4D5_RAT (+1)	12 kDa
191	Lamin-B1	LMNB1_RAT	67 kDa
192	60S acidic ribosomal protein P1	RLA1_RAT	11 kDa
193	Protein Col6a3	D4A111_RAT (+1)	306 kDa
194	Lactoylglutathione lyase	LGUL_RAT	21 kDa
195	Carboxypeptidase Q	CBPQ_RAT	52 kDa
196	Isoform 2 of Elongation factor 1-delta	sp|Q68FR9-2|EF1D_RAT (+1)	72 kDa
197	Protein Rcn1	D3ZUB0_RAT	38 kDa
198	Protein RGD1310507	E9PST1_RAT	51 kDa
199	Periostin, osteoblast specific factor (Predicted), isoform CRA_a	D3ZAF5_RAT	90 kDa
200	Heterogeneous nuclear ribonucleoprotein H	D3ZYW2_RAT (+1)	47 kDa
201	Thymosin beta-4	TYB4_RAT	5 kDa

202	Protein Pgm5	D3ZVR9_RAT	62 kDa
203	Aspartate aminotransferase, mitochondrial	AATM_RAT	47 kDa
204	Protein Srsf1	D4A9L2_RAT	28 kDa
205	Uncharacterized protein	F1LN61_RAT (+1)	37 kDa
206	Copper transport protein ATOX1	ATOX1_RAT	7 kDa
207	14-3-3 protein zeta/delta	1433Z_RAT	28 kDa
208	Isoform Short of 14-3-3 protein beta/alpha	sp|P35213-2|1433B_RAT (+1)	28 kDa
209	Alpha-actinin-4	ACTN4_RAT	105 kDa
210	Ceruloplasmin	G3V7K3_RAT	121 kDa
211	Rab GDP dissociation inhibitor alpha	GDIA_RAT	51 kDa
212	Adenine phosphoribosyltransferase	APT_RAT	20 kDa
213	Murinoglobulin-1	sp|Q03626|MUG1_RAT	165 kDa
214	Aldose reductase	ALDR_RAT	36 kDa
215	Tropomyosin alpha-3 chain	sp|Q63610|TPM3_RAT	29 kDa
216	Protein S100-A11	S10AB_RAT	11 kDa
217	Hemopexin	HEMO_RAT	51 kDa
218	ATP synthase subunit beta, mitochondrial	ATPB_RAT (+1)	56 kDa
219	Prostaglandin E synthase 3 (Fragment)	R9PXR7_RAT (+1)	19 kDa

220	Vimentin	G3V8C3_RAT (+1)	54 kDa
221	Galectin-1	LEG1_RAT	15 kDa
222	Malate dehydrogenase, cytoplasmic	MDHC_RAT	36 kDa
223	Inositol monophosphatase 1	F1M978_RAT (+1)	30 kDa
224	Alpha-1-inhibitor 3	A1I3_RAT	164 kDa
225	Isoform 2 of Gelsolin	sp|Q68FP1-2|GELS_RAT (+1)	81 kDa
226	NADH dehydrogenase [ubiquinone] flavoprotein 2, mitochondrial	NDUV2_RAT	27 kDa
227	Polyubiquitin-C	F1LML2_RAT (+3)	91 kDa
228	Cytochrome c oxidase subunit 5A, mitochondrial	COX5A_RAT	16 kDa
229	Cysteine and glycine-rich protein 1	CSRP1_RAT	21 kDa
230	Heat shock 27kDa protein 1	G3V913_RAT (+1)	23 kDa
231	Proteasome activator complex subunit 1	PSME1_RAT (+1)	29 kDa
232	Apolipoprotein A-I	APOA1_RAT	30 kDa
233	Protein Ube2l3	B2RZA9_RAT	18 kDa
234	Glutathione peroxidase 1	GPX1_RAT	22 kDa
235	14-3-3 protein theta	1433T_RAT	28 kDa
236	Protein Inmt	D3ZNJ5_RAT	29 kDa
237	Prothymosin alpha	PTMA_RAT	12 kDa
238	Transaldolase	TALDO_RAT	37 kDa

239	Protein Rsu1	D4A8F2_RAT	29 kDa
240	Heterogeneous nuclear ribonucleoproteins A2/B1	F1LM82_RAT	32 kDa
241	Isocitrate dehydrogenase [NADP] cytoplasmic	IDHC_RAT	47 kDa
242	Phosphoglycerate mutase 1	PGAM1_RAT	29 kDa
243	Myosin regulatory light chain 12B	ML12B_RAT	20 kDa
244	Histidine triad nucleotide-binding protein 1	HINT1_RAT	14 kDa
245	Lamina-associated polypeptide 2, isoform beta	LAP2_RAT	50 kDa
246	Alcohol dehydrogenase [NADP(+)]	AK1A1_RAT	37 kDa
247	Translationally-controlled tumor protein	TCTP_RAT	19 kDa
248	Heterogeneous nuclear ribonucleoprotein A3	sp|Q6URK4|ROA3_RAT	40 kDa
249	Alpha-enolase	ENOA_RAT	47 kDa
250	Thioredoxin	THIO_RAT	12 kDa
251	L-lactate dehydrogenase B chain	LDHB_RAT	37 kDa
252	14-3-3 protein epsilon	1433E_RAT	29 kDa
253	Uncharacterized protein	M0R9D5_RAT	572 kDa

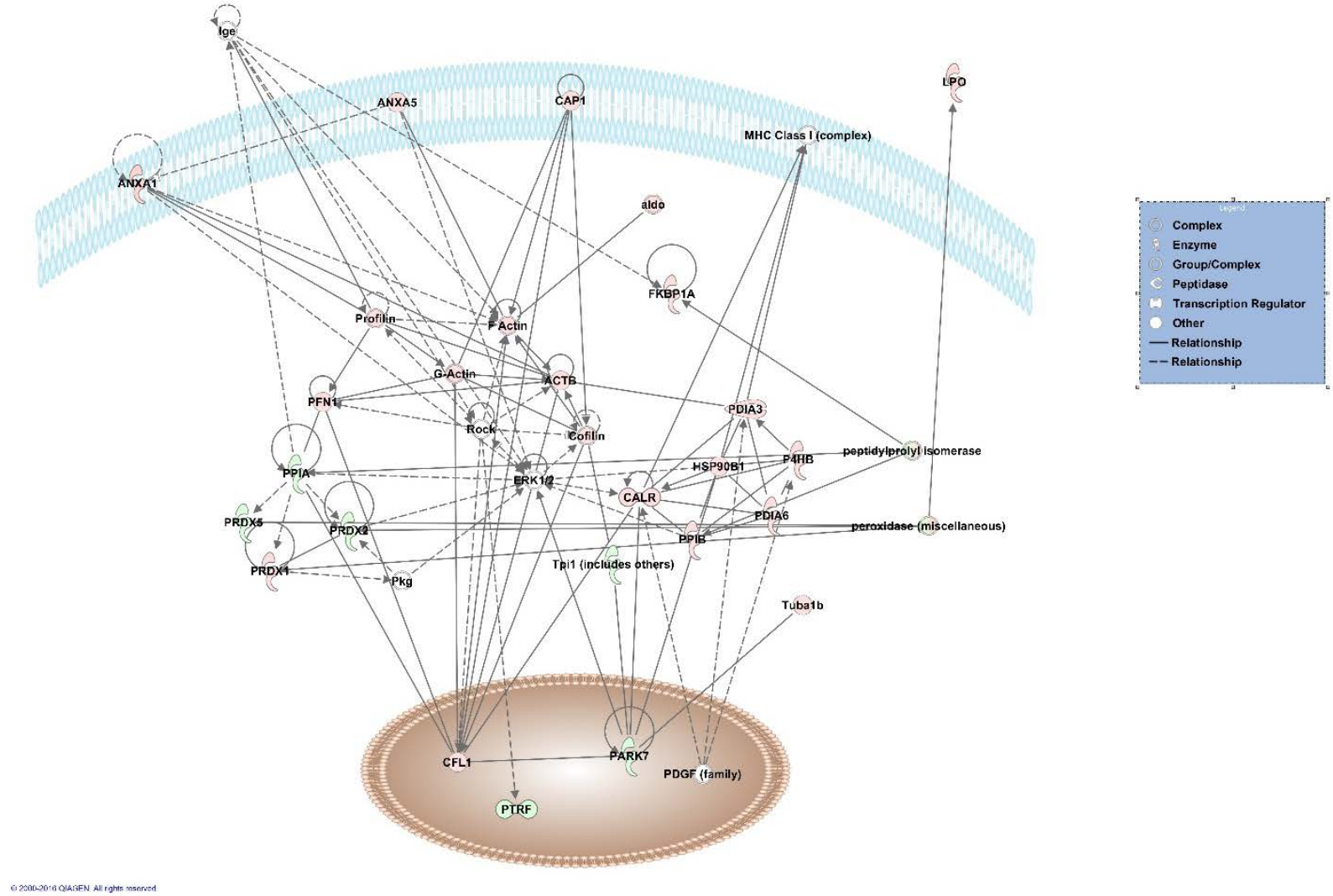

Figure 2.1. Network 1 of 9 constructed through Ingenuity Pathway Analysis from rat uterus proteins affected by E2 exposure.

From all (143) up- and down-regulated proteins, we mapped 139 across 9 networks. Network 1 is the top scoring network in the E2-

regulated dataset, showing 22 molecules from our dataset. Top diseases and functions relevant to the uterus included: Cancer, organismal injury and abnormalities, and immunological diseases. Single lines indicate protein-protein interactions from the network diagram and arrows specify proteins/compounds that regulate another protein. The intensity of green and red molecule colors represents the degree of down- or up-regulation, respectively. Solid or dashed lines show direct or indirect interactions, respectively.

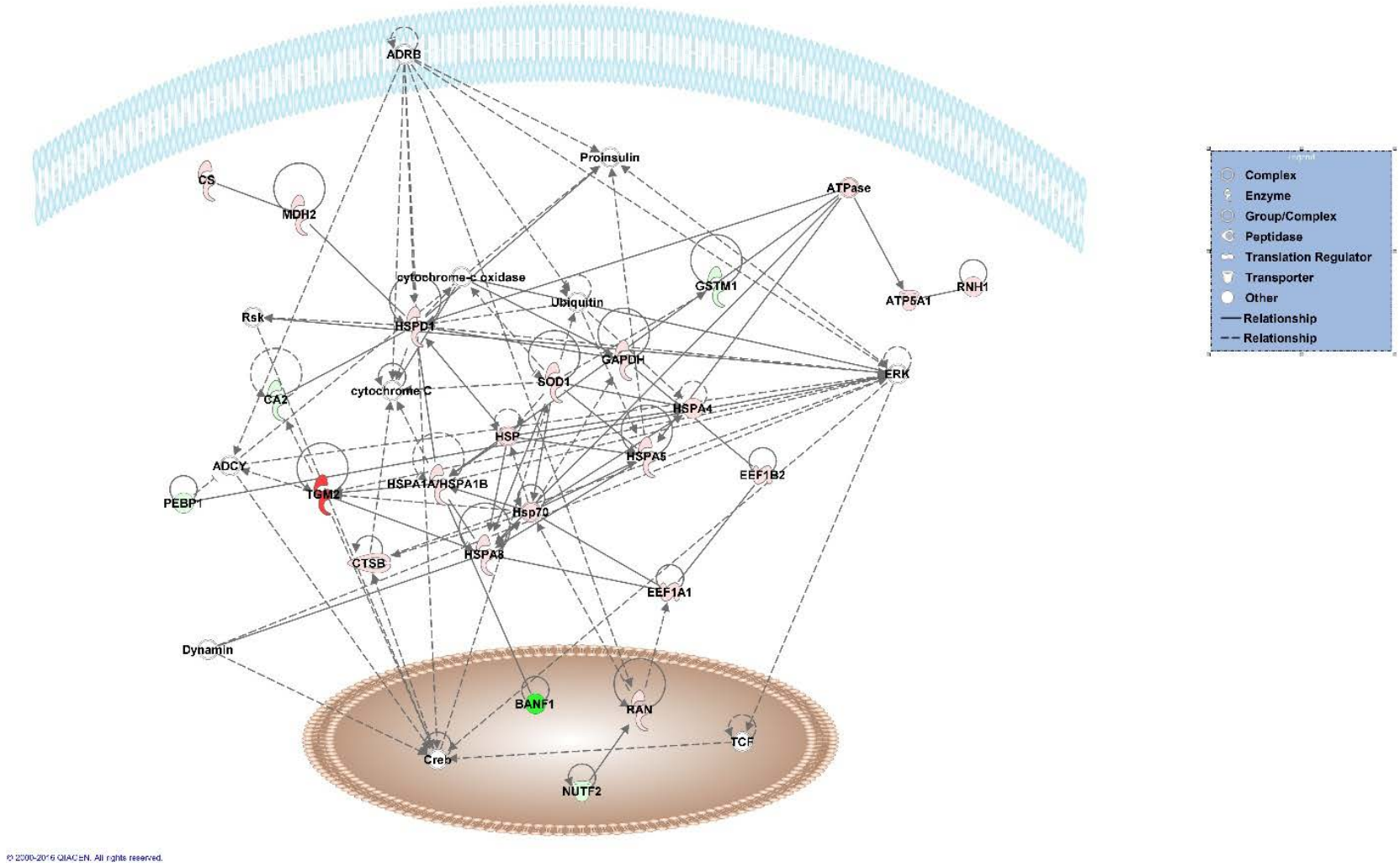

Figure 2.2. Network 2 of 9 constructed through Ingenuity Pathway Analysis from rat uterus proteins affected by E2 exposure.

From all (143) up- and down-regulated proteins, we mapped 139 across 9 networks. Network 2 is the second highest scoring network

in the E2-regulated dataset, showing 21 molecules from our dataset. Top diseases and functions relevant to the uterus included: Cell death and survival, and metabolic diseases. Single lines indicate protein-protein interactions from the network diagram and arrows specify proteins/compounds that regulate another protein. The intensity of green and red molecule colors represents the degree of down- or up-regulation, respectively. Solid or dashed lines show direct or indirect interactions, respectively.

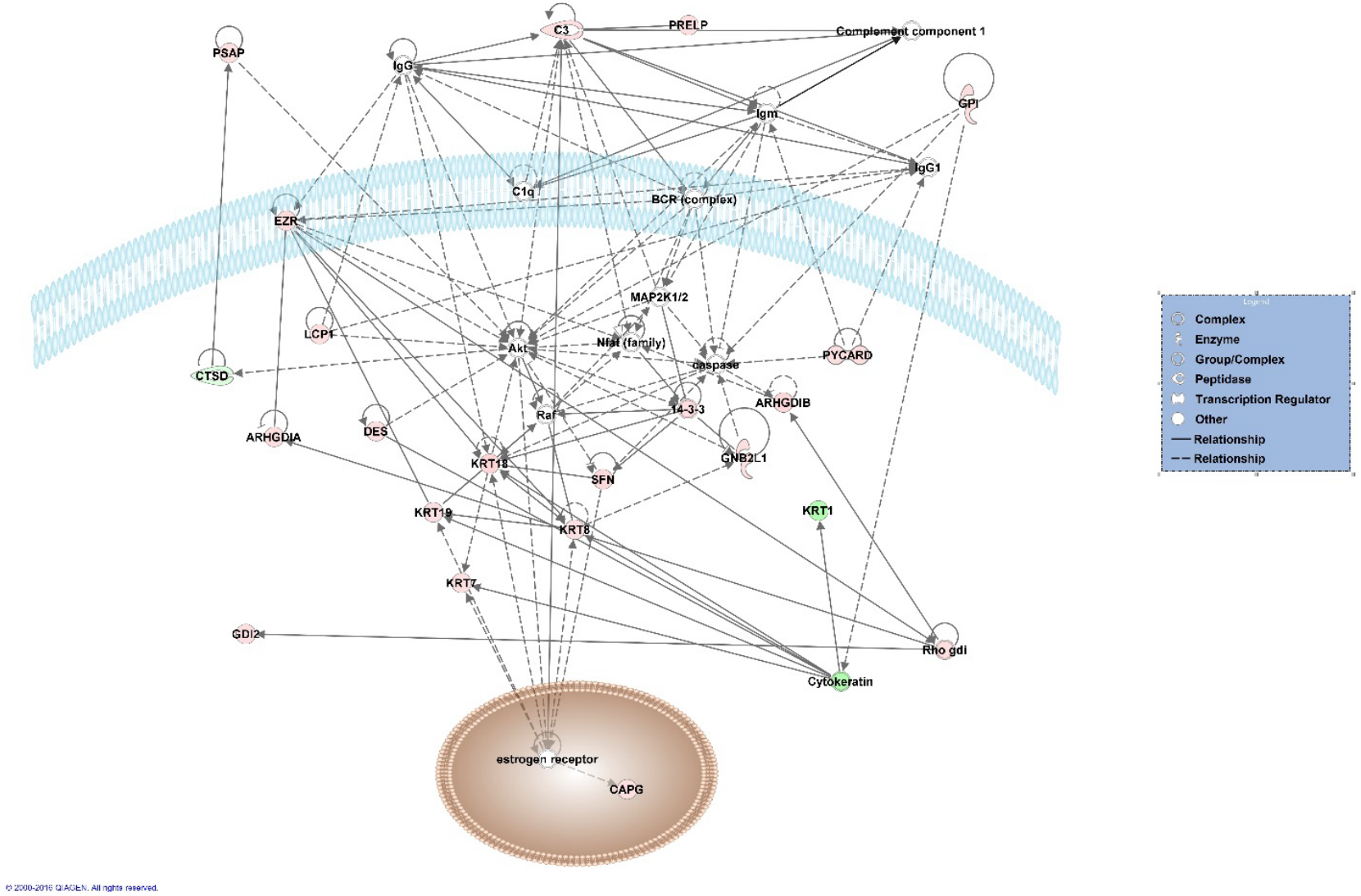

Figure 2.3. Network 3 of 9 constructed through Ingenuity Pathway Analysis from rat uterus proteins affected by E2 exposure.

From all (143) up- and down-regulated proteins, we mapped 139 across 9 networks. Network 3 is the third highest scoring network in

the E2-regulated dataset, showing 20 molecules from our dataset. Top diseases and functions relevant to the uterus included: Cell morphology. Single lines indicate protein-protein interactions from the network diagram and arrows specify proteins/compounds that regulate another protein. The intensity of green and red molecule colors represents the degree of down- or up-regulation, respectively. Solid or dashed lines show direct or indirect interactions, respectively.

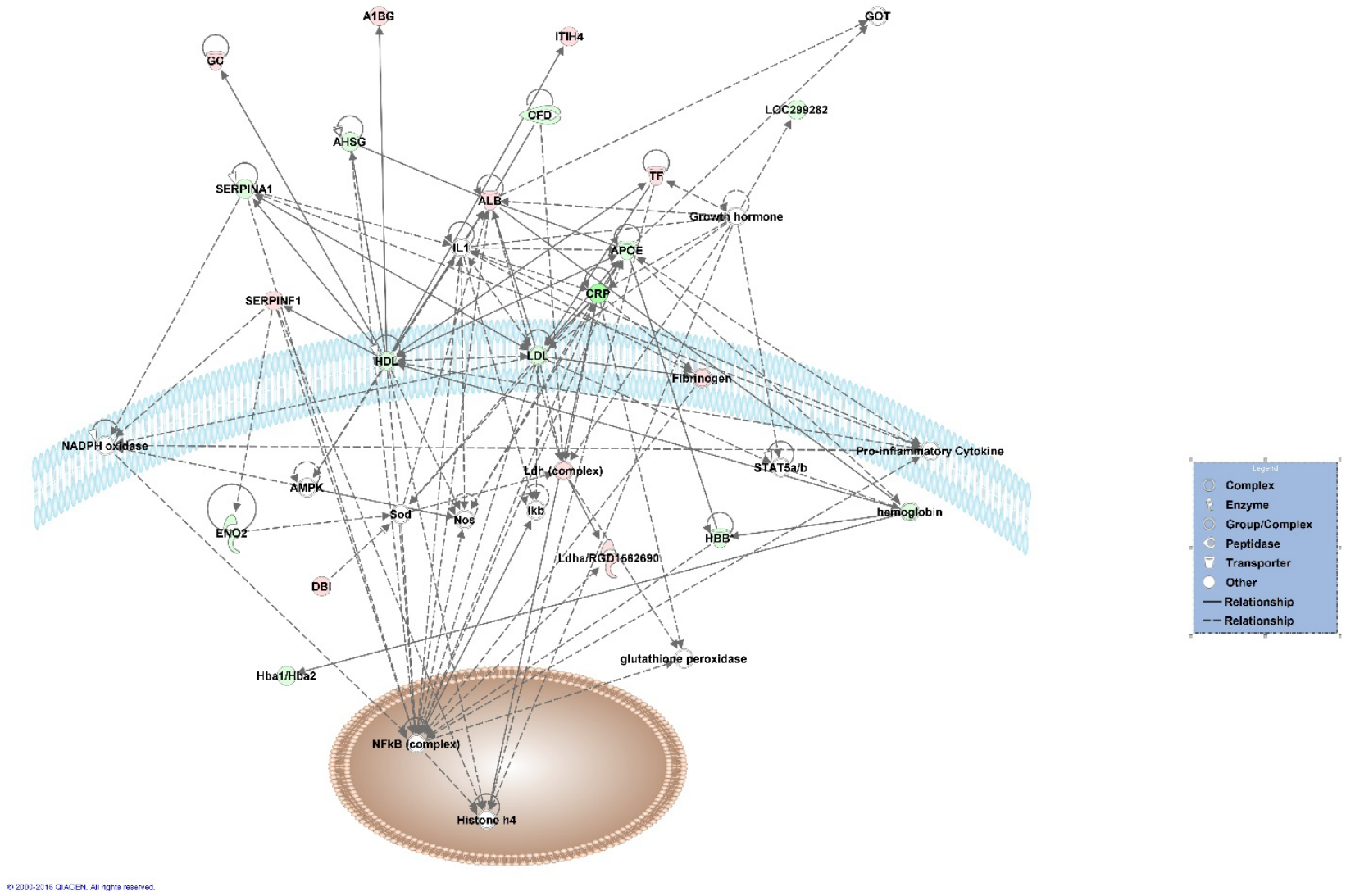

Figure 2.4. Network 4 of 9 constructed through Ingenuity Pathway Analysis from rat uterus proteins affected by E2 exposure.

From all (143) up- and down-regulated proteins, we mapped 139 across 9 networks. Network 4 is the fourth highest scoring network

in the E2-regulated dataset, showing 17 molecules from our dataset. Top diseases and functions relevant to the uterus included: Free radical scavenging, and organismal injury and abnormalities. Single lines indicate protein-protein interactions from the network diagram and arrows specify proteins/compounds that regulate another protein. The intensity of green and red molecule colors represents the degree of down- or up-regulation, respectively. Solid or dashed lines show direct or indirect interactions, respectively.

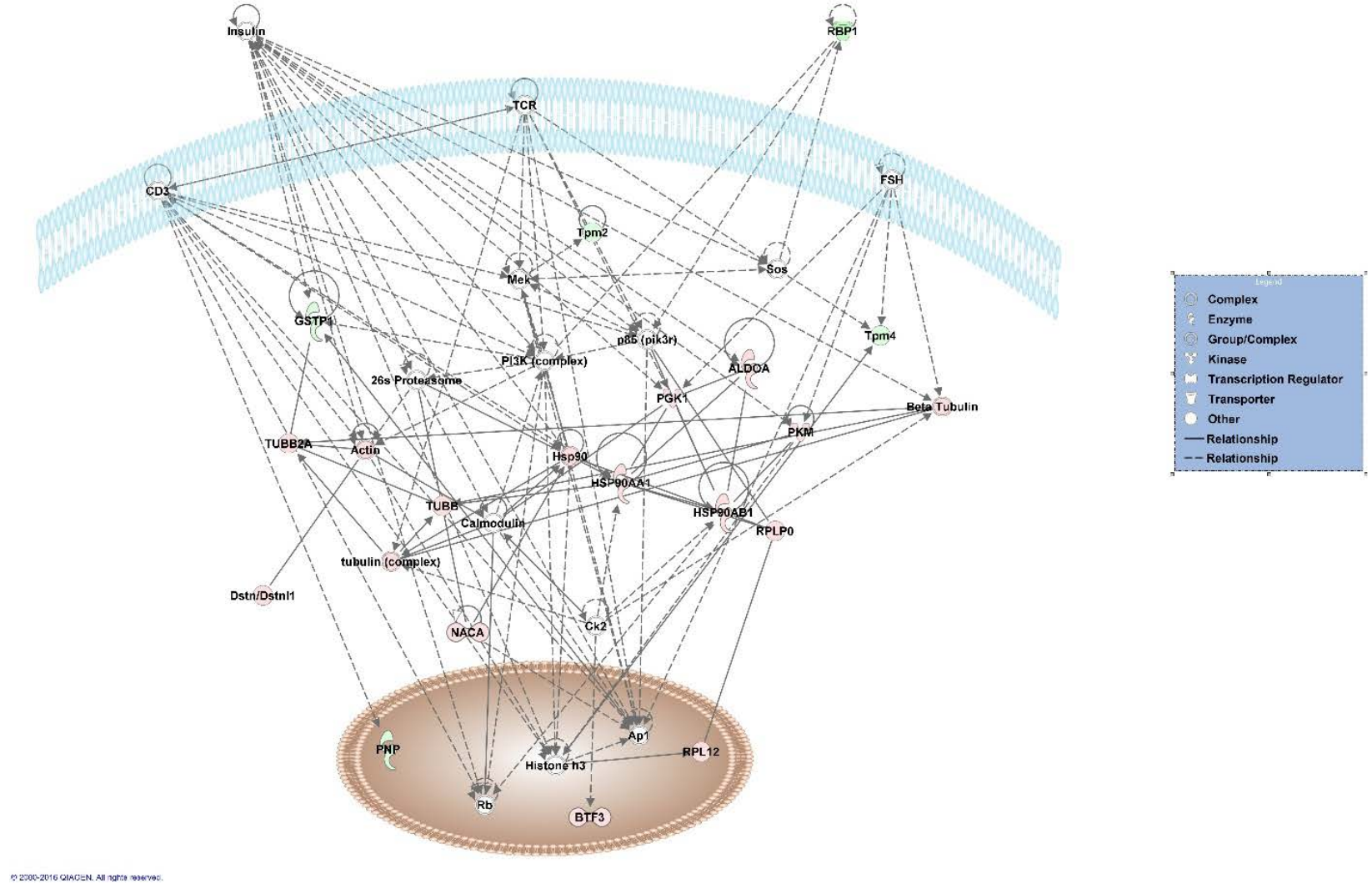

Figure 2.5. Network 5 of 9 constructed through Ingenuity Pathway Analysis from rat uterus proteins affected by E2 exposure.

From all (143) up- and down-regulated proteins, we mapped 139 across 9 networks. Network 5 is the fifth highest scoring network in

the E2-regulated dataset, showing 17 molecules from our dataset. Top diseases and functions relevant to the uterus included: Cancer. Single lines indicate protein-protein interactions from the network diagram and arrows specify proteins/compounds that regulate another protein. The intensity of green and red molecule colors represents the degree of down- or up-regulation, respectively. Solid or dashed lines show direct or indirect interactions, respectively.

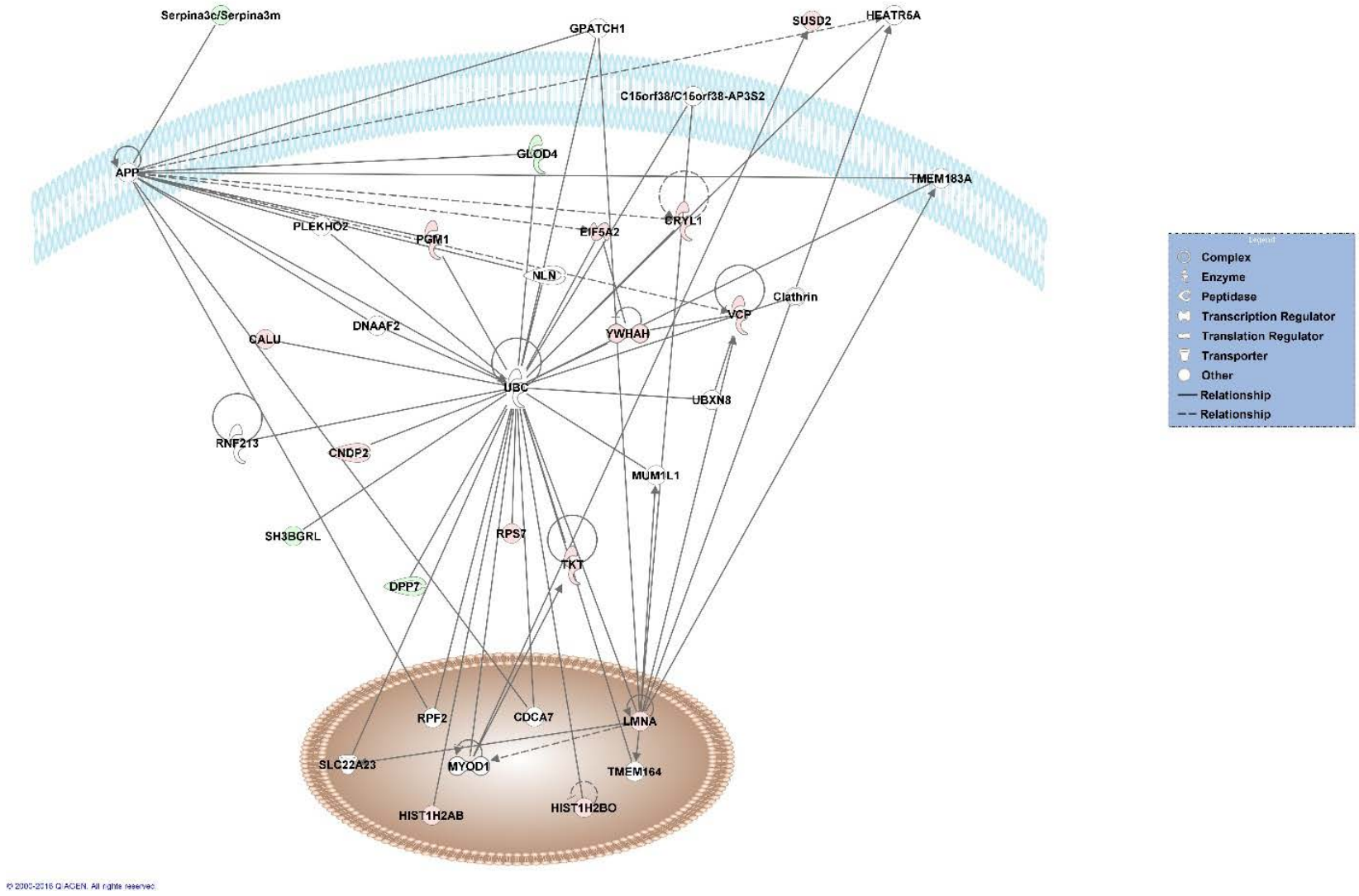

Figure 2.6. Network 6 of 9 constructed through Ingenuity Pathway Analysis from rat uterus proteins affected by E2 exposure.

From all (143) up- and down-regulated proteins, we mapped 139 across 9 networks. Network 6 is the sixth highest scoring network in

the E2-regulated dataset, showing 17 molecules from our dataset. Top diseases and functions relevant to the uterus included: Carbohydrate metabolism, nucleic acid metabolism, and cell morphology. Single lines indicate protein-protein interactions from the network diagram and arrows specify proteins/compounds that regulate another protein. The intensity of green and red molecule colors represents the degree of down- or up-regulation, respectively. Solid or dashed lines show direct or indirect interactions, respectively.

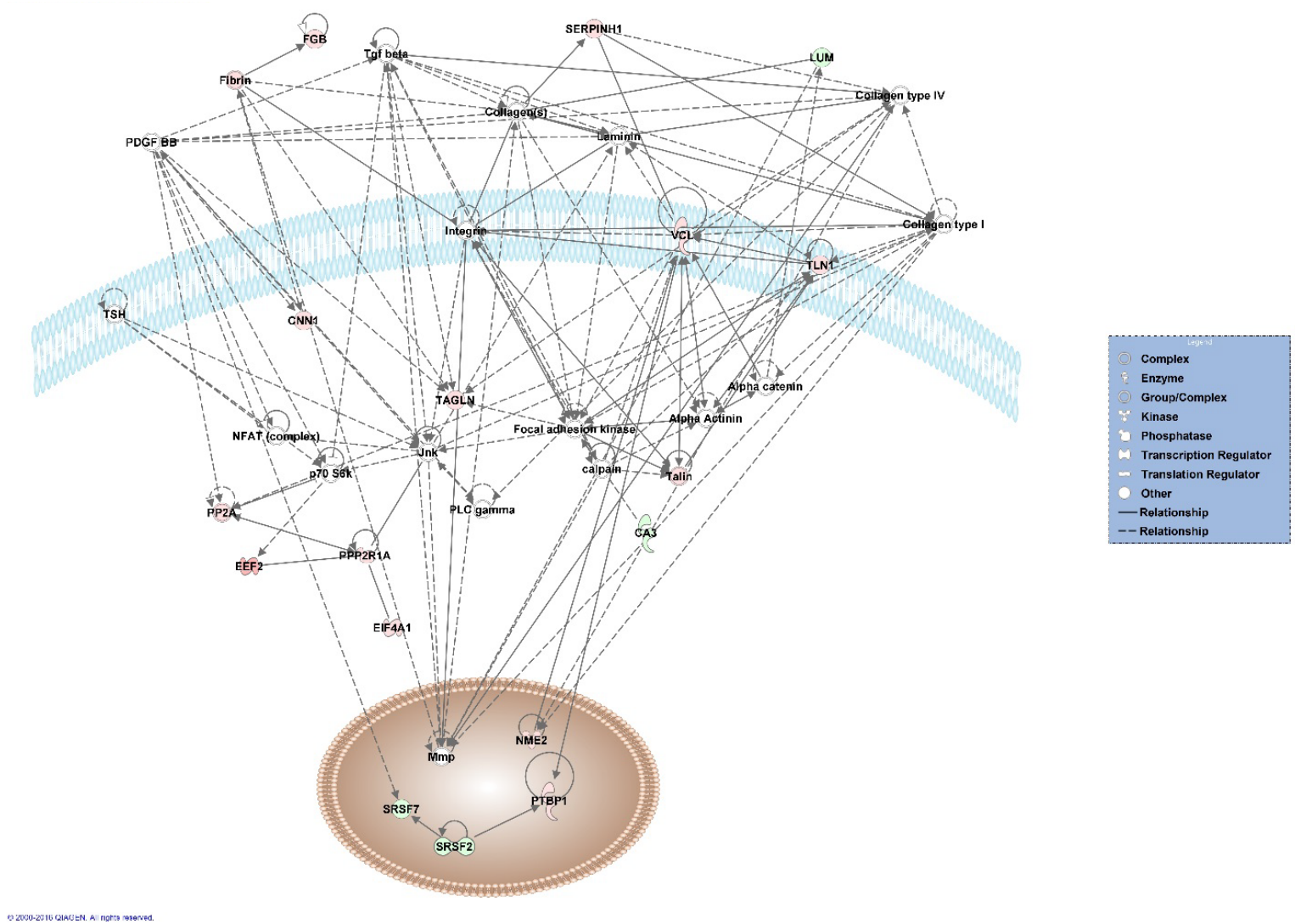

Figure 2.7. Network 7 of 9 constructed through Ingenuity Pathway Analysis from rat uterus proteins affected by E2 exposure.

From all (143) up- and down-regulated proteins, we mapped 139 across 9 networks. Network 7 is the seventh highest scoring network

in the E2-regulated dataset, showing 15 molecules from our dataset. Top diseases and functions relevant to the uterus included: Cell morphology, cellular assembly and organization, and connective tissue disorders. Single lines indicate protein-protein interactions from the network diagram and arrows specify proteins/compounds that regulate another protein. The intensity of green and red molecule colors represents the degree of down- or up-regulation, respectively. Solid or dashed lines show direct or indirect interactions, respectively.

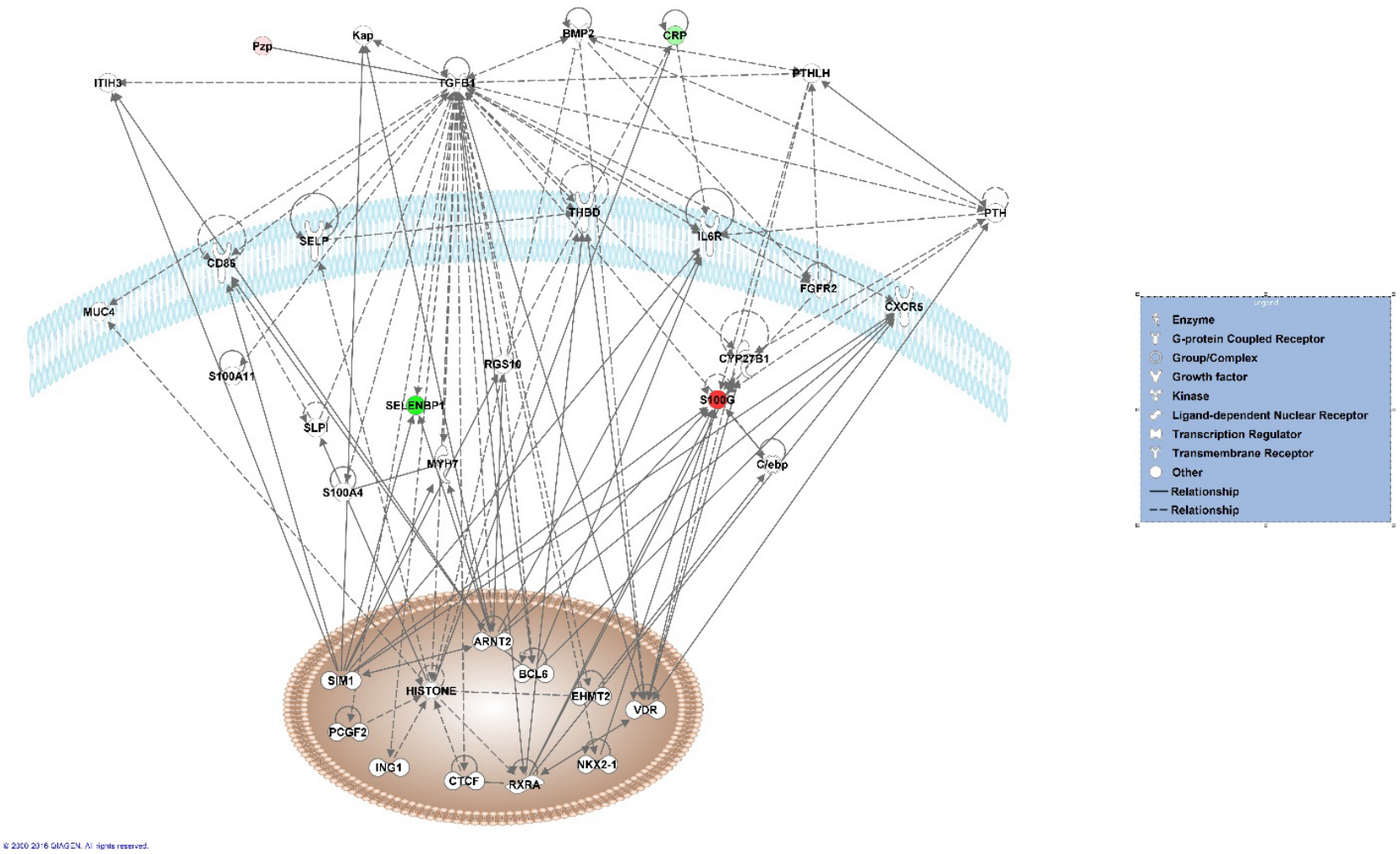

Figure 2.8. Network 8 of 9 constructed through Ingenuity Pathway Analysis from rat uterus proteins affected by E2 exposure.

From all (143) up- and down-regulated proteins, we mapped 139 across 9 networks. Network 8 is the eighth highest scoring network in the E2-regulated dataset, showing 4 molecules from our dataset. Top diseases and functions relevant to the uterus included: Organ

morphology, and inflammatory disease. Single lines indicate protein-protein interactions from the network diagram and arrows specify proteins/compounds that regulate another protein. The intensity of green and red molecule colors represents the degree of down- or up-regulation, respectively. Solid or dashed lines show direct or indirect interactions, respectively.

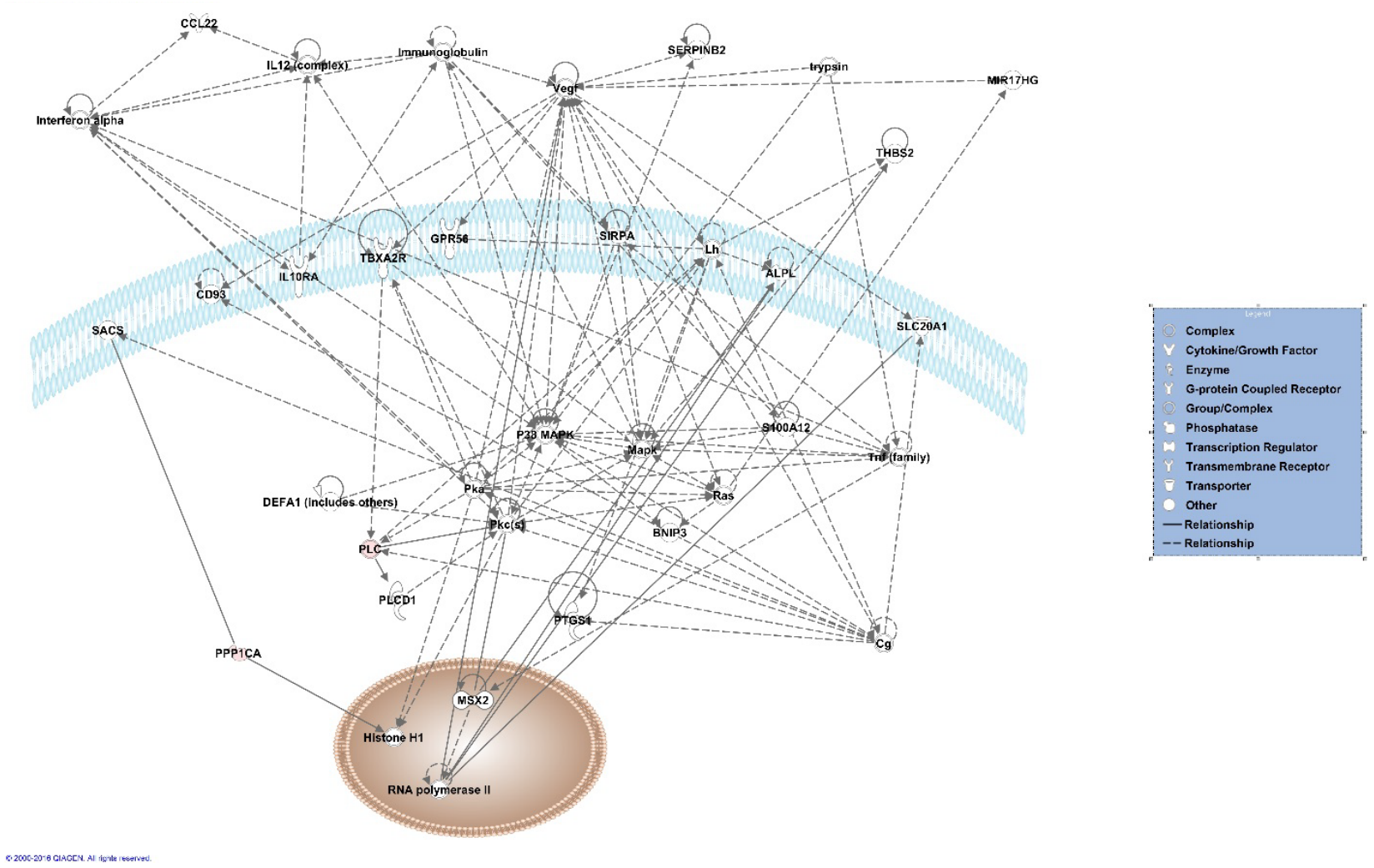

Figure 2.9. Network 9 of 9 constructed through Ingenuity Pathway Analysis from rat uterus proteins affected by E2 exposure.

From all (143) up- and down-regulated proteins, we mapped 139 across 9 networks. Network 9 is the lowest scoring network in the

E2-regulated dataset, showing 1 molecule from our dataset. Top diseases and functions relevant to the uterus included: Cellular movement, and inflammatory response. Single lines indicate protein-protein interactions from the network diagram and arrows specify proteins/compounds that regulate another protein. The intensity of green and red molecule colors represents the degree of down- or up-regulation, respectively. Solid or dashed lines show direct or indirect interactions, respectively.

REFERENCES

1. Vizcaino, J. A.; Deutsch, E. W.; Wang, R.; Csordas, A.; Reisinger, F.; Rios, D.; Dianes, J. A.; Sun, Z.; Farrah, T.; Bandeira, N.; Binz, P. A.; Xenarios, I.; Eisenacher, M.; Mayer, G.; Gatto, L.; Campos, A.; Chalkley, R. J.; Kraus, H. J.; Albar, J. P.; Martinez-Bartolome, S.; Apweiler, R.; Omenn, G. S.; Martens, L.; Jones, A. R.; Hermjakob, H., ProteomeXchange provides globally coordinated proteomics data submission and dissemination. *Nat. Biotechnol.* **2014,** 32, (3), 223-6.

2. UniProt, C., UniProt: a hub for protein information. *Nucleic Acids Res.* **2015,** 43, (Database issue), D204-12.

3. Keller, A.; Nesvizhskii, A. I.; Kolker, E.; Aebersold, R., Empirical statistical model to estimate the accuracy of peptide identifications made by MS/MS and database search. *Anal. Chem.* **2002,** 74, (20), 5383-5392.

4. Nesvizhskii, A. I.; Keller, A.; Kolker, E.; Aebersold, R., A statistical model for identifying proteins by tandem mass spectrometry. *Anal. Chem.* **2003,** 75, (17), 4646-4658.

5. United States Environmental Protection Agency, Endocrine Disruptor Screening Program Test Guidelines OPPTS 890.1600: Uterotrophic Assay. In Oct 2009 EPA 740-C-09-0010 ed.; Office of Prevention Pesticides and Toxic Substances (OPPTS), Ed. 2009.

6. United States Environmental Protection Agency, OPPTS 890.1600: Uterotrophic Assay Standard Evaluation Procedure. In Sep 2011 ed.; Office of Prevention Pesticides and Toxic Substances (OPPTS), Ed. 2011.

7. Szarka, S.; Nguyen, V.; Prokai, L.; Prokai-Tatrai, K., Separation of dansylated 17beta-estradiol, 17alpha-estradiol, and estrone on a single HPLC column for simultaneous quantitation by LC-MS/MS. *Anal. Bioanal. Chem.* **2013,** 405, (10), 3399-406.

8. Prokai, L.; Stevens, S. M., Jr.; Rauniyar, N.; Nguyen, V., Rapid label-free identification of estrogen-induced differential protein expression in vivo from mouse brain and uterine tissue. *J. Proteome Res.* **2009,** 8, (8), 3862-71.

9. Tu, C.; Li, J.; Sheng, Q.; Zhang, M.; Qu, J., Systematic assessment of survey scan and MS2-based abundance strategies for label-free quantitative proteomics using high-resolution MS data. *J. Proteome Res.* **2014,** 13, (4), 2069-79.

10. Watanabe, H.; Suzuki, A.; Kobayashi, M.; Takahashi, E.; Itamoto, M.; Lubahn, D. B.; Handa, H.; Iguchi, T., Analysis of temporal changes in the expression of estrogen-regulated genes in the uterus. *J. Mol. Endocrinol.* **2003,** 30, (3), 347-358.

11. Watanabe, H.; Suzuki, A.; Mizutani, T.; Khono, S.; Lubahn, D. B.; Handa, H.; Iguchi, T., Genome-wide analysis of changes in early gene expression induced by oestrogen. *Genes Cells* **2002,** 7, (5), 497-507.

12. Bauersachs, S.; Mitko, K.; Ulbrich, S. E.; Blum, H.; Wolf, E., Transcriptome studies of bovine endometrium reveal molecular profiles characteristic for specific stages of estrous cycle and early pregnancy. *Exp. Clin. Endocrinol. Diabetes* **2008,** 116, (7), 371-84.

13. Zhu, Z.; Boobis, A. R.; Edwards, R. J., Identification of estrogen-responsive proteins in MCF-7 human breast cancer cells using label-free quantitative proteomics. *Proteomics* **2008,** 8, (10), 1987-2005.

14. Collodoro, M.; Lemaire, P.; Eppe, G.; Bertrand, V.; Dobson, R.; Mazzucchelli, G.; Widart, J.; De Pauw, E.; De Pauw-Gillet, M. C., Identification and quantification of concentration-dependent biomarkers in MCF-7/BOS cells exposed to 17beta-estradiol by 2-D DIGE and label-free proteomics. *J. Proteomics* **2012,** 75, (14), 4555-69.

15. Dang, V. H.; Choi, K. C.; Hyun, S. H.; Jeung, E. B., Induction of uterine calbindin-D9k through an estrogen receptor-dependent pathway following single injection with xenobiotic agents in immature rats. *J. Toxicol. Environ. Health A* **2007,** 70, (2), 171-82.

16. Choi, K. C.; Leung, P. C.; Jeung, E. B., Biology and physiology of Calbindin-D9k in female reproductive tissues: involvement of steroids and endocrine disruptors. *Reprod. Biol. Endocrinol.* **2005,** 3, 66.

17. Choi, Y.; Seo, H.; Shim, J.; Kim, M.; Ka, H., Regulation of S100G Expression in the Uterine Endometrium during Early Pregnancy in Pigs. *Asian Australas. J. Anim. Sci.* **2012,** 25, (1), 44-51.

18. Vo, T. T.; Jeung, E. B., An evaluation of estrogenic activity of parabens using uterine calbindin-d9k gene in an immature rat model. *Toxicol. Sci.* **2009,** 112, (1), 68-77.

19. Vo, T. T.; An, B. S.; Yang, H.; Jung, E. M.; Hwang, I.; Jeung, E. B., Calbindin-D9k as a sensitive molecular biomarker for evaluating the synergistic impact of estrogenic chemicals on GH3 rat pituitary cells. *Int. J. Mol. Med.* **2012,** 30, (5), 1233-40.

20. Boverhof, D. R.; Fertuck, K. C.; Burgoon, L. D.; Eckel, J. E.; Gennings, C.; Zacharewski, T. R., Temporal- and dose-dependent hepatic gene expression changes in immature ovariectomized mice following exposure to ethynyl estradiol. *Carcinogenesis* **2004,** 25, (7), 1277-91.

21. Kiraly, R.; Demeny, M.; Fesus, L., Protein transamidation by transglutaminase 2 in cells: a disputed Ca^{2+}-dependent action of a multifunctional protein. *FEBS J.* **2011,** 278, (24), 4717-39.

22. Yoon, K.; Kwack, S. J.; Kim, H. S.; Lee, B. M., Estrogenic endocrine-disrupting chemicals: molecular mechanisms of actions on putative human diseases. *J. Toxicol. Environ. Health B Crit. Rev.* **2014,** 17, (3), 127-74.

23. Øverbye, A.; Brinchmann, M. F.; Seglen, P. O., Proteomic Analysis of Membrane-Associated Proteins from Rat Liver Autophagosomes. *Autophagy* **2014,** 3, (4), 300-322.

24. Zhang, Z.; Zhang, J.; Xiao, J., Selenoproteins and selenium status in bone physiology and pathology. *Biochim. Biophys. Acta* **2014,** 1840, (11), 3246-3256.

25. Porat, A.; Sagiv, Y.; Elazar, Z., A 56-kDa Selenium-binding Protein Participates in Intra-Golgi Protein Transport. *J. Biol. Chem.* **2000,** 275, (19).

26. Zhang, S.; Li, F.; Younes, M.; Liu, H.; Chen, C.; Yao, Q., Reduced selenium-binding protein 1 in breast cancer correlates with poor survival and resistance to the anti-proliferative effects of selenium. *PLoS One* **2013,** 8, (5), e63702.

27. Salgado, R. M.; Favaro, R. R.; Martin, S. S.; Zorn, T. M., The estrous cycle modulates small leucine-rich proteoglycans expression in mouse uterine tissues. *Anat. Rec.* **2009,** 292, (1), 138-53.

28. Salgado, R. M.; Favaro, R. R.; Zorn, T. M., Modulation of small leucine-rich proteoglycans (SLRPs) expression in the mouse uterus by estradiol and progesterone. *Reprod. Biol. Endocrinol.* **2011,** 9, 22.

29. Lucariello, A.; Trabucco, E.; Boccia, O.; Perna, A.; Sellitto, C.; Castaldi, M. A.; De Falco, M.; De Luca, A.; Cobellis, L., Small leucine rich proteoglycans are differently distributed in normal and pathological endometrium. *In Vivo* **2015,** 29, (2), 217-22.

30. Orlandi, A.; Ferlosio, A.; Ciucci, A.; Francesconi, A.; Lifschitz-Mercer, B.; Gabbiani, G.; Spagnoli, L. G.; Czernobilsky, B., Cellular retinol binding protein-1 expression in endometrial hyperplasia and carcinoma: diagnostic and possible therapeutic implications. *Mod. Pathol.* **2006,** 19, (6), 797-803.

31. Clawitter, J.; Trout, W.; Burke, M.; Araghi, S.; Roberts, R., A novel family of progesterone-induced, retinol-binding proteins from uterine secretions of the pig. *J. Biol. Chem.* **1990,** 265, (6), 3248-3255.

32. Moreno-Moya, J. M.; Vilella, F.; Martinez, S.; Pellicer, A.; Simon, C., The transcriptomic and proteomic effects of ectopic overexpression of miR-30d in human endometrial epithelial cells. *Mol. Hum. Reprod.* **2014,** 20, (6), 550-66.

33. Forde, N.; McGettigan, P. A.; Mehta, J. P.; O'Hara, L.; Mamo, S.; Bazer, F. W.; Spencer, T. E.; Lonergan, P., Proteomic analysis of uterine fluid during the pre-implantation period of pregnancy in cattle. *Reproduction* **2014,** 147, (5), 575-87.

34. Al Saleh, S.; Al Mulla, F.; Luqmani, Y. A., Estrogen receptor silencing induces epithelial to mesenchymal transition in human breast cancer cells. *PLoS One* **2011,** 6, (6), e20610.

35. Prokai-Tatrai, K.; Szarka, S.; Nguyen, V.; Sahyouni, F.; Walker, C.; White, S.; Talamantes, T.; Prokai, L., "All in the mind"? Brain-targeting chemical delivery system of 17beta-estradiol (Estredox) produces significant uterotrophic side effect. *Pharm. Anal. Acta.* **2012,** Suppl 7.

CHAPTER III

TARGETED PROTEOMIC ASSAY DEVELOPMENT AND OPTIMIZATION FOR THE VERIFICATION OF ESTROGEN-REGULATED PROTEINS

INTRODUCTION

In the previous chapter, we surveyed the rat uterus proteome after estrogen exposure to identify proteins showing statistically significant differences in expression levels using an untargeted mass spectrometry-based proteomics approach. In addition to identifying and quantifying those proteins affected by exposure to estrogen, we mapped those proteins to interaction networks to understand the impact E2 has on the uterus. From our untargeted experiment, we selected several, profoundly up- and down-regulated proteins for targeted validation, and also considering that they represent the pathways, biological functions, and diseases listed in Table 2.4 as fully as possible. Therefore, in this chapter we seek to validate these selected targets of E2's action found from our discovery-driven study of chapter 2. We approached validation by two methods: stable isotope dimethyl labeling and using heavy-isotope labeled internal standards.

EXPERIMENTAL STRATEGY

Chemicals

HPLC grade solvents were all obtained from Fisher Scientific (Atlanta, GA). Sequencing grade trypsin was from Applied Biosystems (Foster City, CA). All other chemicals were acquired through Sigma-Aldrich (St. Louis, MO), unless otherwise stated.

Animals

Ovariectomized adult Sprague Dawley rats weighing 200− 250 g were obtained from Charles Rivers Laboratories (Wilmington, DE, USA). Animals were kept under the standard 12 h light/12 h dark cycle, and the room temperature was maintained at 21 °C. Animals had full access to standard diet and water. Rats were treated according to institutional animal care and use guidelines.

Ovariectomy of the animals was done by their supplier (Charles River Laboratories, Wilmington, MA). The animals were shipped approximately one week after ovariectomy and were allowed to adapt in the animal facility of the University of North Texas Health Science Center for approximately two weeks before starting daily injections with the vehicle (corn oil, 60 µL per injection) control or E2 (50 µg/kg body weight in corn oil vehicle) for 5 consecutive days between 10:00 a.m. and 12:00 a.m. The animals were sacrificed by cervical dislocation, decapitated, and their brains were removed. An abdominal incision was then made and the uterus was removed by cutting at the junction of the uterus and vagina and at the site of the ovariectomy on each horn. Excess fat and connective tissues were removed, and the organ was blotted and weighed. All tissues were stored at -80 °C until sample preparation and analysis.

Trypsin Digestion

Approximately one-tenth of the whole uterus (10 mg control and 50 mg E2-treated) was incubated in 200 µL of 8M urea for 30 minutes. The samples were centrifuged for 5 minutes at 1400x g and the supernatant was collected. Protein content of uterine extracts was determined by a microBCA assay (Bio-RAD, CA). Approximately 100 µg of protein from each sample was used for further processing. Samples were reduced with 1 mM dithiothreitol (DTT) for 30 minutes at 65°C to reduce the disulfide bonds. Carbamidomethylation of the thiol groups was performed by the addition of 5 mM iodoacetamide (IAA) and incubation for 30 minutes at room temperature in the dark. Excess IAA was quenched by the addition of DTT for 5 minutes. The samples were diluted with 50 mM ammonium bicarbonate to lower the urea concentration to less than 2M. Samples were digested with sequencing grade trypsin (1:50, Applied Biosystems, Foster City, CA) overnight. Following tryptic digestion, the enzymatic reaction was terminated by acidifying the samples to pH <2.0 with acetic acid and the digests were desalted using C18 Sep-Pak solid-phase extraction cartridges (Waters, Milford, MA). The desalted uterine tryptic digests were further dried with a SpeedVac and subsequently reconstituted in 20 µL of 5% (v/v) acetonitrile in water containing 0.1% (v/v) acetic acid and aliquots of 5 µL were used for LC-MS/MS analyses.

Design of MRM Transitions for Targeted Quantitation

The initial protein panel was comprised of 12 candidate proteins (6 up- and 6 down-regulated) identified from our untargeted analysis (Table 3.1). Candidates were selected based on the criteria previously outlined (1, 2). Proteins that had at least 2 peptides identified and peptides that were identified in Scaffold with >95% probability, 2 proteotypic peptides were selected and

subjected to BLASTP analysis to confirm 100% homology, peptides did not have any missed cleavages, peptides did not have extensive post-translational modifications, and carbamidomethylated Cys was incorporated as a fixed modification in all peptides.

Initial method development for validation was done using a stable isotope dimethyl labeling approach (3-6). Synthetic peptides purchased from Synthetic Biomolecules (San Diego, CA) will be differentially labeled with light, intermediate and heavy dimethyl groups, resulting in mass shifts of +28 Da, +32 Da, and +36 Da, respectively, for each isotope variant. This reductive dimethylation allows for multiplexing of samples (5, 6). First, peptides in 100 mM TEAB (tetraethylammonium borohydride) (at 1 mg/mL) were incubated for 1 hr at 40°C with 0.5% formaldehyde (CH_2O) for light, formaldehyde-d_2 (CD_2O) for intermediate, and formaldehyde-^{13}C, d_2 ($^{13}CD_2O$) for heavy with 50 mM sodium cyanoborohydride ($NaBH_3CN$) for light and intermediate samples or sodium cyanoborodeuteride ($NaBD_3CN$) for heavy samples to block the N-termini and ε-amino groups of Lys of tryptic peptides. Excess formaldehyde (light, intermediate and heavy) was quenched with 0.5% ammonium hydroxide (NH_4OH). Samples were then acidified to pH ~3 with formic acid to decompose the sodium cyanoborohydride (or sodium cyanobordeuteride). The labeled peptides were then desalted by solid phase extraction (SPE, C18 Sep-Pak, Waters, Milford, MA). Peptides were used for direct infusion for method development (i.e., optimal transition selection and collision energy selection) and as quality control standards in this approach.

For method optimization involving stable isotope labeled internal standards (SIS), the target panel was narrowed down to 6 candidate proteins (3 up- and 3 down-regulated). This approach involves a comparison of the SRMs for native tryptic peptide levels (NAT) to the SRMs of the added SISs, which were purchased from New England Peptide (Gardner, MA).

Incorporation of the ^{13}C and ^{15}N isotopes was done at the C-terminal residue of tryptic peptides yielding mass shifts of +8 Da (from $^{13}C_6{}^{15}N_2$-lysine), +10 Da (from $^{13}C_6{}^{15}N_4$-arginine), and +7 Da (from $^{13}C_6{}^{15}N$-leucine) compared to their unlabeled counterparts. SIS peptides were used for refining the transition list, and as a mixture for quality control.

Sample Preparation for Targeted Analysis

Uterine protein extracts were first digested as described above. Then samples were either: a) put into pseudo-triplex by stable isotope dimethylation for initial method development using control and E2-treated samples, or b) spiked with SIS internal standards for method optimization using control and E2-treated samples. For the pseudo triplex approach, approximately 100 μg of each group of uterine protein extract was used for each isotope variant light, intermediate or heavy, and then mixed together (i.e. 2 controls to 1 treated or 2 treated to 1 control). For the SIS approach, approximately 200 μg of uterine protein extract was used and spiked with 25 ng of mixture of all SIS peptides.

Targeted LC-MRM-MS/MS Data Acquisition

The samples were analyzed in triplicate using a TSQ Quantum Ultra triple-quadrupole mass spectrometer (TSQ, Thermo Electron Corporation, Trace Chemical Analysis, Austin, TX) equipped with either a nano-electrospray ionization (NSI) or heated electrospray ionization (H-ESI) source and operated with Xcalibur (version 2.2) and LTQ Tune Plus (version 2.2) data acquisition software.

For NSI analysis, online reversed-phase high performance liquid chromatography (RP-HPLC) was performed with an Eksigent nano-LC-2D (Eksigent, Dublin, CA) system. An

amount of 5 µL of the sample was automatically loaded onto the IntegraFrit™ sample trap (2.5 cm x 75 µm) (New Objective, Woburn, MA), for sample concentration and desalting, at a flow rate of 1.5 µl/min in a loading solvent containing 0.1% (v/v) acetic acid and 5% (v/v) acetonitrile in 94.9% (v/v) water prior to injection onto a reverse-phase column (NAN75-15-03-C18-PM; 75 µm i.d. x 15 cm, LC Packings, Sunnyvale, CA) packed with C_{18} beads (3 µm, 100 Å pore size, PepMap). Mobile-phase buffer A consisted of 0.1% (v/v) acetic acid and 99.9% (v/v) water, and mobile-phase buffer B consisted of 0.1% (v/v) acetic acid and 99.9% (v/v) acetonitrile. Following desalting and injection onto the analytical column, peptides were separated using the following gradient program: 5% B to 40% B in 30 min, then ramped to 90% B in 5 min and held for 5 min, finally the column was ramped to 5% B in 2 min and equilibrated for 13 minutes. The flow rate through the column was 250 nL/min. Peptides eluted through a Picotip emitter (internal diameter 10 ± 1 µm; New Objective, Woburn, MA) and were directly sampled by the nano-electrospray source of the mass spectrometer. Spray voltage and capillary temperature during the gradient run were maintained at 2.0 kV and 250 ºC. Collision-induced dissociation was performed with argon at 1.5 mTorr pressure. Selected reaction monitoring (SRM) with unit mass resolution for the precursor and product ions was used for quantitation of peptides. Data acquisition and processing were controlled by the XCalibur software (version 2.1) of the instrument.

For H-ESI analysis, gradient separations were carried out using a Surveyor LC system (Thermo). The Phenomenex Aeris™ PEPTIDE XB-C18 column (150 x 2.10 mm, 3.6 µm particles) was operated at 0.4 mL/min flow rate and with the following gradient program: 2% B to 65% B in 30 min, then ramped to 95% B in 0.5 min and held for 3.5 min, finally the column was ramped to 2% B in 0.5 min and equilibrated for 10.5 minutes. The autosampler injection

volume was 10 μL and the tray temperature was maintained at 18 °C. H-ESI spray voltage, H-ESI temperature, and capillary temperature were maintained at 3.5 kV, 275 °C, and 300 °C, respectively. Nitrogen sheath gas and auxiliary gas flow rates were 30 and 20 arbitrary unit (corresponding to approximately 0.45 and 6.0 L/min according to the manufacturer's specification), respectively. Collision-induced dissociation was performed with argon at 1.5 mTorr pressure. Selected reaction monitoring (SRM) with unit mass resolution for the precursor and product ions was used for quantitation of peptides. Data acquisition and processing were controlled by the XCalibur software (version 2.1) of the instrument. A complete list of the MRM transitions used in this study is provided in Tables 3.2 and 3.3. To identify the MS/MS product ions of the peptides listed in these tables, we used the nomenclature introduced by Roepstorff and Fohlman (7), which is summarized schematically in Figure 3.1.

Targeted Quantitation Data Analysis

Manual verification of the extracted ion chromatogram peak selections was performed with XCalibur software (version 2.1). Area under the curve (AUC) of the relative abundance of each peak for each transition was calculated from within the Xcalibur software. Relative quantitation was done by first taking the average from the technical replicates of all samples for each peptide, and then comparing the ratio of AUC of control samples to treated samples in pseudo-triplex samples, or using the ratio of native proteotypic peptide (NAT) to SIS peptide, to obtain fold change increase or decrease.

RESULTS AND DISCUSSION

Using the selection criteria described, an initial panel of 12 proteins from our shotgun analysis (6 up- and 6 down-regulated) were chosen as putative markers of estrogenicity for targeted validation (Table 3.1). In selecting proteins for our biomarker panel, not only did we want those proteins that showed the greatest degree of differential expression from our shotgun study, but we also sought to strike a balance with selecting proteins in consensus with previous establishment as estrogen-regulated, as well as to probing novel findings. Of the 12 candidate proteins selected, 11 have been shown previously either by transcriptomics or proteomics (8-11) to be estrogen-regulated (TGM2, S100G, EF2, ATPA, RAN, SBP1, LUM, GSTP1, GSTM2, RBP1, CAPG). To our knowledge, one of these proteins is a completely novel finding with regards to estrogen (DPP2) and 6 of those that are established as estrogen-regulated are findings that are novel *in vivo* using proteomics (TGM2, S100G, SBP1, RAN, RBP1, CAPG). Figure 3.2 shows a heuristic network we built from these proteins. Pathways, biological functions and diseases captured by this network included, but not limited to, cell death and survival, metabolic disease, dermatological diseases and conditions, cell morphology, cancer, carbohydrate metabolism, nucleic acid metabolism, cellular assembly and organization, connective tissue disorders, organ morphology, and inflammatory disease.

Initial method development, using nanoLC-MS, involved the use of a pseudo-triplex dimethylation approach to increase throughput (5, 6). This technique also is cost-effective, because stable isotope labeling relies on a few, inexpensive reagents. A full list of all MRM transitions used in method development is provided in Table 3.2. Synthetic peptides were differentially labelled with stable isotope dimethyl groups, which label the N-terminus and lysine

residues. The labeling scheme of the pseudo triplex is shown in Figure 3.3. Labeled peptides were analyzed individually and in mixtures to select the optimal conditions for MRM targeted quantitation. Because of the number of transitions, and the limitations with retention time scheduling, we used 2 methods to cover all transitions for all peptides.

Once the conditions were established, control and E2-treated uterus protein extracts were digested and differentially labeled. We verified the conditions in biological matrix using the control and treated uterus digests individually spiked with labeled QC peptides in varying combinations (for example, light labeled tissue digest mixed with medium and heavy labeled QC peptides, etc.). Then, each pseudo triplex was combined into one vial for analysis (i.e., light labeled control, medium labeled E2-treated, and heavy labeled control). While this approach allowed for the multiplexing of samples and the labeling was reliable, interferences were introduced that did not allow for accurate quantitation, and in most cases left complete noise.

In attempting to multiplex the samples in the assay using stable isotope-coded dimethylation (5, 6), we encountered a number of issues. While this approach seemed promising, as it increased throughput while keeping costs low compared to the use of specific isotope-labeled internal standards, the drawbacks were too great to overcome. The additional sample preparation introduced sample complexities, which manifested as “chemical noise” in the spectra and potential matrix effects that suppressed signals. Also, the approach was more labor-intensive, and did not work in our practice for the purpose of validation by the LC-MRM-based targeted proteomics method. We were able to verify one protein, EF2, but all other proteins were not verified convincingly due to spectral interference. Altogether, we considered this a failed effort and instead chose to use stable isotope labeled internal standards that, while more expensive, have been a proven methodology for quantitation (3, 4, 12).

In order to continue method optimization, we simplified the sample preparation and used stable isotope labeled internal standards spiked into digests (Figure 3.4). In this approach, the proteotypic tryptic peptide level from the endogenous protein ("native," NAT) is compared to a known concentration of its stable isotope labeled internal standard (SIS). The ratio of the area under the curve of NAT/SIS is what is compared to determine the relative fold change differences between treatments. Although more expensive, this approach is more reliable given the samples do not undergo as much processing and less interferences are introduced. In addition, we narrowed down the panel to 6 proteins (3 up- and 3 down-regulated) that were the most amenable to targeted analysis and showed the most promise as part of a panel as markers of estrogenicity. Figure 3.5 shows a heuristic network we built from these proteins, which also captured the majority of pathways, biological functions and diseases represented in Figure 3.2 including cell death and survival, metabolic disease, carbohydrate metabolism, nucleic acid metabolism, cell morphology, cellular assembly and organization, connective tissue disorders, organ morphology, and inflammatory disease. Initial conditions were established from the SIS peptides, which were also used as quality control (QC) peptides. These QC samples were used to monitor the performance of the LC-MS system, the method, the sample preparation, and to assess the integrity and validity of the results of the unknown samples analyzed based on shifts in retention times and relative fragment ratios (13-15). We chose small-bore (2.1mm) LC-MS because of robustness and easy method transfer among platforms compared to nanoflow separation (16). Once MRM conditions were established, control and E2-treated tissue digests were spiked with a mixture of all SIS peptides. Here, we were able to set up one method with retention time scheduling of the peptides. We verified the use of NAT/SIS approach with the biological matrix. A list of the optimized MRM transitions is shown in Table 3.3.

CONCLUSIONS

In developing a targeted proteomics assay for markers of estrogenicity, we aimed to validate the discovery-driven findings from chapter 2. Development of a valid assay will complement the assay for uterotrophic effects by providing a complementary testing technology that makes use of molecular targets. We have been able to develop a targeted assay suitable for validation of our findings using our selected panel of 6 candidate proteins to a known estrogenic EDC.

Table 3.1. A putative panel of candidate biomarkers of estrogenicity identified by untargeted analysis.

Protein Name	Gene Name	Peptide Sequences	Induction Status Upon E2 exposure
Protein S100-G**	*S100g*	LLIQSEFPSLLK ASSTLDNLFK	Activated
Transglutaminase 2**	*Tgm2*	YSGCLTESNLIK SEGTYCCGPVSVR	Activated
Elongation factor 2**	*Ef2*	EGIPALDNFLDKL TFCQLILDPIFK	Activated
Macrophage-capping protein	*Capg*	EVQGNESDLFMSYFPQGLK QAALQVADGFISR	Activated
ATP synthase subunit alpha, mitochondrial	*Atpa*	TGTAEMSSILEER VVDALGNAIDGK	Activated
GTP-binding nuclear protein	*Ran*	SNYNFEKPFLWLAR VCENIPIVLCGNK	Activated

Selenium-binding protein 1**	*Sbp1*	HEIIQTLQMK LILPSIISSR	Repressed
Lumican**	*Lum*	NNQIDHIDEK SLEYLDLSFNQMSK	Repressed
Dipeptidyl peptidase 2**	*Dpp2*	ASNSEDPPSVVEVR DLTQLFGFAR	Repressed
Glutathione S-transferase P	*Gstp1*	YGTLIYTNYENGKDDYVK EAALVDMVNDGVEDLR	Repressed
Glutathione S-transferase Mu 2	*Gstm2*	LQLAMVCYSPDFER PMTLGYWDIR	Repressed
Retinol-binding protein 1	*Rbp1*	CMTTVSWDGDKLQCVQK MLSNENFEEYLR	Repressed

**Subset of proteins selected for validation by targeted proteomics using the stable isotope labeled internal standard (SIS) method

Table 3.2. List of all MRM transitions used for relative quantitation analysis with pseudo-triplex approach of reductive dimethylation.

Peptide Sequence	Light Precursor *m/z*	Light Fragment *m/z*	Intermediate Precursor *m/z*	Intermediate Fragment *m/z*	Heavy Precursor *m/z*	Heavy Fragment *m/z*	Collison Energy	Fragment Ion	Protein ID
YSGC[@]LTESNLIK	720.8	163.9	724.8	167.9	728.8	171.9	35	a1	TGM2
YSGC[@]LTESNLIK	720.8	1250.1	724.8	1254.1	728.8	1258.1	26	y11	TGM2
SEGTYC[@]C[@]GPVSVR	750.3	216.9	752.3	220.9	754.3	224.9	32	a2	TGM2
SEGTYC[@]C[@]GPVSVR	750.3	934.5	752.3	934.5	754.3	934.5	29	y8	TGM2
LLIQSEFPSLLK	722.0	113.9	726.0	117.9	730.0	121.9	34	a1	S100G
LLIQSEFPSLLK	722.0	584.3	726.0	588.3	730.0	592.3	31	y5 or b5	S100G
ASSTLDNLFK	575.8	548.3	579.8	552.3	583.8	556.3	23	y4	S100G
ASSTLDNLFK	575.8	1051.7	579.8	1055.7	583.8	1059.7	21	y9	S100G
EGIPALDNFLDKL	751.0	129.9	755.0	133.9	759.0	137.9	35	a1	EF2
EGIPALDNFLDKL	751.0	214.9	755.0	218.9	759.0	222.9	34	b2	EF2
TFC[@]QLILDPIFK	776.0	101.9	780.0	105.9	784.0	109.9	35	a1	EF2
TFC[@]QLILDPIFK	776.0	532.3	780.0	536.3	784.0	540.3	33	y4	EF2
TGTAEMSSILEER	726.4	101.9	728.4	105.9	730.4	109.9	35	a1	ATPA

TGTAEMSSILEER	726.4	1323.1	728.4	1323.1	730.4	1323.1	28	y12	ATPA
VVDALGNAIDGK	614.3	231.9	618.3	235.9	622.3	239.9	33	y2	ATPA
VVDALGNAIDGK	614.3	702.3	618.3	706.3	622.3	710.3	31	y7	ATPA
EVQGNESDLFMSYFPQGLK	749.4	570.3	752.0	574.3	754.7	578.3	22	y5	CAPG
EVQGNESDLFMSYFPQGLK	749.4	717.4	752.0	721.4	754.7	725.4	16	y6	CAPG
QAALQVADGFISR	702.4	128.9	704.4	132.9	706.4	136.9	35	a1	CAPG
QAALQVADGFISR	702.4	579.2	704.4	579.2	706.4	579.2	33	y5	CAPG
SNYNFEKPFLWLAR	920.9	229.9	924.9	233.9	928.9	237.9	42	b2	RAN
SNYNFEKPFLWLAR	920.9	902.6	924.9	902.6	928.9	902.6	36	y7	RAN
VC$^{@}$ENIPIVLC$^{@}$GNK	786.5	287.8	790.5	291.8	794.5	295.8	29	b2	RAN
VC$^{@}$ENIPIVLC$^{@}$GNK	786.5	928.6	790.5	932.6	794.5	936.6	27	y8	RAN
HEIIQTLQMK	648.9	137.9	652.9	141.9	656.9	145.9	36	a1	SBP1
HEIIQTLQMK	648.9	1131.9	652.9	1135.9	656.9	1139.9	26	y9	SBP1
LILPSIISSR	563.9	113.9	565.9	117.9	567.9	121.9	35	a1	SBP1
LILPSIISSR	563.9	985.7	565.9	985.7	567.9	985.7	21	y9	SBP1
NNQIDHIDEK	641.3	114.9	645.3	118.9	649.3	122.9	35	a1	LUM

NNQIDHIDEK	641.3	784.3	645.3	788.3	649.3	792.3	26	y6	LUM
SLEYLDLSFNQMSK	866.1	357.9	870.1	361.9	874.1	365.9	36	b3	LUM
SLEYLDLSFNQMSK	866.1	521.2	870.1	525.2	874.1	529.2	32	y4	LUM
ASNSEDPPSVVEVR	757.4	632.2	759.4	636.2	761.4	640.2	32	b6	DPP
ASNSEDPPSVVEVR	757.4	882.5	759.4	882.5	761.4	882.5	27	y8	DPP
DLTQLFGFAR	598.4	115.8	600.4	119.8	602.4	123.8	34	a1	DPP
DLTQLFGFAR	598.4	597.2	600.4	597.2	602.4	597.2	22	y5	DPP
YGTLIYTNYENGKDDYVK	747.8	163.9	751.8	167.9	755.8	171.9	34	a1	GSTP1
YGTLIYTNYENGKDDYVK	747.8	437.1	751.8	441.1	755.8	445.1	28	y3	GSTP1
EAALVDMVNDGVEDLR	887.6	129.9	889.6	133.9	891.6	137.9	36	a1	GSTP1
EAALVDMVNDGVEDLR	887.6	299.9	889.6	303.9	891.6	307.9	39	b3	GSTP1
LQLAMVCYSPDFER	878.9	114.0	880.9	118.0	882.9	122.0	35	a1	GSTM2
LQLAMVCYSPDFER	878.9	454.4	880.9	458.4	882.9	462.4	30	b4	GSTM2
#PMTLGYWDIR	633.4	214.9	634.4	216.9	635.4	218.9	28	a2	GSTM2
#PMTLGYWDIR	633.4	288.0	634.4	288.0	635.4	288.0	28	y2	GSTM2
MLSNENFEEYLR	786.5	131.9	788.5	135.9	790.5	139.9	33	a1	RBP1

MLSNENFEEYLR	786.5	1413.3	788.5	1413.3	790.5	1413.3	26	y11	RBP1
$C^{@}$MTTVSWDGDKLQ$C^{@}$VQK	nd	nd	nd	nd	nd	nd	nd	nd	RBP1
$C^{@}$MTTVSWDGDKLQ$C^{@}$VQK	nd	nd	nd	nd	nd	nd	nd	nd	RBP1

Light is peptide labeled on N-terminal amino acid and lysine with C_2H_4, giving mass shift of +28 Da compared to non-labeled counterpart.

Intermediate is peptide labeled on N-terminal amino acid and lysine with $C_2{}^2H_4$, giving mass shift of +32 Da compared to non-labeled counterpart.

Heavy is peptide labeled on N-terminal amino acid and lysine with $^{13}C_2{}^2H_5$, giving mass shift of +36 Da compared to non-labeled counterpart.

$C^{@}$ is carbamidomethylated cysteine.

$^{\#}$P is N-terminal proline where the amino acid is observed to be labeled with monomethyl CH_2, giving mass shift of +14 Da compared to non-labeled counterpart.

nd means not detected.

Table 3.3. List of final optimized MRM transitions used for relative quantitation analysis with isotope labeled internal standards.

Peptide Sequence	NAT Precursor *m/z*	NAT Fragment *m/z*	SIS Precursor *m/z*	SIS Fragment *m/z*	Collison Energy	Fragment Ion	Retention Time Segment (in min)	Dwell Time (in ms)	Protein ID
YSGC[@]LTESNLIK	692.8	804.5	696.9	812.7	24	**y7**	0-12	17	TGM2
YSGC[@]LTESNLIK	692.8	917.6	696.9	925.8	24	y8	0-12	17	TGM2
SEGTYC[@]C[@]GPVSVR	736.2	934.7	741.4	944.6	33	y8	0-12	17	TGM2
SEGTYC[@]C[@]GPVSVR	736.2	614.5	741.4	624.3	24	**y6**	0-12	17	TGM2
LLIQSEFPSLLK	694	919.7	698.5	928.6	27	**y8**	0-12	17	S100G
LLIQSEFPSLLK	694	556.3	698.5	565.4	27	y5	0-12	17	S100G
ASSTLDNLFK	547.8	748.4	552.3	757.5	20	y6	0-12	17	S100G
ASSTLDNLFK	547.8	459.7	552.3	464.2	19	**y8-H_2O^{++}**	0-12	17	S100G
HEIIQTLQMK	620.9	266.9	624.9	266.9	28	**b2**	0-12	17	SBP1
HEIIQTLQMK	620.9	362.0	624.9	362.0	33	b3-H2O	0-12	17	SBP1
NNQIDHIDEK	613.3	257.9	617.3	265.9	24	**y2-H_2O**	0-12	17	LUM
NNQIDHIDEK	613.3	275.9	617.3	283.9	27	y2	0-12	17	LUM
ASNSEDPPSVVEVR	743.4	882.5	748.4	892.6	24	**y8**	0-12	17	DPP

ASNSEDPPSVVEVR	743.4	997.6	748.4	1007.7	21	y9	0-12	17	DPP
TFC[@]QLILDPIFK	747.8	504.2	752	512.3	29	**y4**	12-15	25	EF2
TFC[@]QLILDPIFK	747.8	845.9	752	853.6	25	y7	12-15	25	EF2
LLIQSEFPSLLK	694	919.7	698.5	928.6	27	**y8**	12-15	25	S100G
LLIQSEFPSLLK	694	556.3	698.5	565.4	27	y5	12-15	25	S100G
ASSTLDNLFK	547.8	748.4	552.3	757.5	20	y6	12-15	25	S100G
ASSTLDNLFK	547.8	459.7	552.3	464.2	19	**y8-H_2O^{++}**	12-15	25	S100G
LILPSIISSR	549.9	759.5	554.9	769.5	24	y7	12-15	25	SBP1
LILPSIISSR	549.9	227.0	554.9	227.0	20	**b2**	12-15	25	SBP1
SLEYLDLSFNQMSK	838.1	841.4	842.1	849.5	25	**y7**	12-15	25	LUM
SLEYLDLSFNQMSK	838.1	1069.6	842.1	1077.8	23	y9	12-15	25	LUM
EGIPALDNFLDKL	722.8	573.5	726.4	576.8	23	**$y10^{++}$**	15-45	25	EF2
EGIPALDNFLDKL	722.8	186.8	726.4	186.8	29	b2	15-45	25	EF2
TFC[@]QLILDPIFK	747.8	504.2	752	512.3	29	**y4**	15-45	25	EF2
TFC[@]QLILDPIFK	747.8	845.9	752	853.6	25	y7	15-45	25	EF2
DLTQLFGFAR	584.3	597.3	589.3	607.3	16	**y5**	15-45	25	DPP

DLTQLFGFAR	584.3	710.4	589.3	720.4	23	y6	15-45	25	DPP
LLIQSEFPSLLK	694	919.7	698.5	928.6	27	**y8**	15-45	25	S100G
LLIQSEFPSLLK	694	556.3	698.5	565.4	27	y5	15-45	25	S100G
SLEYLDLSFNQMSK	838.1	841.4	842.1	849.5	25	**y7**	15-45	25	LUM
SLEYLDLSFNQMSK	838.1	1069.6	842.1	1077.8	23	y9	15-45	25	LUM

NAT is endogenous proteotypic tryptic peptide.
SIS is stable isotope labeled peptide labeled on C-terminal amino acid, giving mass shift of +8 Da (from $^{13}C_6{}^{15}N_2$-lysine), +10 Da (from $^{13}C_6{}^{15}N_4$-arginine), and +7 Da (from $^{13}C_6{}^{15}N$-leucine) compared to non-labeled counterpart (NAT).
$C^{@}$ is carbamidomethylated cysteine.
Bolded fragment ion indicates quantifier ion, and other fragment ion for each peptide is qualifier ion.

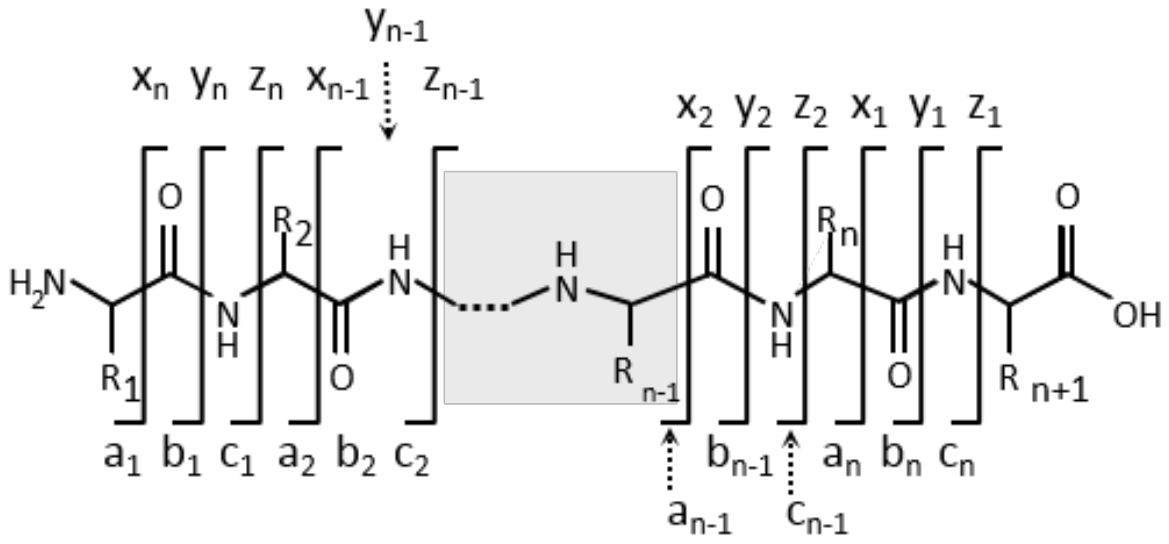

Figure 3.1. The nomenclature of fragment ions for peptides according to Roepstorff and Fohlman (7).

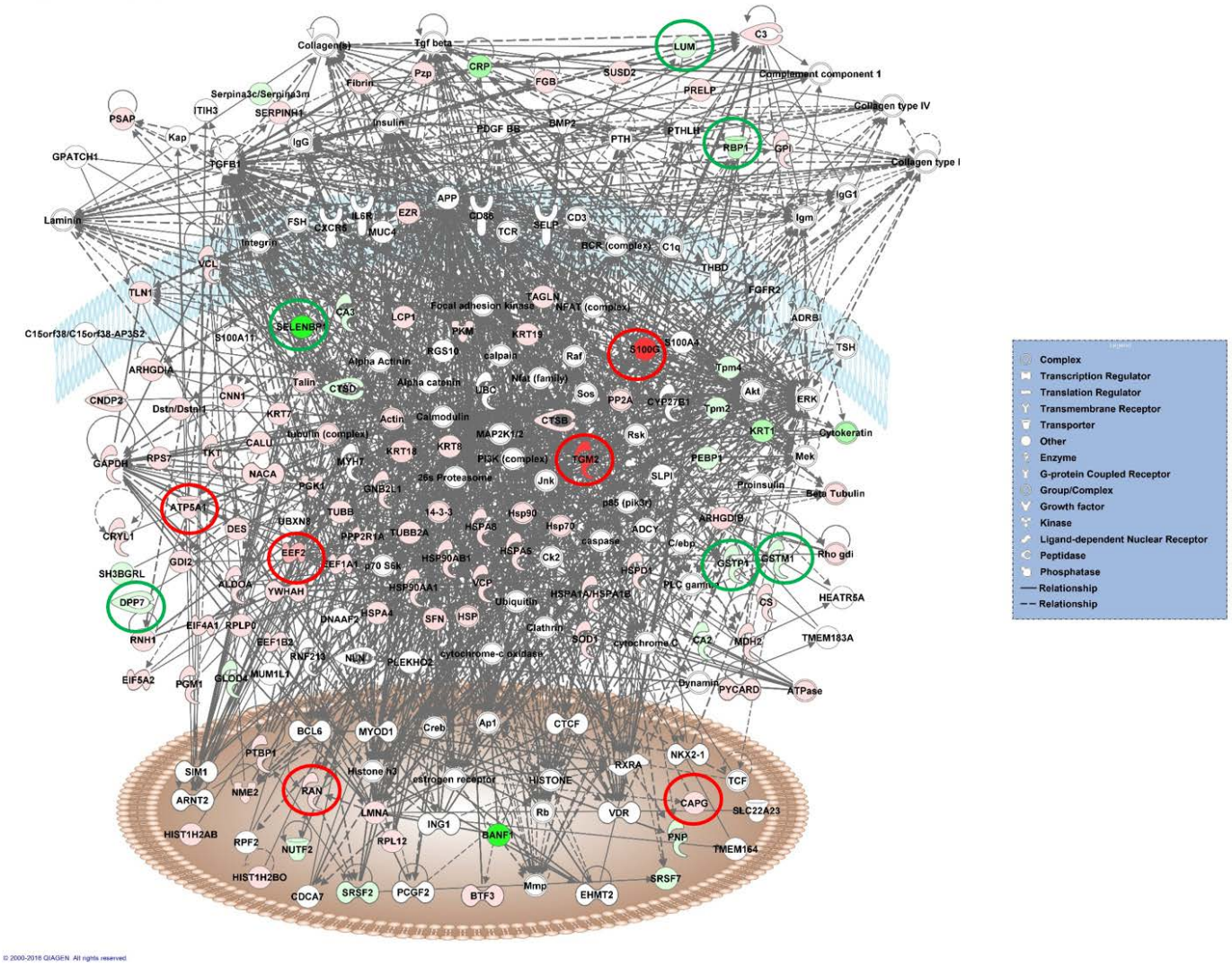

Figure 3.2. A heuristic IPA network we built from the proteins listed in Table 3.1. It captures biological processes and diseases associated with cell death and survival, metabolic disease, dermatological diseases and conditions, cell morphology, cancer,

carbohydrate metabolism, nucleic acid metabolism, cellular assembly and organization, connective tissue disorders, organ morphology, and inflammatory disease.

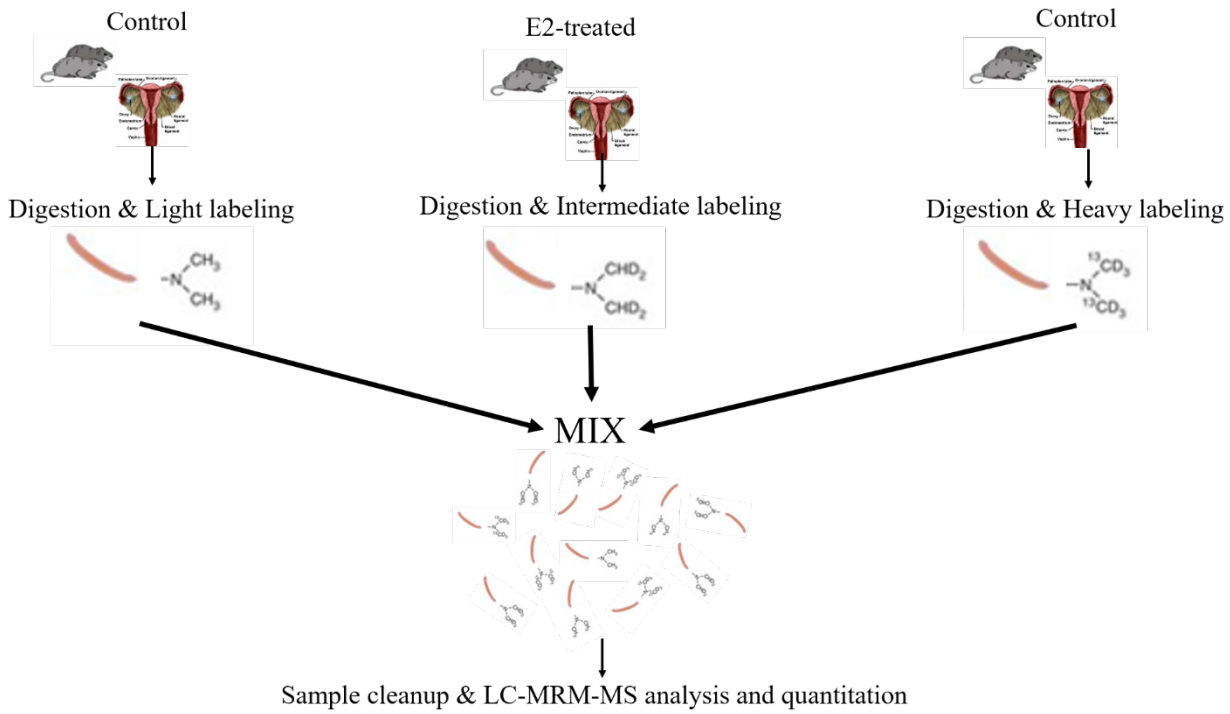

Figure 3.3. A schematic representation of the pseudo-triplex reductive dimethylation approach for targeted quantitation.

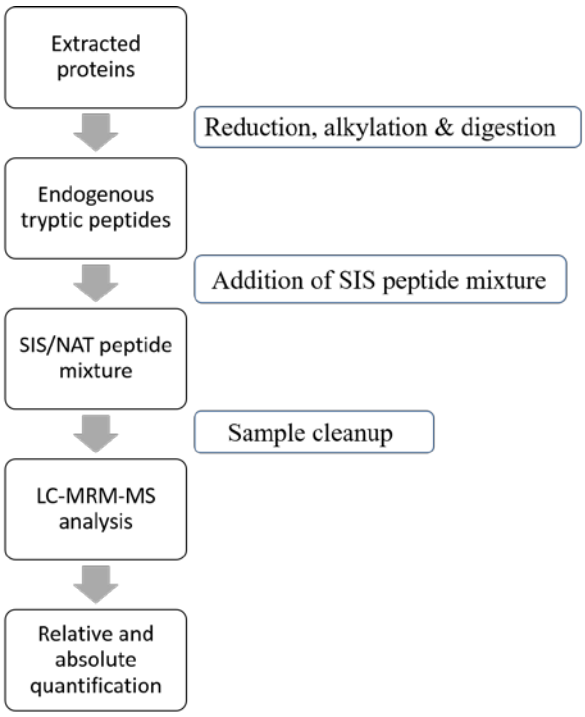

Figure 3.4. A schematic representation of the stable isotope dilution, or AQUA, approach for targeted quantitation.

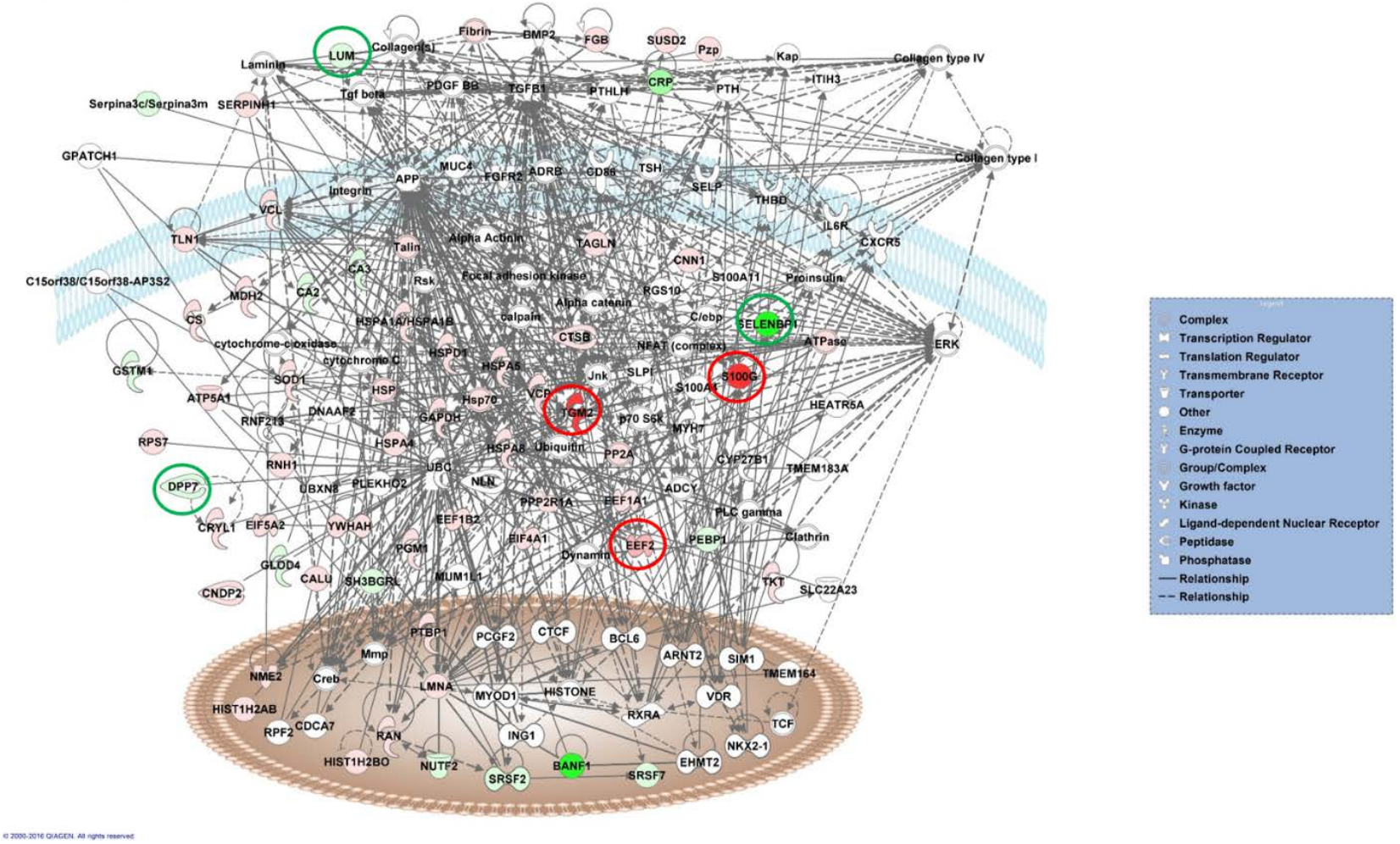

Fig. 3.5. A heuristic IPA network we built from a subset of proteins listed in Table 3.1 and selected for validation by targeted proteomics using the stable isotope labeled internal standard (SIS) method of Figure 3.4. It captures biological processes and

diseases associated with cell death and survival, metabolic disease, carbohydrate metabolism, nucleic acid metabolism, cell morphology, cellular assembly and organization, connective tissue disorders, organ morphology, and inflammatory disease.

REFERENCES

1. Lange, V.; Picotti, P.; Domon, B.; Aebersold, R., Selected reaction monitoring for quantitative proteomics: a tutorial. *Mol. Syst. Biol.* **2008,** 4, 222.

2. Picotti, P.; Aebersold, R., Selected reaction monitoring-based proteomics: workflows, potential, pitfalls and future directions. *Nat. Methods* **2012,** 9, (6), 555-66.

3. Bantscheff, M.; Schirle, M.; Sweetman, G.; Rick, J.; Kuster, B., Quantitative mass spectrometry in proteomics: a critical review. *Anal. Bioanal. Chem.* **2007,** 389, (4), 1017-31.

4. Bantscheff, M.; Lemeer, S.; Savitski, M. M.; Kuster, B., Quantitative mass spectrometry in proteomics: critical review update from 2007 to the present. *Anal. Bioanal. Chem.* **2012,** 404, (4), 939-65.

5. Boersema, P. J.; Raijmakers, R.; Lemeer, S.; Mohammed, S.; Heck, A. J., Multiplex peptide stable isotope dimethyl labeling for quantitative proteomics. *Nat. Protoc.* **2009,** 4, (4), 484-94.

6. Song, C.; Wang, F.; Ye, M.; Cheng, K.; Chen, R.; Zhu, J.; Tan, Y.; Wang, H.; Figeys, D.; Zou, H., Improvement of the quantification accuracy and throughput for phosphoproteome analysis by a pseudo triplex stable isotope dimethyl labeling approach. *Anal. Chem.* **2011,** 83, (20), 7755-62.

7. Roepstorff, P.; Fohlman, J., Proposal for a common nomenclature for sequence ions in mass spectra of peptides. *Biomed. Mass Spectrom.* **1984,** 11, (11), 601.

8. Bauersachs, S.; Mitko, K.; Ulbrich, S. E.; Blum, H.; Wolf, E., Transcriptome studies of bovine endometrium reveal molecular profiles characteristic for specific stages of estrous cycle and early pregnancy. *Exp. Clin. Endocrinol. Diabetes* **2008,** 116, (7), 371-84.

9. Watanabe, H.; Suzuki, A.; Kobayashi, M.; Takahashi, E.; Itamoto, M.; Lubahn, D. B.; Handa, H.; Iguchi, T., Analysis of temporal changes in the expression of estrogen-regulated genes in the uterus. *J. Mol. Endocrinol.* **2003,** 30, (3), 347-358.

10. Watanabe, H.; Suzuki, A.; Mizutani, T.; Khono, S.; Lubahn, D. B.; Handa, H.; Iguchi, T., Genome-wide analysis of changes in early gene expression induced by oestrogen. *Genes Cells* **2002,** 7, (5), 497-507.

11. Prokai, L.; Stevens, S. M., Jr.; Rauniyar, N.; Nguyen, V., Rapid label-free identification of estrogen-induced differential protein expression in vivo from mouse brain and uterine tissue. *J. Proteome Res.* **2009,** 8, (8), 3862-71.

12. Villanueva, J.; Carrascal, M.; Abian, J., Isotope dilution mass spectrometry for absolute quantification in proteomics: concepts and strategies. *J. Proteomics* **2014,** 96, 184-99.

13. United States Department of Health and Human Services Food and Drug Administration, Guide for Industry Bioanalytical Method Validation. In May 2001 ed.; Center for Drug Evaluation and Research, Ed. 2001.

14. Albar, J. P.; Canals, F., Standardization and quality control in proteomics. *J. Proteomics* **2013,** 95, 1-2.

15. Teleman, J.; Waldemarson, S.; Malmstrom, J.; Levander, F., Automated quality control system for LC-SRM setups. *J. Proteomics* **2013,** 95, 77-83.

16. Percy, A. J.; Chambers, A. G.; Yang, J.; Domanski, D.; Borchers, C. H., Comparison of standard- and nano-flow liquid chromatography platforms for MRM-based quantitation of putative plasma biomarker proteins. *Anal. Bioanal. Chem.* **2012,** 404, (4), 1089-101.

CHAPTER IV

APPLICATION OF TARGETED PROTEOMIC ASSAY FOR THE VALIDATION OF ESTROGENIC EFFECTS IN RATS USING BPA AS A PROTOTYPIC EDC

INTRODUCTION

In the previous chapter, a targeted proteomics assay was developed to validate putative protein markers of estrogenicity in the rat uterus. In this chapter, we aim at validating the panel of 6 uterus protein markers in rats exposed to two doses of BPA, a known estrogenic EDC.

EXPERIMENTAL STRATEGY

Chemicals

HPLC grade solvents were all obtained from Fisher Scientific (Atlanta, GA). Sequencing grade trypsin was from Applied Biosystems (Foster City, CA). All other chemicals were acquired through Sigma-Aldrich (St. Louis, MO), unless otherwise stated.

Animals

Ovariectomized adult Sprague Dawley rats weighing 200− 250 g were obtained from Charles Rivers Laboratories (Wilmington, DE, USA). Animals were kept under the standard 12 h

light/12 h dark cycle, and the room temperature was maintained at 21 °C. Animals had full access to standard diet and water. Rats were treated according to institutional animal care and use guidelines.

Ovariectomy of the animals was done by their supplier (Charles River Laboratories, Wilmington, MA). The animals were shipped approximately one week after ovariectomy and were allowed to adapt in the animal facility of the University of North Texas Health Science Center for approximately two weeks before starting daily injections with the vehicle (corn oil, 60 µL per injection) control, E2 (50 µg/kg body weight in corn oil vehicle), or BPA (100 mg/kg or 300 mg/kg body weight in corn oil vehicle) for 5 consecutive days between 10:00 a.m. and 12:00 a.m. The animals were sacrificed by cervical dislocation, decapitated, and their brains were removed. An abdominal incision was then made and the uterus was removed by cutting at the junction of the uterus and vagina and at the site of the ovariectomy on each horn. Excess fat and connective tissues were removed, and the organ was blotted and weighed. All tissues were stored at -80 °C until sample preparation and analysis.

Trypsin Digestion

Approximately one-tenth of the whole uterus (10 mg control and 50 mg E2-treated) was incubated in 200 µL of 8M urea for 30 minutes. The samples were centrifuged for 5 minutes at 1400x g and the supernatant was collected. Protein content of uterine extracts was determined by a microBCA assay (Bio-RAD, CA). Approximately 100 µg of protein from each sample was used for further processing. Samples were reduced with 1 mM dithiothreitol (DTT) for 30 minutes at 65°C to reduce the disulfide bonds. Carbamidomethylation of the thiol groups was performed by the addition of 5 mM iodoacetamide (IAA) and incubation for 30 minutes at room temperature in

the dark. Excess IAA was quenched by the addition of DTT for 5 minutes. The samples were diluted with 50 mM ammonium bicarbonate to lower the urea concentration to less than 2M. Samples were digested with sequencing grade trypsin (1:50, Applied Biosystems, Foster City, CA) overnight. Following tryptic digestion, the enzymatic reaction was terminated by acidifying the samples to pH <2.0 with acetic acid and the digests were desalted using C18 Sep-Pak solid-phase extraction cartridges (Waters, Milford, MA). The desalted uterine tryptic digests were further dried with a SpeedVac and subsequently reconstituted in 20 µL of 5% (v/v) acetonitrile in water containing 0.1% (v/v) acetic acid and aliquots of 5 µL were used for LC-MS/MS analyses.

Target panel and internal standards

The target panel was comprised of 6 candidate proteins (3 up- and 3 down-regulated) (Table 3.1). This approach involved the use of stable isotope labeled internal standards (SIS) for comparison against native tryptic peptide levels (NAT). The internal standards were stable isotope labeled synthetic analogs of each endogenous peptide which were purchased from New England Peptide (Gardner, MA). Incorporation of the ^{13}C and ^{15}N isotopes was done at the C-terminal residue of tryptic peptides yielding mass shifts of +8 Da (from $^{13}C_6{}^{15}N_2$-lysine), +10 Da (from $^{13}C_6{}^{15}N_4$-arginine), and +7 Da (from $^{13}C_6{}^{15}N$-leucine) compared to their unlabeled counterparts. SIS peptides were used as a mixture for quality control.

Sample Preparation for Targeted Analysis

Uterine protein extracts were first digested as described above. Then, samples were spiked with SIS internal standards for analysis using control, E2-, and BPA-treated (100 mg/kg

and 300 mg/kg) samples. Approximately 200 µg of uterine protein extract was used and spiked with 25 ng of a mixture of all SIS peptides.

Targeted LC-MRM-MS/MS Data Acquisition

The samples were analyzed in triplicate using a TSQ Quantum Ultra tripe-quadrupole mass spectrometer (TSQ, Thermo Electron Corporation, Trace Chemical Analysis, Austin, TX) equipped with either a nano-electrospray ionization (NSI) or heated electrospray ionization (H-ESI) source and operated with Xcalibur (version 2.2) and LTQ Tune Plus (version 2.2) data acquisition software.

For NSI analysis, online reversed-phase high performance liquid chromatography (RP-HPLC) was performed with an Eksigent nano-LC-2D (Eksigent, Dublin, CA) system. An amount of 5 µL of the sample was automatically loaded onto the IntegraFrit™ sample trap (2.5 cm x 75 µm) (New Objective, Woburn, MA), for sample concentration and desalting, at a flow rate of 1.5 µl/min in a loading solvent containing 0.1% (v/v) acetic acid and 5% (v/v) acetonitrile in 94.9% (v/v) water prior to injection onto a reverse-phase column (NAN75-15-03-C18-PM; 75 µm i.d. x 15 cm, LC Packings, Sunnyvale, CA) packed with C_{18} beads (3 µm, 100 Å pore size, PepMap). Mobile-phase buffer A consisted of 0.1% (v/v) acetic acid and 99.9% (v/v) water, and mobile-phase buffer B consisted of 0.1% (v/v) acetic acid and 99.9% (v/v) acetonitrile. Following desalting and injection onto the analytical column, peptides were separated using the following gradient program: 5% B to 40% B in 30 min, then ramped to 90% B in 5 min and held for 5 min, finally the column was ramped to 5% B in 2 min and equilibrated for 13 minutes. The flow rate through the column was 250 nL/min. Peptides eluted through a Picotip emitter (internal diameter 10 ± 1 µm; New Objective, Woburn, MA) and were directly sampled by the nano-

electrospray source of the mass spectrometer. Spray voltage and capillary temperature during the gradient run were maintained at 2.0 kV and 250 ºC. Collision-induced dissociation was performed with argon at 1.5 mTorr pressure. Selected reaction monitoring (SRM) with unit mass resolution for the precursor and product ions was used for quantitation of peptides. Data acquisition and processing were controlled by the XCalibur software (version 2.1) of the instrument.

For H-ESI analysis, gradient separations were carried out using a Surveyor LC system (Thermo). The Phenomenex Aeris™ PEPTIDE XB-C18 column (150 x 2.10 mm, 3.6 µm particles) was operated at 0.4 mL/min flow rate and with the following gradient program: 2% B to 65% B in 30 min, then ramped to 95% B in 0.5 min and held for 3.5 min, finally the column was ramped to 2% B in 0.5 min and equilibrated for 10.5 minutes. The autosampler injection volume was 10 µL and the tray temperature was maintained at 18 °C. H-ESI spray voltage, H-ESI temperature, and capillary temperature were maintained at 3.5 kV, 275 °C, and 300 °C, respectively. Nitrogen sheath gas and auxiliary gas flow rates were 30 and 20 arbitrary unit (corresponding to approximately 0.45 and 6.0 L/min according to the manufacturer's specification), respectively. Collision-induced dissociation was performed with argon at 1.5 mTorr pressure. Selected reaction monitoring (SRM) with unit mass resolution for the precursor and product ions was used for quantitation of peptides. Data acquisition and processing were controlled by the XCalibur software (version 2.1) of the instrument. A complete list of the MRM transitions used in this study is provided in Table 3.3.

Targeted Quantitation Data Analysis

Manual verification of the extracted ion chromatogram peak selections was performed with XCalibur software (version 2.1). Area under the curve (AUC) of the relative abundance of each peak for each transition was calculated from within the Xcalibur software. Relative quantitation was done by first taking the average from the technical replicates of all samples for each peptide, and then using the ratio of native peptide (NAT) to SIS peptide, comparing controls and treated samples to get any fold change increase or decrease. Relative ratios of SIS internal standards to endogenous peptide, for each peptide, were normalized to control to get fold change differences.

Statistical analysis of the relative fold change of peptides was performed using a one-way ANOVA with Tukey's post hoc test. $P<0.05$ was considered statistically significant.

RESULTS AND DISCUSSION

For validating our panel of 6 estrogen-regulated uterus proteins (Table 3.1), we used high and low doses of BPA (100 mg/kg and 300 mg/kg) exposure in comparison to E2 and control-treated animals, as shown previously (1-3). We applied our NAT/SIS targeted assay to find the relative abundance change from control, E2- and BPA-treated animals. As expected, the administration of E2 and BPA to these animals resulted in a visibly pronounced effect on the uterus. By using the classical we weight measurements, as is used in the uterotrophic assay, we were able to verify estrogenicity (Figure 4.1). In addition, we were able to verify the up- and/or down-regulation upon exposure to estrogen and estrogen-like compounds for our 6 candidate markers of estrogenicity (Figures 4.2-4.7).

While we were able to verify the 6 candidate proteins from our panel, S100G proved to be somewhat difficult to confirm. Specifically, we detected little to no endogenous peptide from S100G using either small-bore or nanoflow LC-MS/MS upon targeted analysis of the tissue harvested from vehicle-treated control animals. This is most likely due to the low abundance of the protein in the uterus in the absence of estrogen (4-6). While it is a well-established marker of estrogenicity (7-11), it is not as abundant a protein as the other candidate markers are in the uterus (4-6). Previous studies investigating calbindin-D9k (an alternative name for S100G) gene expression levels at the transcription level, as well as using North blot analysis, were unable to detect S100G in the uterus without estrogen present (4-6). They showed the low level expression of S100G in the uterus, and the subsequent detectable increase in expression upon E2 exposure, which we also showed at the protein level.

CONCLUSIONS

In summary, we successfully validated our preliminary panel of 6 candidate markers of estrogenicity using stable isotope dilution-based targeted quantitation, based on the principles of AQUA (12). To our knowledge, this is the first study using quantitative proteomics to the identification of molecular markers of estrogenicity in the mammalian uterus. With further panel expansion and after rigorous validation, we propose the application of these markers in an assessment strategy that complements the currently used uterotrophic assay. Specifically, the proposed strategy would permits multiple-measure informed prioritization of suspected EDCs for additional tests regarding estrogenicity.

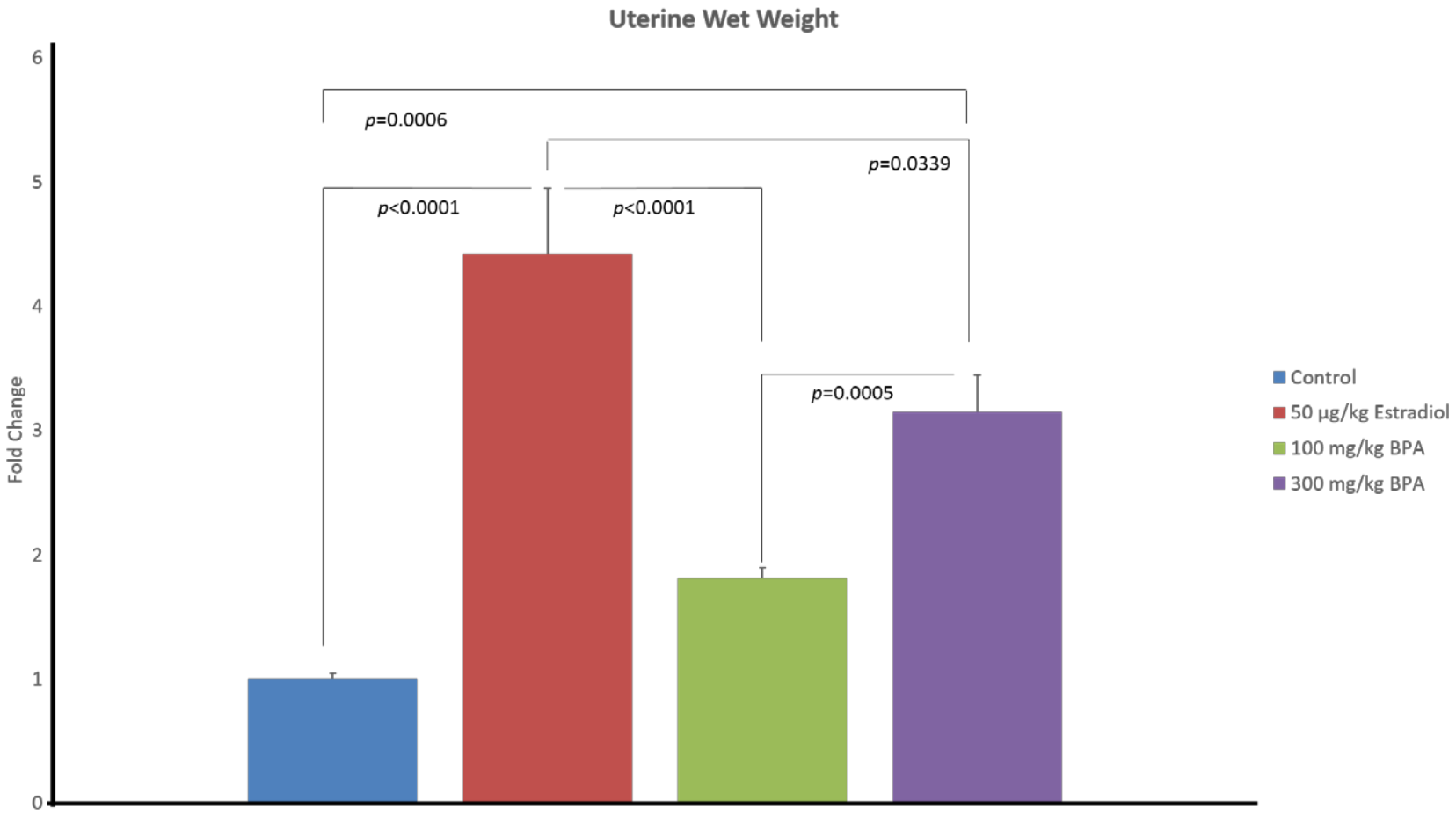

Figure 4.1. Changes in uterine wet weights of OVX Sprague-Dawley rats compared to vehicle-treated controls after daily injections of E2 (50 µg/kg) and BPA in two doses for 5 days. Wet weight of the uteri in the control group: 119.3 ± 9.9 mg, error bars are standard errors of the mean (SEM).

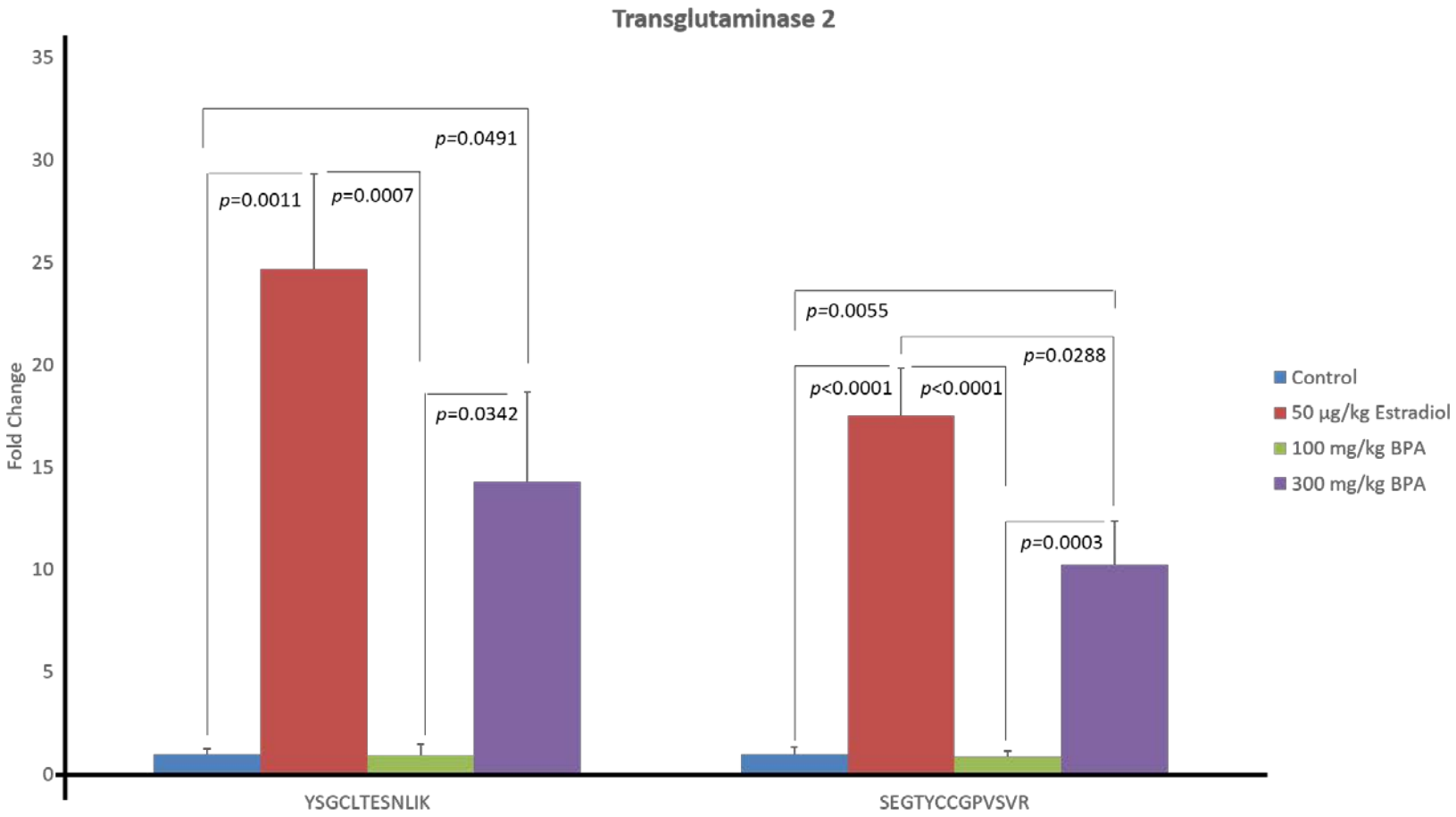

Figure 4.2. Comparison of the fold change difference across treatment groups, normalized to control, for each proteotypic peptide of transglutaminase 2 (*Tgm2*) from the candidate marker panel of estrogenicity. Error bars are standard errors of the mean (SEM).

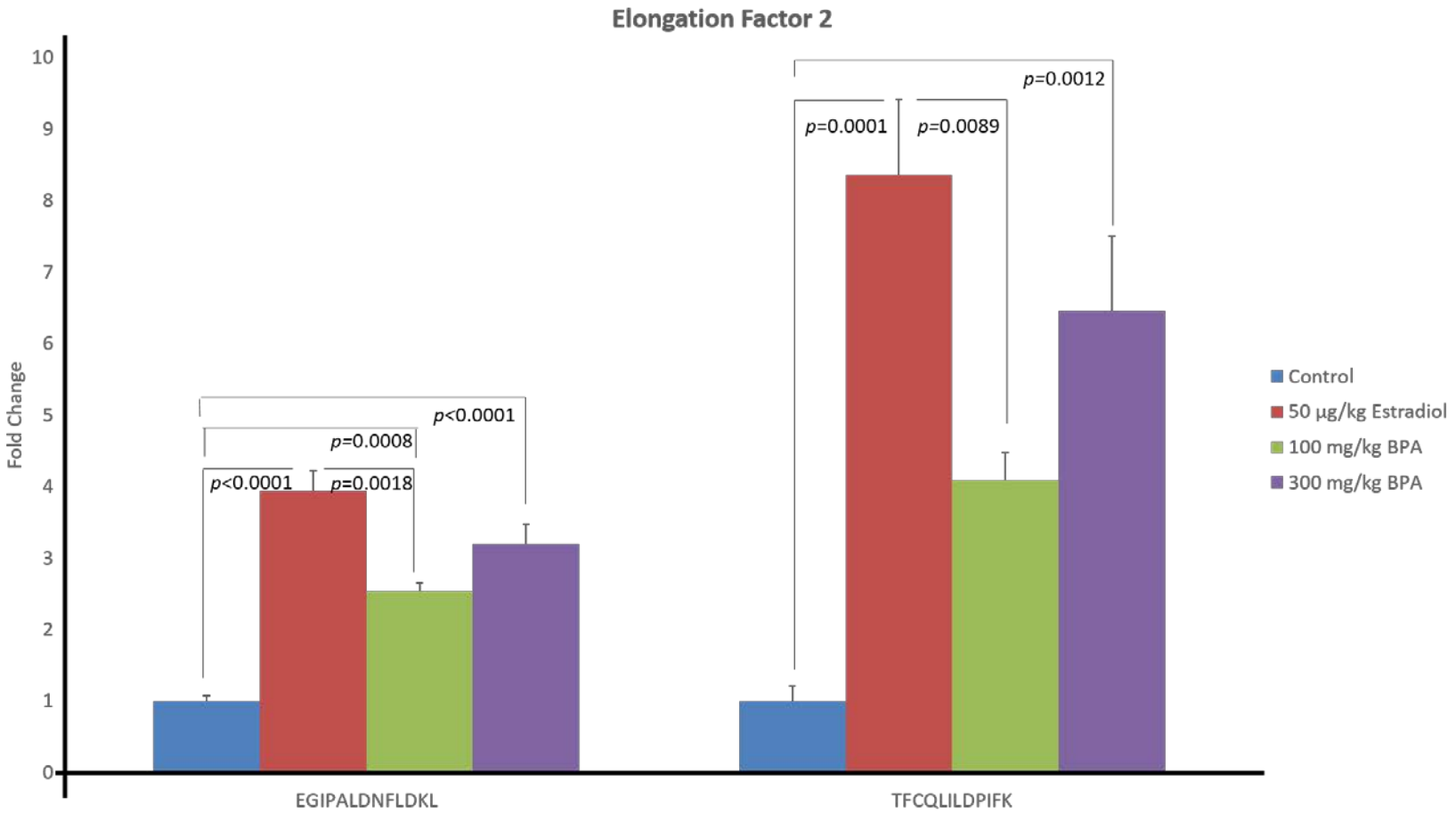

Figure 4.3. Comparison of the fold change difference across treatment groups, normalized to control, for each proteotypic peptide of elongation factor 2 (*Ef2*) from the candidate marker panel of estrogenicity. Error bars are standard errors of the mean (SEM).

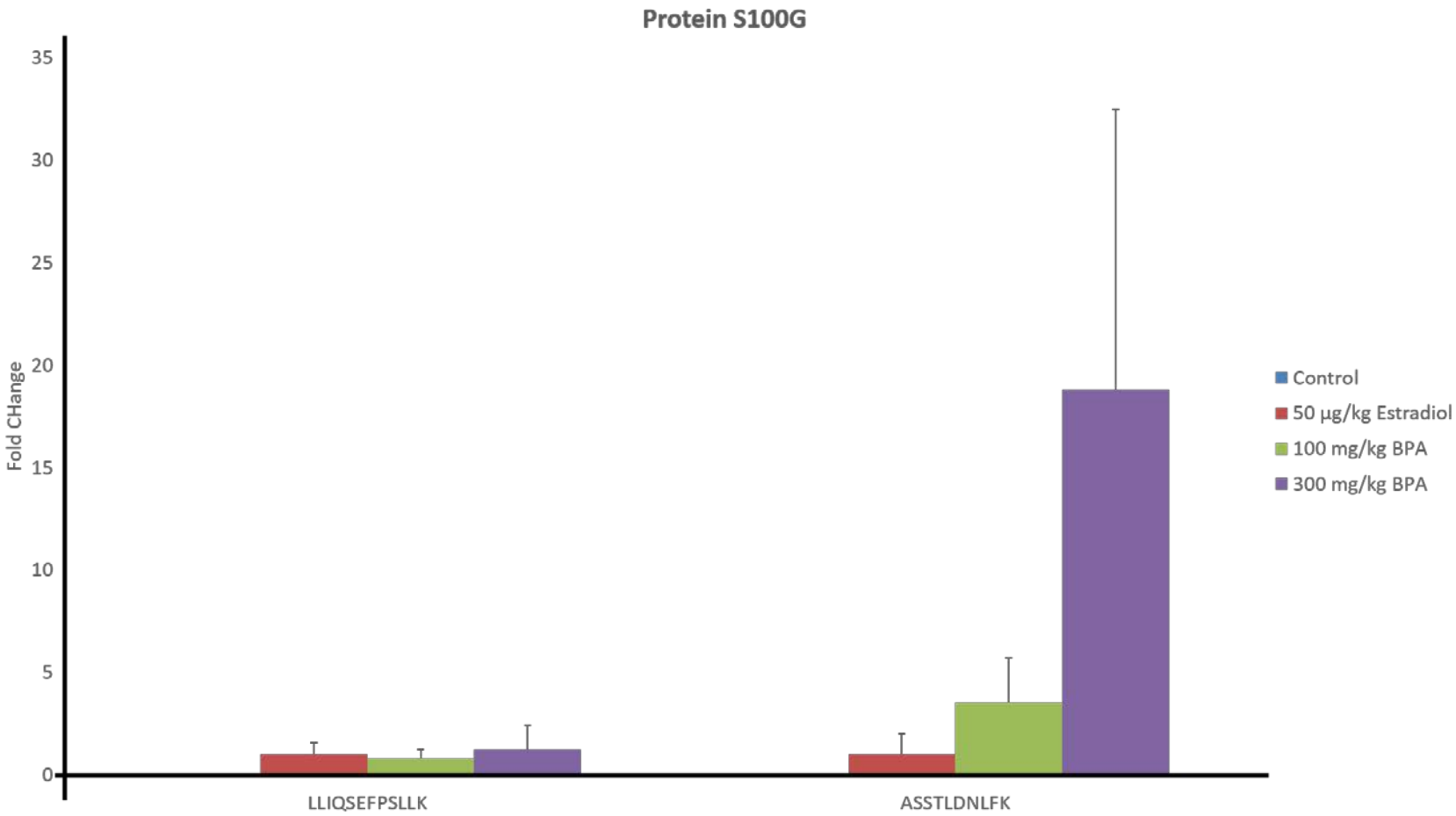

Figure 4.4. Comparison of the fold change difference across treatment groups, normalized to E2, for each proteotypic peptide of S100G from the candidate marker panel of estrogenicity. Error bars are standard errors of the mean (SEM).

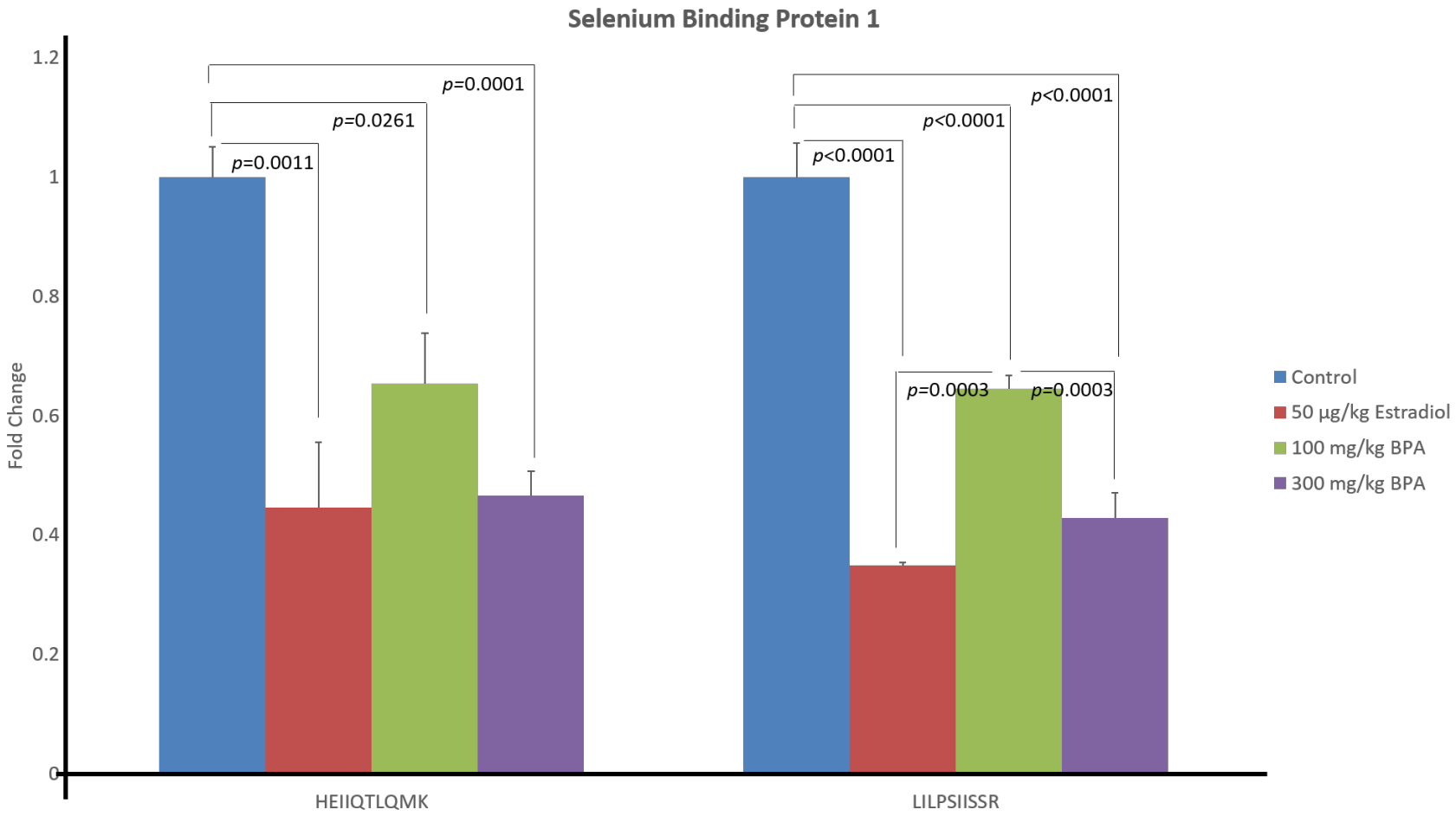

Figure 4.5. Comparison of the fold change difference across treatment groups, normalized to control, for each proteotypic peptide of selenium-binding protein 1 (*Sbp1*) from the candidate marker panel of estrogenicity in the rat uterus. Error bars are standard errors of the mean (SEM).

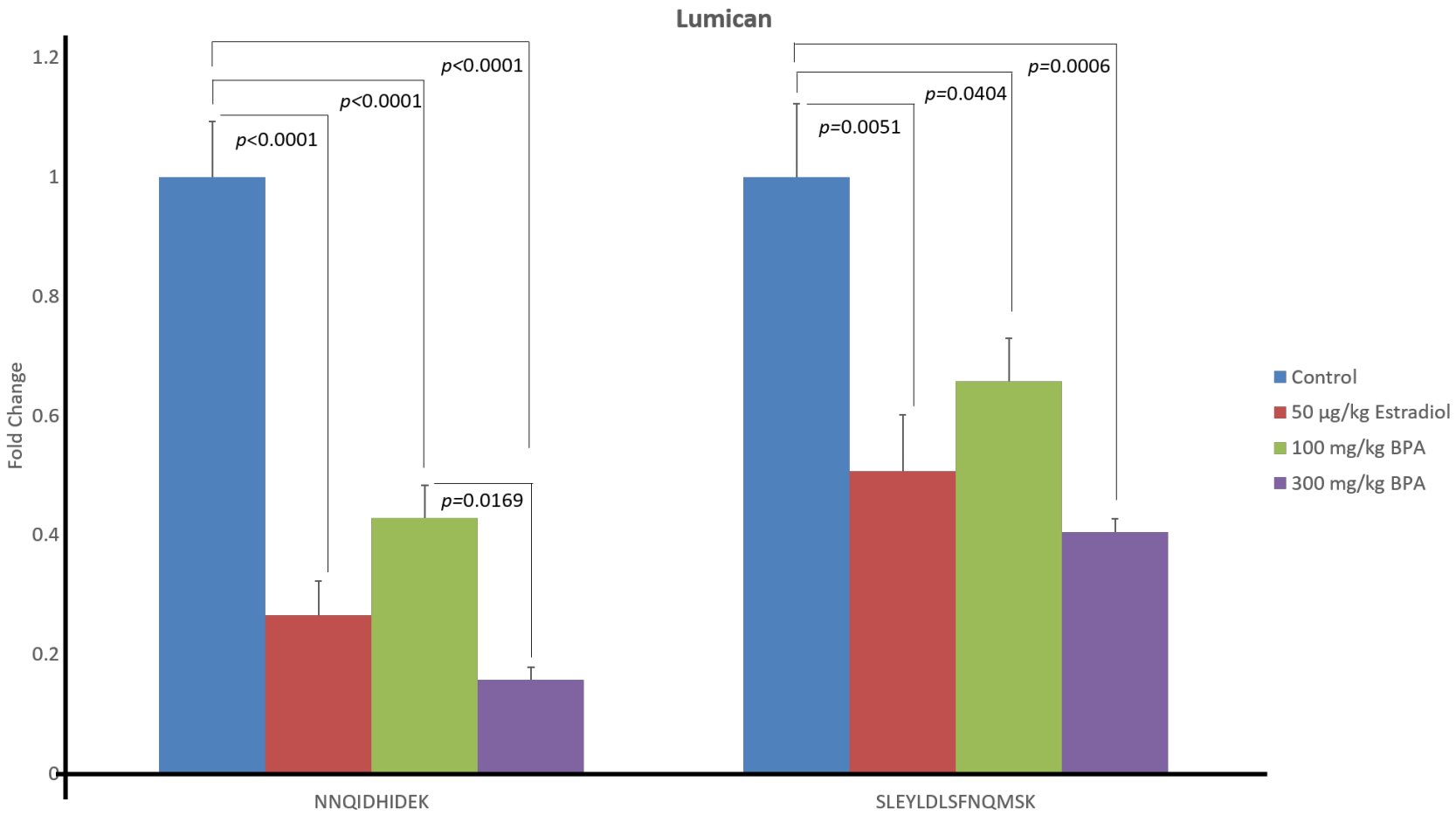

Figure 4.6. Comparison of the fold change difference across treatment groups, normalized to control, for each proteotypic peptide from lumican (*Lum*) from the candidate marker panel of estrogenicity in the rat uterus. Error bars are standard errors of the mean (SEM).

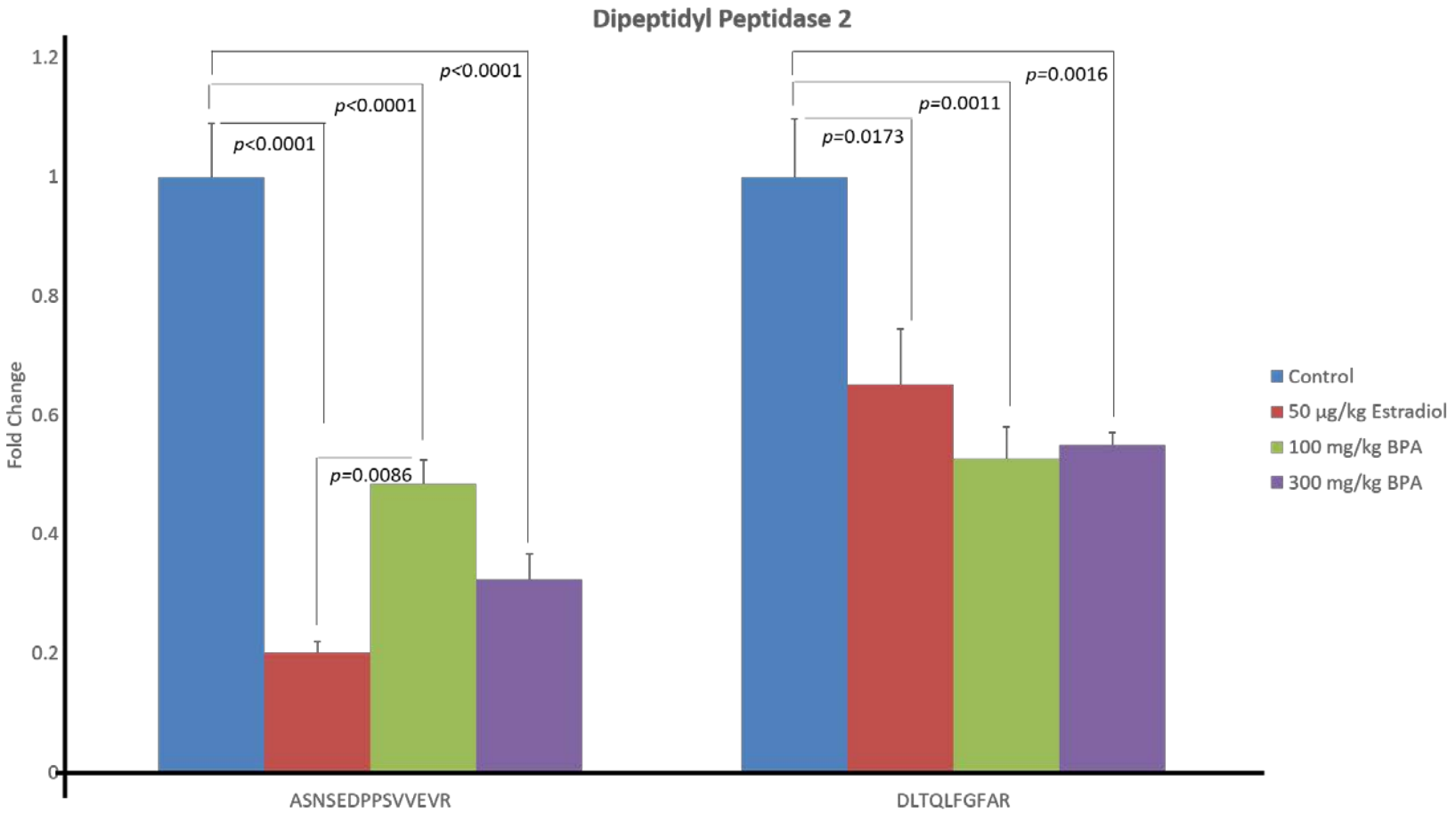

Figure 4.7. Comparison of the fold change difference across treatment groups, normalized to control, for each proteotypic peptide of dipeptidyl peptidase 2 (*Dpp2*) from the candidate marker of estrogenicity in the rat uterus. Error bars are standard errors of the mean (SEM).

REFERENCES

1. Kitamura, S.; Suzuki, T.; Sanoh, S.; Kohta, R.; Jinno, N.; Sugihara, K.; Yoshihara, S.; Fujimoto, N.; Watanabe, H.; Ohta, S., Comparative study of the endocrine-disrupting activity of bisphenol A and 19 related compounds. *Toxicol. Sci.* **2005,** 84, (2), 249-59.

2. Ashby, J., Increasing the sensitivity of the rodent uterotrophic assay to estrogens, with particular reference to bisphenol A. *Environ. Health Perspect.* **2001,** 109, (11), 1091-4.

3. Tinwell, H.; Joiner, R.; Pate, I.; Soames, A.; Foster, J.; Ashby, J., Uterotrophic activity of bisphenol A in the immature mouse. *Regul. Toxicol. Pharmacol.* **2000,** 32, (1), 118-26.

4. Krisinger, J.; Dann, J. L.; Applegarth, O.; Currie, W. D.; Jeung, E. B.; Staun, M.; Leung, P. C., Calbindin-D9k gene expression during the perinatal period in the rat: correlation to estrogen receptor expression in uterus. *Mol. Cell. Endocrinol.* **1993,** 97, (1-2), 61-9.

5. Jeung, E. B.; Leung, P. C.; Krisinger, J., The human calbindin-D9k gene. Complete structure and implications on steroid hormone regulation. *J. Mol. Biol.* **1994,** 235, (4), 1231-8.

6. L'Horset, F.; Perret, C.; Brehier, A.; Thomasset, M., 17 beta-estradiol stimulates the calbindin-D9k (CaBP9k) gene expression at the transcriptional and posttranscriptional levels in the rat uterus. *Endocrinology* **1990,** 127, (6), 2891-7.

7. Choi, K. C.; Leung, P. C.; Jeung, E. B., Biology and physiology of Calbindin-D9k in female reproductive tissues: involvement of steroids and endocrine disruptors. *Reprod. Biol. Endocrinol.* **2005,** 3, 66.

8. Choi, Y.; Seo, H.; Shim, J.; Kim, M.; Ka, H., Regulation of S100G Expression in the Uterine Endometrium during Early Pregnancy in Pigs. *Asian Australas. J. Anim. Sci.* **2012,** 25, (1), 44-51.

9. Dang, V. H.; Choi, K. C.; Hyun, S. H.; Jeung, E. B., Induction of uterine calbindin-D9k through an estrogen receptor-dependent pathway following single injection with xenobiotic agents in immature rats. *J. Toxicol. Environ. Health A* **2007,** 70, (2), 171-82.

10. Vo, T. T.; An, B. S.; Yang, H.; Jung, E. M.; Hwang, I.; Jeung, E. B., Calbindin-D9k as a sensitive molecular biomarker for evaluating the synergistic impact of estrogenic chemicals on GH3 rat pituitary cells. *Int. J. Mol. Med.* **2012,** 30, (5), 1233-40.

11. Vo, T. T.; Jeung, E. B., An evaluation of estrogenic activity of parabens using uterine calbindin-d9k gene in an immature rat model. *Toxicol. Sci.* **2009,** 112, (1), 68-77.

12. Gerber, S. A.; Rush, J.; Stemman, O.; Kirschner, M. W.; Gygi, S. P., Absolute quantification of proteins and phosphoproteins from cell lysates by tandem MS. *Proc. Natl. Acad. Sci. USA* **2003,** 100, (12), 6940-5.

CHAPTER V

SUMMARY

The need for advanced testing to evaluate the safety of the tens of thousands of man-made chemicals in the environment has been brought to light as the traditional testing methodologies do not adequately address the complex risk exposure can have (1). Therefore, more efforts need to be made to discover advanced testing methodologies, but also apply established technologies, such as quantitative proteomics, for the testing of these compounds.

Previously in our lab, we reported on the rapid label-free proteomic approach to identify estrogen-regulated proteins in the mouse brain and uterus (2). In the present study, we used uterus proteins extracted from rats exposed to E2 along with their controls in order to gain more insight into the effects of E2 on the proteome level, in addition to developing a targeted LC-MS/MS MRM-based assay for validation of potential markers of hormonal effects identified from proteomic discovery, as well as understanding signaling networks affected. We used a label-free quantitative approach to discover, described in **Chapter II**, and then validate markers of estrogenicity, described in **Chapters III and IV**. In developing a targeted proteomics assay, we are making use of a more advanced technology over the currently used uterotrophic assay (3), which can be implemented seamlessly in the arsenal of assays for the screening of compounds concerning potential estrogenic activity. Currently, the uterotrophic assay merely considers the uterine weight gain as an endpoint. Complementing this simple assay with suitable molecular-

level endpoint data could diminish chances of dismissing potential estrogenic EDCs from further investigations because they do not meet statistical significance criteria for organ weight gain only, especially in studies involving a small number of animal subjects in the treatment groups. Such multiple-measure assessment that includes biological information could also justify further targeted studies to identify specific links between chemical interactions and toxicological effects.

Targeted proteomics was recognized by Nature Methods as method of the year in 2012 (4, 5). It is a specific and selective way to assay specific proteins of interest. We were able to take a page from small-molecule methodologies and apply it to proteins, monitoring only those selected proteotypic peptides, from a complex mixture of peptides, allows for an increase in sensitivity, reproducibility, as well as specificity and robustness. Using targeted proteomics allows for determining a peptide's presence and quantity in and across samples, which can be used for relative or absolute quantification. These targeted assays are inherently more accurate than Western blots and do not require the use of antibodies and, thus, avoid the problems associated with antibody-based quantitative measurements (6). These LC-MRM-based assays are faster and capable of measuring upwards of several hundred peptides in a single analysis. This methodology holds huge promise for targeted screening and for use as a diagnostic tool in this and other fields.

In summary, we performed differential proteome analyses focusing on estrogen-regulated rat uterus proteins using two quantitative approaches: a label-free shotgun method followed by targeted quantitation based on an initial panel of candidate markers using stable isotope labeled internal standards. To our knowledge, this is the first study using quantitative proteomics to the identification of molecular markers of estrogenicity. With further panel expansion and after rigorous validation, we propose the use of these biological markers in an assessment strategy that

complements the currently used uterotrophic assay and permits multiple-measure informed prioritization of suspected EDCs to additional tests for estrogenicity.

FUTURE DIRECTIONS

Our preliminary panel can be expanded to give a more comprehensive evaluation. Each protein apparently exhibits differing response to EDCs, showing the vast complexities regarding exposure. Because the nature of the proteome is dynamic, we must look past simple compilations of lists of proteins as potential biomarkers but rather to take a systems approach and look at protein interactions and networks, similarly to what we employed as a guiding principle in this dissertation. Future studies can, and should, further explore these interactions and networks in depth to help identify links between chemical exposure and toxicological effects. In addition to expansion, a proposed panel also needs to undergo rigorous validation to meet regulatory criteria for use in a battery of assays evaluating suspected estrogenic EDCs.

REFERENCES

1. United States Environmental Protection Agency, Next Generation Risk Assessment: Incorporation of Recent Advances in Molecular, Computational, and Systems Biology. In Sept 2014 EPA/600/R-14/004 ed.; National Center for Environmental Assessment Office of Research and Development, Ed. 2014.

2. Prokai, L.; Stevens, S. M., Jr.; Rauniyar, N.; Nguyen, V., Rapid label-free identification of estrogen-induced differential protein expression in vivo from mouse brain and uterine tissue. *J. Proteome Res.* **2009,** 8, (8), 3862-71.

3. United States Environmental Protection Agency, OPPTS 890.1600: Uterotrophic Assay Standard Evaluation Procedure. In Sep 2011 ed.; Office of Prevention Pesticides and Toxic Substances (OPPTS), Ed. 2011.

4. Method of the Year 2012. *Nat. Methods* **2013,** 10, (1), 1.

5. Marx, V., Targeted proteomics. *Nat. Methods* **2013,** 10, (1), 19-22.

6. Aebersold, R.; Burlingame, A. L.; Bradshaw, R. A., Western blots versus selected reaction monitoring assays: time to turn the tables? *Mol. Cell. Proteomics* **2013,** 12, (9), 2381-2.